

# Top Quark Mass <sup>1</sup>

Jonathan L. Rosner<sup>2</sup>

*CERN, 1211-CH Geneva 23, Switzerland*

*Enrico Fermi Institute and Department of Physics  
University of Chicago, Chicago, IL 60637 USA <sup>3</sup>*

## Abstract

The influence of the top quark mass on mixing processes and precise electroweak measurements is described. Experimental observation of the top quark in proton-antiproton collisions is discussed, and some brief remarks are made about electron-positron production. Some speculations are noted about the possible significance of the large top quark mass.

arXiv:hep-ph/9610222v2 6 Jan 1997

CERN-TH/96-245  
September 1996

---

<sup>1</sup>Three lectures given at Cargèse Summer Institute on Particle Physics, *Masses of Fundamental Particles*, August, 1996. Proceeding to be published by Plenum.

<sup>2</sup>rosner@uchepa.uchicago.edu

<sup>3</sup>Permanent address.

# TOP QUARK MASS

Jonathan L. Rosner  
Enrico Fermi Institute and Department of Physics  
University of Chicago  
5640 South Ellis Avenue, Chicago, IL 60637

## 1. INTRODUCTION

In the present article, based on a series of three lectures, we describe ways in which the large top quark mass influences a number of processes, and some ideas about how it might arise. After a brief introduction to the pattern of masses and couplings of quarks and leptons and an overview of the top quark's properties, we discuss in Section 2 the role of the top quark in mixing processes, such as particle-antiparticle mixing in the neutral kaon and  $B$  meson systems, and in other flavor-changing charge-preserving processes. Section 3 is devoted to precision electroweak experiments and the impact upon their interpretation of the precise measurements of the top quark's mass which have recently been achieved at Fermilab (Section 4). Some brief remarks about top quark production in electron-positron collisions occupy Section 5, while Section 6 contains various speculations about the source of the top quark's mass. (See also Graham Ross' lectures at this Institute [1].) Section 7 concludes.

### A. Quark and lepton mass and coupling patterns

The top quark is the heaviest known elementary particle, nearly 200 times as heavy as a proton. Its mass is compared with that of the other known quarks and leptons in Figure 1. Also shown are the patterns of couplings in charge-changing weak transitions. The main coupling of the top ( $t$ ) appears to be to the bottom ( $b$ ) quark [2], while charm ( $c$ ) couples mainly to strange ( $s$ ) and up to down. Each charged lepton, in turn, appears to couple to its own neutrino. However, the pattern for quarks known at present is much richer, including weaker couplings of  $t$  to  $s$  and  $d$ , of  $c$  to  $b$  and  $d$ , and of  $u$  to  $b$  and  $s$ . This pattern is encoded in a unitary  $3 \times 3$  matrix  $V$  known as the *Cabibbo-Kobayashi-Maskawa* [3, 4] matrix.

In these lectures we shall explore a number of aspects of the pattern of masses and couplings in Figure 1 and Table 1 [5]. The large mass of the top quark and its pattern of couplings to the  $b$ ,  $s$ , and  $d$  quarks lead to a number of consequences for processes in which the top quark participates as a virtual particle. Not the least of these is the ability of loop diagrams involving the top quark to generate the observed CP violation in the neutral kaon system [4]. At the same time, the fact that the top quark is about

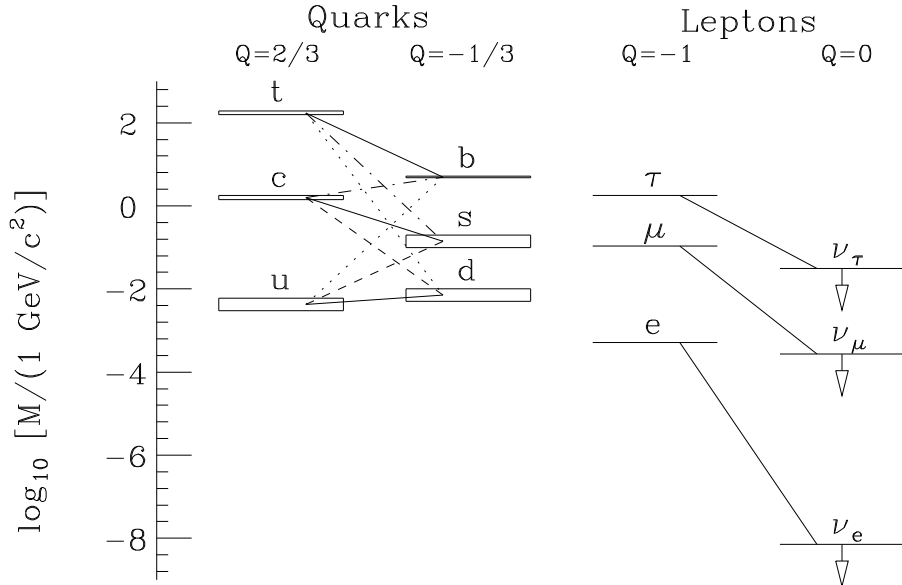


Figure 1: Patterns of charge-changing weak transitions among quarks and leptons. Direct evidence for  $\nu_\tau$  does not yet exist. The strongest inter-quark transitions correspond to the solid lines, with dashed, dot-dashed, and dotted lines corresponding to successively weaker transitions.

twice as heavy as the gauge bosons  $W$  and  $Z$  of the electroweak interactions [6] offers a hint that it may play a crucial role in the understanding of all the quark and lepton masses.

A note of caution: if its mass is viewed on a logarithmic scale, as in Figure 1, the top quark is not all that exceptional. Although it is more than 100 times as heavy as the next lightest quark of charge  $2/3$ , the charmed quark, we have not yet explored similar logarithmic mass intervals above the bottom quark or  $\tau$  lepton. But the  $Z$  decays to just three pairs of light neutrinos [7]. so the pattern of any fermions heavier than those in Figure 1 must at least change to a significant extent.

Table 1: Relative strengths of charge-changing weak transitions.

Relative amplitude	Transition	Source of information (example)
$\sim 1$	$u \leftrightarrow d$	Nuclear $\beta$ -decay
$\sim 1$	$c \leftrightarrow s$	Charmed particle decays
$\sim 0.22$	$u \leftrightarrow s$	Strange particle decays
$\sim 0.22$	$c \leftrightarrow d$	Neutrino prod. of charm
$\sim 0.04$	$c \leftrightarrow b$	$b$ decays
$\sim 0.003$	$u \leftrightarrow b$	Charmless $b$ decays
$\sim 1$	$t \leftrightarrow b$	Dominance of $t \rightarrow Wb$
$\sim 0.04$	$t \leftrightarrow s$	Only indirect evidence
$\sim 0.01$	$t \leftrightarrow d$	Only indirect evidence

## B. Quark and lepton families

The case for a quark-lepton analogy is suggested by the doublets

$$\begin{pmatrix} \nu_e \\ e^- \end{pmatrix} : \text{leptons} \quad ; \quad \begin{pmatrix} u \\ d \end{pmatrix} : \text{quarks} \quad . \quad (1)$$

In both cases the states in the upper and lower rows are connected by emission or absorption of a  $W$  boson. This pattern was extended to the second family by several authors [8], who inferred the existence of a fourth quark (charm) coupling mainly to the strange quark from the existence of the  $\mu - \nu_\mu$  doublet:

$$\begin{pmatrix} \nu_\mu \\ \mu^- \end{pmatrix} : \text{leptons} \Rightarrow \begin{pmatrix} c \\ s \end{pmatrix} : \text{quarks} \quad . \quad (2)$$

The suppression of processes involving weak decays of strange particles as compared with strangeness-preserving weak decays could be made compatible with the universal strength of the weak interactions if the  $u$  quark coupled to an appropriately normalized linear combination of  $d$  and  $s$ :

$$u \leftrightarrow d \cos \theta_c + s \sin \theta_c \quad . \quad (3)$$

This universality property was proposed by Gell-Mann and Lévy [9] and used by Cabibbo [3] (hence the subscript on the angle) to relate successfully a number of beta-decay processes of non-strange and strange particles. The strength of the charge-changing weak current could be normalized by considering it and its hermitian adjoint to be members of an  $SU(2)$  triplet. The neutral member of this triplet contained strangeness-changing terms and thus had to be interpreted as unphysical, since no strangeness-changing neutral-current processes had been seen. However, if one then considered the charmed quark to couple to the orthogonal combination,

$$c \leftrightarrow -d \sin \theta_c + s \cos \theta_c \quad , \quad (4)$$

the corresponding neutral current would couple to the combination  $u\bar{u} + c\bar{c} - d\bar{d} - s\bar{s}$ , and would preserve flavor [8, 10]. This property was preserved in higher orders of perturbation theory, and neutral strangeness-changing processes were induced only to the extent that the charm and  $u$  quark masses differed from one another [10].

A further motivation for the quark-lepton analogy was noted by Bouchiat, Iliopoulos, and Meyer [11] in 1972. In a gauge theory of the electroweak interactions, triangle anomalies associated with graphs of the type shown in Figure 2 have to be avoided. This cancellation requires the fermions  $f$  in the theory to contribute a total of zero to the sum over  $f$  of  $Q_f^2 I_{3L}^f$ . Such a cancellation can be achieved by requiring quarks and leptons to occur in complete families of the type mentioned above, so that the terms

$$\text{Leptons : } (0)^2 \left(\frac{1}{2}\right) + (-1)^2 \left(-\frac{1}{2}\right) = -\frac{1}{2} \quad (5)$$

$$\text{Quarks : } 3 \left[ \left(\frac{2}{3}\right)^2 \left(\frac{1}{2}\right) + \left(-\frac{1}{3}\right)^2 \left(-\frac{1}{2}\right) \right] = \frac{1}{2} \quad (6)$$

sum to zero for each family.

Some history of how the quark and lepton families were pieced together may be of interest [12]. In the family (1), the first particle to be discovered was the electron, whose unique properties were clinched by J. J. Thomson's measurement of its enormous

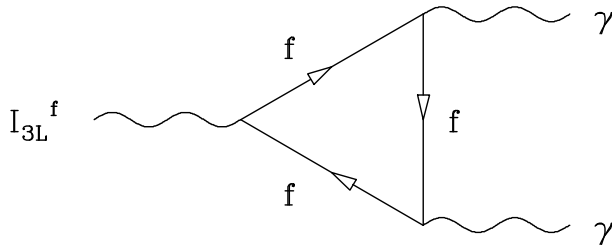


Figure 2: Example of triangle diagram for which leading behavior must cancel in a renormalizable electroweak theory.

charge-to-mass ratio (nearly 2000 times that of the proton) in 1897. The corresponding neutrino was proposed by W. Pauli [13] in 1931. As for the  $u$  and  $d$  quark, the need for two constituents of hadrons differing in charge by a unit but with very similar behaviour under the strong interactions dates back to the recognition of isotopic spin as a good symmetry [14], in the 1930's.

Evidence for the second family (2) began with the discovery in 1937 by S. Neddermeyer and C. Anderson of the muon in cosmic radiation [15]. The corresponding neutrino  $\nu_\mu$  was proved distinct from the electron neutrino  $\nu_e$  in 1962 by a group led by L. Lederman, M. Schwartz, and J. Steinberger [16]. Meanwhile, evidence for particles containing one or more strange ( $s$ ) quarks, initially seen in cosmic radiation and later produced at accelerators, began accumulating over the period 1946-53. The charmed ( $c$ ) quark was discovered initially in the form of a  $c\bar{c}$  bound state, the  $J$  [17] or  $\psi$  [18] (the dual name  $J/\psi$  has survived). Particles containing a single charmed quark (“bare charm”) were identified a bit later [19].

At the same time evidence for the charmed quark was accumulating in electron-positron annihilations, the first member of a third family:

$$\begin{pmatrix} \nu_\tau \\ \tau^- \end{pmatrix} : \text{leptons} \quad ; \quad \begin{pmatrix} t \\ b \end{pmatrix} : \text{quarks} \quad . \quad (7)$$

was making its appearance. This was the  $\tau$  lepton, identified by M. Perl and collaborators [20]. If this were to be a lepton like the  $e$  and  $\mu$ , having its own neutrino, the anomaly-cancellation mechanism mentioned earlier [11] then required there to be a third pair of quarks: the “top” and “bottom” [21], our present names for the quarks proposed by Kobayashi and Maskawa [4] as candidates for explaining CP violation.

The bottom quark made its appearance in the form of  $b\bar{b}$  bound states discovered at Fermilab in 1977 by a group led by L. Lederman [22] and in “bare bottom” (otherwise known as “beauty”) mesons containing single  $b$  quarks seen at the Cornell Electron Storage Ring (CESR) somewhat later [23]. Eagerly awaited, the top quark finally made its appearance 17 years after the bottom, in proton-antiproton collisions at Fermilab at a center-of-mass energy of 1.8 TeV [24].

Even up to the present day, in the absence of direct evidence for the  $\nu_\tau$ , we have never had a complete set of quark and lepton families without hints of the next family. By the time the  $\nu_\tau$  is discovered, perhaps at a forthcoming experiment at Fermilab [25], who knows what other particles may appear?

### C. Top quark properties

The most recent measurements of the top quark mass, reported at the 1996 Warsaw

Conference, are [26]

$$m_t = 176.8 \pm 4.4 \pm 4.8 \text{ GeV}/c^2 \text{ (CDF)} ; 169 \pm 8 \pm 8 \text{ GeV}/c^2 \text{ (D0)} ; 175 \pm 6 \text{ GeV}/c^2 \text{ (avg.)} . \quad (8)$$

The top is expected to decay essentially 100% ( $\simeq |V_{tb}|^2$ ) to  $W + b$ , with branching ratios of only about  $|V_{ts}|^2 \simeq 1.5 \times 10^{-3}$  to  $W + s$  and  $|V_{td}|^2 \simeq 10^{-4}$  to  $W + d$ . We shall see in Sec. 4 that recent data [2] support this expectation.

The predicted rate for the decay  $t \rightarrow W + b$  is

$$\Gamma(t \rightarrow W + b) = \frac{G_F}{8\pi\sqrt{2}} |V_{tb}|^2 m_t^3 \Phi_K K_{\text{QCD}} \quad , \quad (9)$$

where, in the limit in which the  $b$  quark mass can be neglected,

$$\Phi_K \equiv \left(1 - \frac{M_W^2}{m_t^2}\right)^2 \left(1 + 2\frac{M_W^2}{m_t^2}\right) = 0.885 \quad (10)$$

and  $K_{\text{QCD}}$  is a QCD correction factor which is about 0.917 [27]. For  $m_t = 175 \text{ GeV}$ , one thus predicts  $\Gamma = (1.76 \text{ GeV})(0.885)(0.917) \simeq 1.43 \text{ GeV}$ , so that the top quark decays before it can form hadrons. Thus, sad to say, we will not be able to study the properties of  $t\bar{t}$  or  $t\bar{q}$  states (where  $q$  stands for one of the lighter quarks). Nonetheless, some crude information about the  $t\bar{t}$  interaction can be recovered, as we shall mention in Sec. 5.

The spin of the top quark is expected to be 1/2, just like that of the other quarks. Direct evidence for this is lacking, but if we are prepared to admit that  $J(t) = J(b)$ , we can use all of the bottom quark's rich spectroscopy to conclude that  $J(b) = 1/2$  and hence  $J(t) = 1/2$ . The spectra of  $c\bar{c}$ ,  $b\bar{b}$ , charm – light quark and bottom – light quark bound states are shown in Figs. 3, 4, 5, and 6 respectively. We shall use some of the terminology in these figures in what follows, so they are worth getting acquainted with.

The charmonium ( $c\bar{c}$ ) spectrum in Fig. 3 bears strong evidence that the spin of the charmed quark is 1/2, as one might have expected from its partnership with the strange quark. (Spins of strange particles have been directly measured for a number of years and support the notion that  $J(s) = 1/2$ .) The S-wave ( $L = 0$ ) levels have total angular momentum  $J$ , parity  $P$ , and charge-conjugation eigenvalue  $C$  equal to  $J^{PC} = 0^{+-}$  and  $1^{--}$  as one would expect for  $^1S_0$  and  $^3S_1$  states, respectively, of a quark and antiquark. The P-wave ( $L = 1$ ) levels have  $J^{PC} = 1^{+-}$  for the  $^1P_1$ ,  $0^{++}$  for the  $^3P_0$ ,  $1^{++}$  for the  $^3P_1$ , and  $2^{++}$  for the  $^3P_2$ . The  $J^{PC} = 1^{--}$  levels are identified as such by their copious production through single virtual photons in  $e^+e^-$  annihilations. The  $0^{-+}$  level  $\eta_c$  is produced via single-photon emission from the  $J/\psi$  (so its  $C$  is positive) and has been directly measured to have  $J^P$  compatible with  $0^-$  [28]. Numerous studies have been made of the electromagnetic (electric dipole) transitions between the S-wave and P-wave levels [29] and they, too, support the assignments shown.

The  $b\bar{b}$  (upsilon) levels shown in Fig. 4 have a very similar structure, aside from an overall shift. The similarity of the  $c\bar{c}$  and  $b\bar{b}$  spectra is in fact an accident of the fact that for the interquark distances in question (roughly 0.2 to 1 fm), the interquark potential interpolates between short-distance Coulomb-like and long-distance linear behavior in a manner roughly compatible with  $V \sim \log r$  [30] or with an effective power near zero [31]. The copious production of  $1^{--}$  candidates in  $e^+e^-$  annihilations and the pattern of electric dipole transitions between S- and P-wave levels again supports the assignments shown.

States consisting of a single charmed quark and light ( $u$ ,  $d$ , or  $s$ ) quarks or anti-quarks, shown in Fig. 5, again support  $J(c) = 1/2$ . The lightest mesons have  $J^P = 0^-$

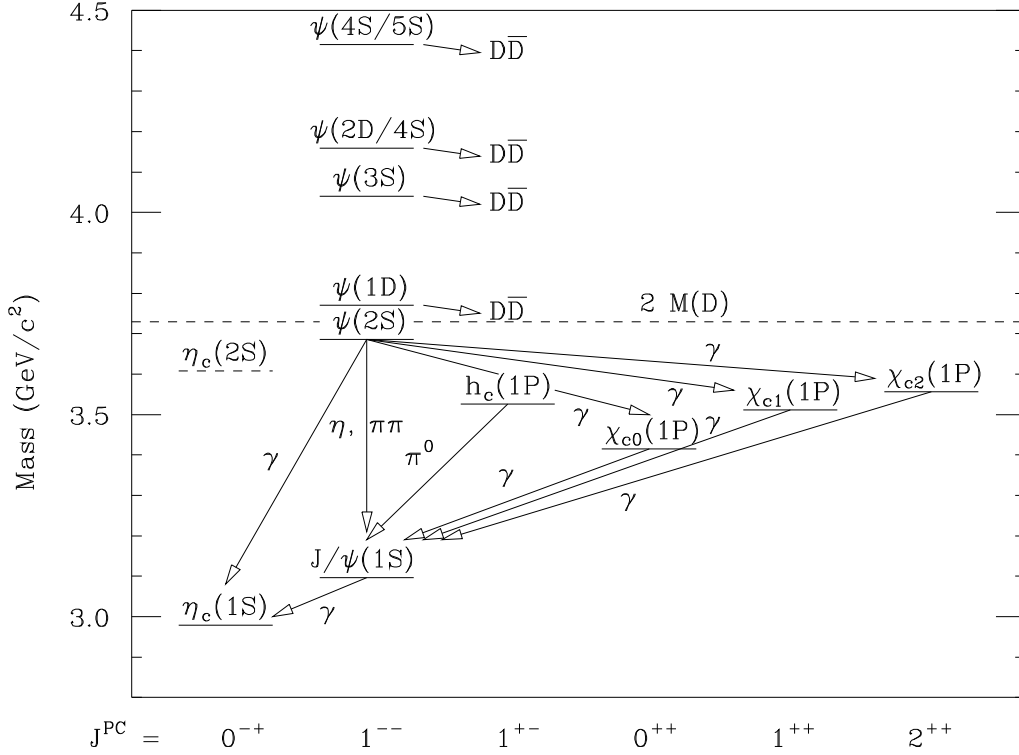


Figure 3: Charmonium ( $c\bar{c}$ ) spectrum. Observed and predicted levels are denoted by solid and dashed horizontal lines, respectively. Arrows denote electromagnetic transitions (labeled by  $\gamma$ ) and hadronic transitions (labeled by emitted hadrons).

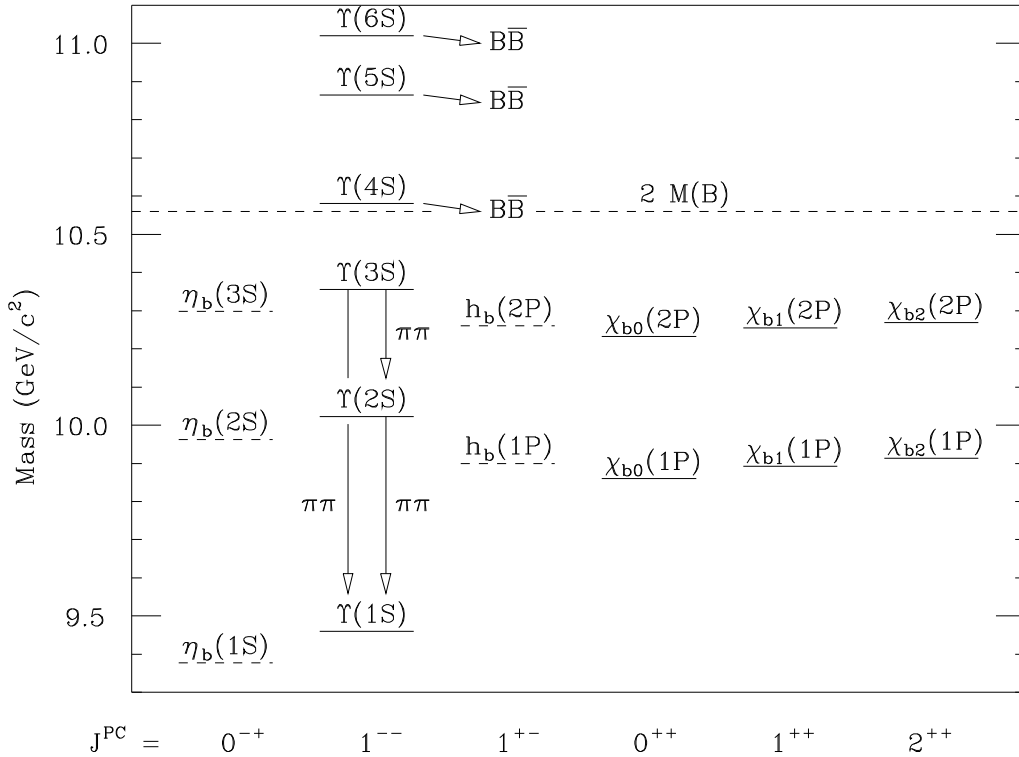


Figure 4: Spectrum of  $b\bar{b}$  states. Observed and predicted levels are denoted by solid and dashed horizontal lines, respectively. In addition to the transitions labeled by arrows, numerous electric dipole transitions and decays of states below  $B\bar{B}$  threshold to hadrons containing light quarks have been seen.

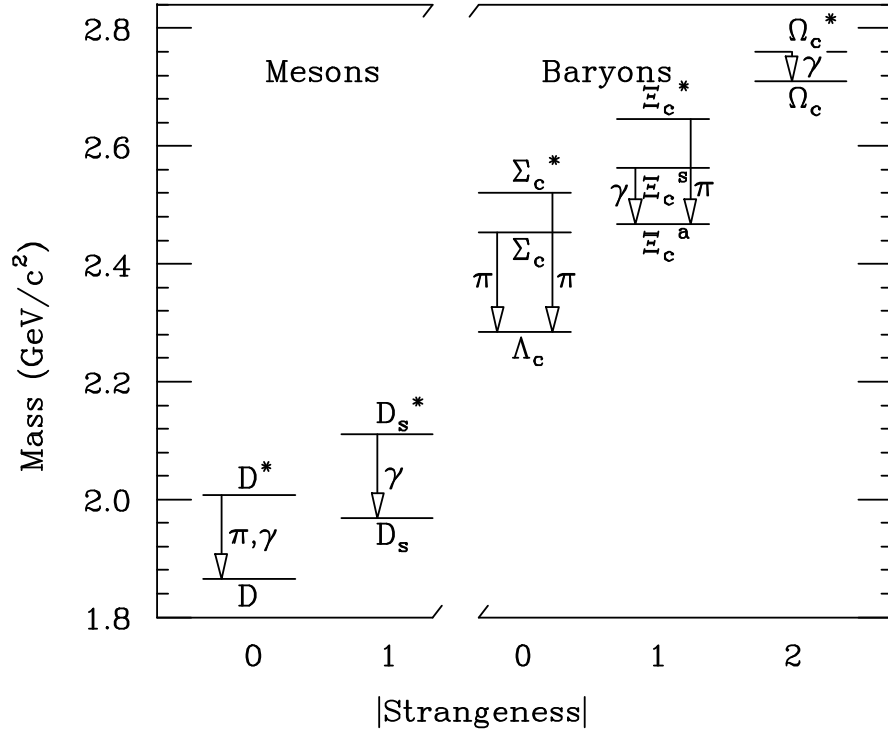


Figure 5: Spectrum of lowest-lying states containing one charmed and one light quark. Observed and predicted levels are denoted by solid and broken horizontal lines, respectively.

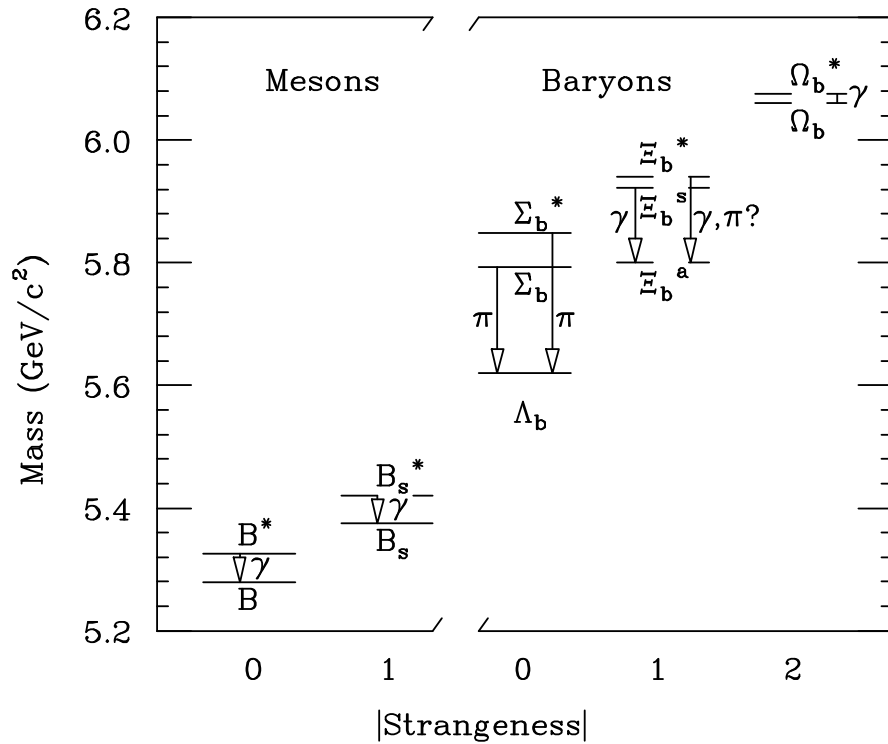


Figure 6: Spectrum of lowest-lying states containing one bottom and one light quark. Observed and predicted levels are denoted by solid and broken horizontal lines, respectively.



( $^1S_0$ ) and  $1^-$  ( $^3S_1$ ). Two charmed baryons discovered fairly recently, both strange [32] and nonstrange [33], are candidates for  $J = 3/2$ . One expects such states as bound states of three spin-1/2 quarks.

Finally, the pattern of states containing a single  $b$  quark (Fig. 6) is very similar to that for singly-charmed states, though not as well fleshed-out. In many cases the splittings between states containing a single  $b$  quark is less than that between the corresponding charmed states by roughly a factor of  $m_c/m_b \simeq 1/3$  as a result of the smaller chromomagnetic moment of the  $b$  quark. (This feature has also been noted by Neubert at this Institute [34].)

The top quark's mass, just like every other mass in the standard electroweak theory, arises as a result of Yukawa interactions of one or more Higgs bosons with the fermions. For the  $t$  and  $b$  quarks, the relevant part of the Lagrangian can be written as

$$\mathcal{L}_{\text{Higgs}}^{t,b} = -g_Y^b[\bar{Q}_L\phi_1 b_R + \text{H.c.}] - g_Y^t[\bar{Q}_L\phi_2 t_R + \text{H.c.}] \quad (11)$$

where

$$Q_L \equiv \begin{pmatrix} t \\ b \end{pmatrix}_L, \quad \phi_1 \equiv \begin{pmatrix} \phi_1^+ \\ \phi_1^0 \end{pmatrix}, \quad \phi_2 \equiv \begin{pmatrix} \phi_2^0 \\ \phi_2^- \end{pmatrix} \quad (12)$$

if there are two Higgs doublets, or  $\phi_2 = i\sigma_2\phi_1^c$  if there is only one. If the neutral member of each Higgs doublet acquires a vacuum expectation value  $\langle\phi_i^0\rangle = v_i/\sqrt{2}$ , then  $m_b = g_Y^b v_1/\sqrt{2}$ ,  $m_t = g_Y^t v_2/\sqrt{2}$ . Here

$$2^{-1/4}G_F^{-1/2} = v_1^2 + v_2^2 = (246 \text{ GeV})^2, \quad (13)$$

while the right-hand side is replaced by  $v_1^2 \equiv v^2$  if  $\phi_2 = i\sigma_2\phi_1^c$ .

Suppose there were just one Higgs doublet, with  $v \simeq 246$  GeV. Then

$$g_Y^t = \frac{246 \text{ GeV}}{\sqrt{2}m_t} = \frac{174 \text{ GeV}}{175 \pm 6 \text{ GeV}} \simeq 1! \quad (14)$$

The significance of this relation may be accidental, however. Quark masses “run” as a result of their interactions with gauge fields (particularly with gluons), and so their values depend on the scale at which the mass is probed. As one example, the top quark’s “pole” mass (what one would measure in a physical process of top quark production) and the value  $\bar{m}_t(\mu)$  in the modified-minimal-subtraction scheme at a mass scale  $\mu$  are related [35] by

$$\frac{m_t^{\text{pole}}}{\bar{m}_t(\mu)} = 1 + \frac{4}{3} \frac{\alpha_s(\mu)}{\pi} + \dots \quad (15)$$

For example, with a pole mass of 175 GeV, and  $\mu = M_W$  (which will frequently be appropriate for the loop calculations we shall perform), so that  $\alpha_s(M_W) \simeq 0.12$ , one has  $m_t^{\text{pole}}/\bar{m}_t(M_W) \simeq 1.05$ . Taking into account higher-order effects as well, we shall take  $\bar{m}_t(M_W) = 165 \pm 6 \text{ GeV}/c^2$  [36] in a number of subsequent calculations.

## 2. THE TOP QUARK IN MIXING PROCESSES

### A. Cabibbo-Kobayashi-Maskawa matrix parameters

The electroweak Lagrangian, before electroweak symmetry breaking, may be written in flavor-diagonal form as

$$\mathcal{L}_{\text{int}} = -\frac{g}{\sqrt{2}}[\bar{U}'_L\gamma^\mu W_\mu^{(+)}D'_L + \text{H.c.}] \quad (16)$$

Table 2: Parameters of KM matrices for  $n$  doublets of quarks.

	$n =$	2	3	4
Number of parameters	$(n - 1)^2$	1	4	9
Number of angles	$n(n - 1)/2$	1	3	6
Number of phases	$(n - 1)(n - 2)/2$	0	1	3

where  $U' \equiv (u', c', t')$  and  $D' \equiv (d', s', b')$  are column vectors describing *weak eigenstates*. Here  $g$  is the weak  $SU(2)_L$  coupling constant, and  $\psi_L \equiv (1 - \gamma_5)\psi/2$  is the left-handed projection of the fermion field  $\psi = U$  or  $D$ .

Quark mixings arise because mass terms in the Lagrangian are permitted to connect weak eigenstates with one another. Thus, the matrices  $\mathcal{M}_{U, D}$  in

$$\mathcal{L}_m = -[\overline{U}'_R \mathcal{M}_U U'_L + \overline{D}'_R \mathcal{M}_D D'_L + \text{H.c.}] \quad (17)$$

may contain off-diagonal terms. One may diagonalize these matrices by separate unitary transformations on left-handed and right-handed quark fields:

$$R_Q^+ \mathcal{M}_Q L_Q = L_Q^+ \mathcal{M}_Q^+ R_Q = \Lambda_Q \quad . \quad (18)$$

where

$$Q'_L = L_Q Q_L; \quad Q'_R = R_Q Q_R \quad (Q = U, D) \quad . \quad (19)$$

Using the relation between weak eigenstates and mass eigenstates:  $U'_L = L_U U_L$ ,  $D'_L = L_D D_L$ , we find

$$\mathcal{L}_{\text{int}} = -\frac{g}{\sqrt{2}}[\overline{U}_L \gamma^\mu W_\mu V D_L + \text{H.c.}] \quad , \quad (20)$$

where  $U \equiv (u, c, t)$  and  $D \equiv (d, s, b)$  are the mass eigenstates, and  $V \equiv L_U^\dagger L_D$ . The matrix  $V$  is just the Cabibbo-Kobayashi-Maskawa matrix. By construction, it is unitary:  $V^\dagger V = V V^\dagger = 1$ . It carries no information about  $R_U$  or  $R_D$ . More information would be forthcoming from interactions sensitive to right-handed quarks or from a genuine theory of quark masses. Because of the unitarity of the matrix, the neutral currents to which the  $Z^0$  couples are flavor-diagonal:  $\overline{Q}' \Gamma Q' = \overline{Q} \Gamma Q$ , where  $\Gamma$  is any combination of  $\gamma^\mu$  and  $\gamma^\mu \gamma_5$ .

For  $n$   $u$ -type quarks and  $n$   $d$ -type quarks,  $V$  is  $n \times n$  and unitary. An arbitrary  $n \times n$  matrix has  $2n^2$  real parameters, but unitarity ( $V^\dagger V = 1$ ) provides  $n^2$  constraints, so only  $n^2$  real parameters remain. We may remove  $2n - 1$  of these by appropriate redefinitions of relative quark phases. The number of remaining parameters is then  $n^2 - (2n - 1) = (n - 1)^2$ . Of these,  $n(n - 1)/2$  (the number of independent rotations in  $n$  dimensions) correspond to angles, while the rest,  $(n - 1)(n - 2)/2$ , correspond to phases. We summarize these results in Table 2.

For  $n = 2$ , we have one angle and no phases. The matrix  $V$  then can always be chosen as orthogonal [3, 8, 10]. For  $n = 3$ , we have three angles and one phase, which in general cannot be eliminated by arbitrary choices of phases in the quark fields. It was this phase that motivated Kobayashi and Maskawa [4] to introduce a third quark doublet. It provides a potential source of CP violation, serving as the leading contender for the observed CP-violating effects in the kaon system and suggesting substantial CP asymmetries in the decays of mesons containing  $b$  quarks.

The CKM matrix  $V$  is then, explicitly,

$$V = \begin{pmatrix} V_{ud} & V_{us} & V_{ub} \\ V_{cd} & V_{cs} & V_{cb} \\ V_{td} & V_{ts} & V_{tb} \end{pmatrix} . \quad (21)$$

We now parametrize its elements.

It is convenient to choose quark phases [37] so that the  $n$  diagonal elements and the  $n - 1$  elements just above the diagonal are real and positive. The parametrization we shall employ is one suggested by Wolfenstein [38].

The diagonal elements of  $V$  are nearly 1, while the dominant off-diagonal elements are  $V_{us} \simeq -V_{cd} \equiv \lambda \simeq 0.22$ . Thus to order  $\lambda^2$ , the upper  $2 \times 2$  submatrix of  $V$  is already known from the four-quark pattern. One may identify  $\lambda = \sin \theta_c$ , where  $\theta_c$  is the Gell-Mann - Lévy - Cabibbo angle mentioned earlier. It is the single parameter needed to describe the mixing in the four-quark ( $n = 2$ ) system. More precisely, analyses of strange particle decays [39] have yielded  $\sin \theta_c = 0.2205 \pm 0.0018$ .

The matrix element  $|V_{ud}|^2$  may be obtained by comparing the strengths of certain beta-decay transitions involving vector transitions with that of muon decay. One can also measure the neutron decay rate (which involves both vector and axial vector transitions), and extract the vector coupling strength by finding  $g_A$  from decay asymmetries. This vector coupling strength may be compared with that obtained in muon decay to learn  $|V_{ud}|^2$ . Finally, one can study the decay  $\pi^+ \rightarrow \pi^0 e^+ \nu_e$ . Overall, one finds [5]  $|V_{ud}| \simeq 0.975 \pm 0.001$ , so that  $|V_{ud}|^2 + |V_{us}|^2 = 0.999 \pm 0.002$ . One cannot deduce the need for the additional contribution of  $|V_{ub}|^2$  in the relation  $|V_{ud}|^2 + |V_{us}|^2 + |V_{ub}|^2 = 1$  required by the unitarity of the CKM matrix. Measurements of  $|V_{cd}|$  and  $|V_{cs}|$  (see Ref. [5]) are also consistent with the predictions of unitarity, but with larger errors.

The long  $b$  quark lifetime (about 1.5 to 1.6 ps [40]) and the predominance of charmed quarks among  $b$  decay products implies that  $V_{cb} \simeq 0.04$ , allowing one to express it as  $A\lambda^2$ , where  $A = \mathcal{O}(1)$ . A recent compilation of results [36, 41] on semileptonic  $b \rightarrow c$  decays yields  $V_{cb} = A\lambda^2 = 0.0393 \pm 0.0028$ , or  $A = 0.808 \pm 0.058$ . [M. Neubert [34] quotes  $V_{cb} = 0.0388 \pm 0.0020_{\text{exp}} \pm 0.0012_{\text{th}}$ .] Unitarity then requires  $V_{ts} \simeq -A\lambda^2$  as long as  $V_{td}$  and  $V_{ub}$  are small enough (which they are).

The magnitude of the element  $V_{ub}$  is learned by comparing charmless  $b$  decays to those with charm. One thus finds that  $|V_{ub}|$  appears to be of order  $A\lambda^3$ . Here one must allow for a phase, so one must introduce two new parameters  $\rho$  and  $\eta$ :  $V_{ub} = A\lambda^3(\rho - i\eta)$ . The measured ratio [36]  $|V_{ub}/V_{cb}| = 0.08 \pm 0.016$ , whose main error is dominated by theoretical extrapolation from a small part of the lepton spectrum in semileptonic  $b \rightarrow u$  decays, implies

$$(\rho^2 + \eta^2)^{1/2} = 0.363 \pm 0.073 \quad . \quad (22)$$

This constraint can be plotted in the  $(\rho, \eta)$  plane as a band bounded by circles centered at  $(0,0)$ .

Finally, unitarity specifies uniquely the form  $V_{td} = A\lambda^3(1 - \rho - i\eta)$ . To summarize, the CKM matrix may be written in terms of the 4 parameters  $\lambda$ ,  $A$ ,  $\rho$ , and  $\eta$  as

$$V \approx \begin{bmatrix} 1 - \lambda^2/2 & \lambda & A\lambda^3(\rho - i\eta) \\ -\lambda & 1 - \lambda^2/2 & A\lambda^2 \\ A\lambda^3(1 - \rho - i\eta) & -A\lambda^2 & 1 \end{bmatrix} . \quad (23)$$

The form (23) is only correct to order  $\lambda^3$  in the matrix elements. For certain purposes it may be necessary to exhibit corrections of higher order to the elements. This can be done using the unitarity of the matrix.

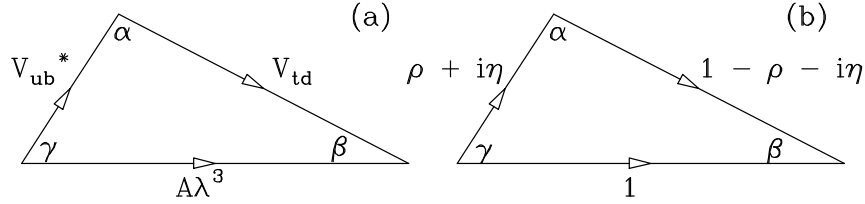


Figure 7: Unitarity triangle for CKM elements. (a) The relation (24) in the complex plane; (b) Eq. (24) divided by the normalizing factor  $A\lambda^3$ .

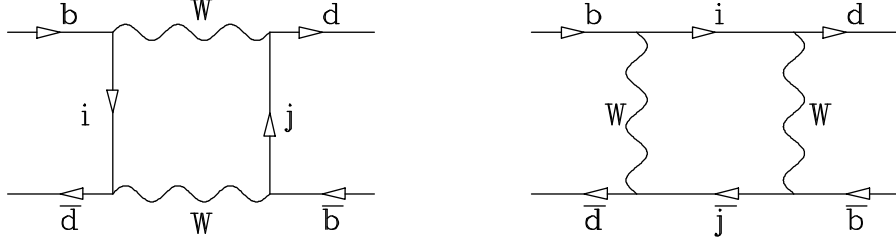


Figure 8: Box diagrams for mixing of  $B^0$  and  $\bar{B}^0$ .

The unitarity of the CKM matrix implies that the scalar product of one row (or column) with the complex conjugate of any other row (or column) must vanish: for example,

$$V_{ud}^*V_{td} + V_{us}^*V_{ts} + V_{ub}^*V_{tb} = 0 \quad . \quad (24)$$

Since  $V_{ud}^* \approx 1$ ,  $V_{us}^* \approx \lambda$ ,  $V_{ts} \approx -A\lambda^2$ , and  $V_{tb} \approx 1$  we have  $V_{td} + V_{ub}^* = A\lambda^3$ , a useful relation expressing the least-known CKM elements in terms of relatively well-known parameters. This result can be visualized as a triangle [42] in the complex plane [Fig. 7(a)]. In this figure the angles  $\alpha, \beta$ , and  $\gamma$  are defined as in the review by Nir and Quinn [43].

Dividing (24) by  $A\lambda^3$ , since  $V_{ub}^*/A\lambda^3 = \rho + i\eta$ ,  $V_{td}/A\lambda^3 = 1 - \rho - i\eta$ , one obtains a triangle of the form shown in Fig. 7(b). The value of  $V_{ub}^*/A\lambda^3$  may then be depicted as a point in the  $(\rho, \eta)$  plane. The major ambiguity which still remains in the determination of the CKM matrix elements concerns the shape of the unitarity triangle. The answer depends on the magnitude of  $V_{td}$ . As we shall see, decays alone will not provide the answer. In order to learn about the elements  $V_{td}$  and  $V_{ts}$  one must resort to indirect means, which involve loop diagrams.

## B. Mixing of neutral $B$ mesons

The box diagrams of Fig. 8 dominate the mixing between  $B^0$  and  $\bar{B}^0$ , leading to a splitting  $\Delta m$  between the mass eigenstates. (We present an abbreviated account of mixing; for more details see [5, 44, 45, 46].) The leading contributions in each of these diagrams cancel one another when one sums over all the intermediate quarks of charge  $2/3$ , since  $V_{ub}V_{ud}^* + V_{cb}V_{cd}^* + V_{tb}V_{td}^* = 0$ . The remaining contributions are dominated by the top quark since the corresponding CKM products of pairs of CKM elements  $V_{ib}V_{id}^*$  are each of order  $\lambda^3$  and  $m_t \gg m_c, m_u$ . One then finds [46]

$$\Delta m = \frac{G_F^2}{6\pi^2} |V_{td}|^2 M_W^2 m_B f_B^2 B_B \eta_B S \left( \frac{m_t^2}{M_W^2} \right) \quad , \quad (25)$$

where

$$S(x) \equiv \frac{x}{4} \left[ 1 + \frac{3 - 9x}{(x - 1)^2} + \frac{6x^2 \ln x}{(x - 1)^3} \right] . \quad (26)$$

This factor behaves as  $x$  for small  $x$  and  $x/4$  for large  $x$  and equals  $3/4$  for  $x = 1$ .

We take  $m_t = 175 \pm 6 \text{ GeV}/c^2$  as noted in Sec. 1 C,  $M_W = 80.34 \pm 0.10 \text{ GeV}/c^2$  (see Sec. 3),  $m_B = 5.279 \text{ GeV}/c^2$  (see [47]), and  $f_B \sqrt{B_B} = 200 \pm 40 \text{ MeV}$  [34, 36]. Here  $f_B$  is the  $B$  meson decay constant, defined in such a way that the matrix element of the weak axial-vector current  $A_\mu \equiv \bar{b} \gamma_\mu \gamma_5 d$  between a  $B^0$  meson and the vacuum is  $\langle 0 | A_\mu | B^0(p) \rangle = i p_\mu f_B$ . With this normalization, the decay constants of the light pseudoscalar mesons are  $f_\pi = 131 \text{ MeV}$  and  $f_K = 160 \text{ MeV}$ . The meson decay constants express the amplitude for the corresponding quark and antiquark (e.g.,  $b$  and  $\bar{d}$ ) to be found at a point, as they must in order to participate in the short-distance processes expressed by Figs. 8.

The factor  $B_B$  expresses the degree to which the diagrams of Fig. 8 actually provide the contribution to  $B - \bar{B}$  mixing. It is sometimes known as the “vacuum saturation parameter” or, more obscurely, as the “bag parameter” since an early estimate of the corresponding quantity for kaons was performed in a “bag” model of quarks confined in hadrons. It has been estimated in lattice gauge theories [48] to be  $1.16 \pm 0.08$ . Finally,  $\eta_B = 0.55$  is a QCD correction. All quantities are quoted in the same consistent renormalization scheme [49] and often appear in the literature with hats.

The first hints of  $B - \bar{B}$  mixing were obtained by the UA1 Collaboration in 1986 [50]. In proton-antiproton collisions, an excess was observed of like-sign muons above background, which could be interpreted as the effects of  $B - \bar{B}$  pair production, followed by oscillation of one of the (probably strange)  $B$ 's to its antiparticle and semileptonic decay of both  $B$ 's. (As we shall see, the mixing amplitude for strange  $B$ 's is expected to be much larger than that for nonstrange ones.)

The first evidence for mixing of nonstrange  $B$ 's was obtained by the ARGUS Collaboration in 1987 [51]. The reaction  $e^+ e^- \rightarrow B^0 \bar{B}^0$  was studied at threshold; the observation of like-sign lepton pairs from the semileptonic decays of  $b$  quarks (e.g.,  $b \rightarrow c \ell^- \nu_\ell$ , where  $\ell = e$  or  $\mu$ ) indicated that one of the neutral  $B$  mesons had oscillated to its antiparticle. The large mixing amplitude,  $\Delta m / \Gamma \simeq 0.7$  (where  $\Delta m$  is the mass difference between mass eigenstates and  $\Gamma$  is the  $B$  meson decay rate), was one early indication of a very heavy top quark.

With the rapidly moving  $B$  mesons and the fine vertex information now available at LEP [52], CDF [53], and SLD [54] (see also the review by [40]), it has become possible to directly observe time-dependent  $B^0 - \bar{B}^0$  oscillations with a modulating factor  $\sin(\Delta m t)$  (where  $t$  is the proper decay time). The current world average [55] is  $\Delta m_d = 0.470 \pm 0.017 \text{ ps}^{-1}$ , where the subscript refers to the mixing between  $B^0 \equiv \bar{b}d$  and  $\bar{B}^0 \equiv b\bar{d}$ . Using the expression (25) and the parameters mentioned above, we can then obtain an estimate of  $|V_{td}|$ , which leads, once we factor out a term  $A\lambda^3$ , to the constraint

$$|1 - \rho - i\eta| = 1.01 \pm 0.22 . \quad (27)$$

This result can be plotted in the  $(\rho, \eta)$  plane as a band bounded by circles with centers at  $(1, 0)$ .

Now that the top quark mass is known so precisely, the dominant source of error in Eq. (27) is uncertainty in the  $B$  meson decay constant  $f_B$ . Pseudoscalar meson decay constants, through the axial-current matrix element mentioned earlier, govern purely leptonic processes such as  $\pi \rightarrow \mu\nu$ ,  $K \rightarrow \mu\nu$ , and the recently observed  $D_s \rightarrow \mu\nu$  and  $D_s \rightarrow \tau\nu$ . (The  $D_s = c\bar{s}$  is the lowest-lying charmed-strange meson; see Fig. 5.) Information on heavy meson decay constants can be improved in several ways [5].

Direct measurements of  $D_s$  leptonic decays have been reported by the WA75, CLEO, BES, and E653 Collaborations [56], and one can also estimate  $D_s$  by assuming factorization in certain  $B$  decays in which the charged weak current produces a  $D_s$  [57]. A recent compilation of experimental values [58] yields  $f_{D_s} = (241 \pm 21 \pm 30)$  MeV.

Estimates based on flavor SU(3), whereby one relates  $f_{D_s}$  to the corresponding decay constant  $f_D$  of the nonstrange charmed meson, yield ratios  $f_D/f_{D_s}$  in the range 0.8 – 0.9. Thus, one expects a value of  $f_D$  not far below the current experimental upper bound [59]  $f_D < 290$  MeV (90% c.l.). This limit was placed by studying the reaction  $e^+e^- \rightarrow D^+D^-$  just above threshold at the SPEAR storage ring, and looking for the distinctive decay  $D \rightarrow \mu\nu$  opposite an identified  $D$ . The Beijing Electron-Positron Collider collaboration [60] has identified one  $D \rightarrow \mu\nu$  event, leading to  $f_D = 300_{-150-80}^{+180+80}$  MeV.

Direct measurements of  $f_B$  are possible once  $|V_{ub}|$  is fairly well known, since the partial width  $\Gamma(B \rightarrow \ell\nu)$  is proportional to  $(f_B|V_{ub}|)^2$ . The expected branching ratios are about  $(1/2) \times 10^{-4}$  for  $\tau\nu$  and  $2 \times 10^{-7}$  for  $\mu\nu$  [5]. Theoretical estimates of  $f_B$  take many forms, including quark models [61] and lattice gauge theory calculations [62], leading to a rough range  $f_B = 180 \pm 40$  MeV.

The same SU(3) estimates [61, 62] for the ratio of  $f_D/f_{D_s}$  also give a very similar ratio of  $f_B/f_{B_s}$ . It has been shown that the equality of these two ratios is to be expected within a few percent [63].

### C. CP-violating $K^0 - \bar{K}^0$ mixing

The top quark (and its charge  $-1/3$  partner, the bottom) were invented [4] to explain CP violation in the neutral kaon system. More than thirty years after its discovery [64], this remarkable phenomenon has only a candidate theory to explain it, with confirmation of the explanation still to come. (For a compendium of literature on CP violation, see [65].)

The  $K^0$  and  $\bar{K}^0$  are strong-interaction eigenstates of opposite strangeness, but the weak interactions do not conserve strangeness. Hence the weak interactions may, and do, pick out linear combinations of  $K^0$  and  $\bar{K}^0$  in decay processes [66]. As of 1957, when the weak interactions were understood to violate charge-conjugation invariance C and spatial reflection P but to preserve their product CP, one expected [67] the linear combination  $K_1^0 \equiv (K^0 + \bar{K}^0)/\sqrt{2}$ , with even CP, to have a much more rapid decay rate since it could decay to the CP-even final state of two pions. The orthogonal linear combination  $K_2^0 \equiv (K^0 - \bar{K}^0)/\sqrt{2}$ , with odd CP, would live much longer since it was forbidden by CP invariance to decay to two pions and would have to decay to three pions or a pion and a lepton-neutrino pair. In fact, a long-lived neutral kaon does exist [68], with a lifetime about 600 times that of the short-lived variety.

In 1964 J. Christenson, J. Cronin, V. Fitch, and R. Turlay reported that in fact the long-lived neutral kaon *did* decay to two pions, with an amplitude whose magnitude is about  $2 \times 10^{-3}$  that for the short-lived  $K \rightarrow 2\pi$  decay. To reach this conclusion they constructed a beam of neutral long-lived kaons and observed their decays in a spark chamber [64].

One then can parametrize the mass eigenstates as

$$K_S \text{ ("short")} \simeq K_1 + \epsilon K_2, \quad K_L \text{ ("long")} \simeq K_2 + \epsilon K_1, \quad (28)$$

where  $|\epsilon| \simeq 2 \times 10^{-3}$  and the phase of  $\epsilon$  turns out to be about  $\pi/4$ . The parameter  $\epsilon$  encodes all that is currently known about CP violation in the neutral kaon system. But where does it come from?

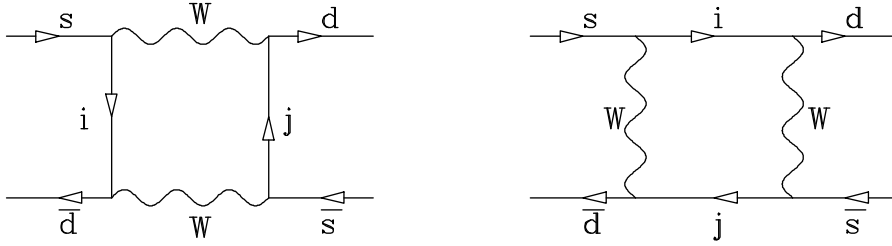


Figure 9: Box diagrams for mixing of a neutral kaon and its antiparticle.

One possibility, proposed [69] immediately after the discovery and still not excluded, is a “superweak” CP-violating interaction which directly mixes  $K^0 = d\bar{s}$  and  $\bar{K}^0 = s\bar{d}$ . This interaction would have no other observable consequences since the  $K^0 - \bar{K}^0$  system is so sensitive to it!

The presence of three quark families [4] poses another opportunity for explaining CP violation through the mixing diagram shown in Fig. 9. With three quark families, phases in complex coupling coefficients cannot be removed by redefinition of quark phases. Within some approximations [5], the parameter  $\epsilon$  is directly proportional to the imaginary part of the mixing amplitude described in Fig. 9. Its magnitude (see [44] or [45] for a calculation in the limit of  $m_t \ll M_W$ ) is [46]

$$|\epsilon| \simeq \frac{G_F^2 m_K f_K^2 B_K M_W^2}{\sqrt{2}(12\pi^2)\Delta m_K} [\eta_1 S(x_c) I_{cc} + \eta_2 S(x_t) I_{tt} + 2\eta_3 S(x_c, x_t) I_{ct}] \quad , \quad (29)$$

where  $I_{ij} \equiv \text{Im}(V_{id}^* V_{is} V_{jd}^* V_{js})$ . In order to evaluate these expressions we need to work to sufficiently high order in small parameters in  $V$ . The application of the unitarity relation to the first and second rows tells us, in fact, that a more precise expression for  $V_{cd}$  is  $V_{cd} = -\lambda - A^2 \lambda^5 (\rho + i\eta)$ . We then find  $I_{cc} = -2A^2 \lambda^6 \eta$ ,  $I_{ct} = A^2 \lambda^6 \eta$ , and  $I_{tt} = 2A^2 \lambda^6 \eta [A^2 \lambda^4 (1 - \rho)]$ . The factors  $\eta_1 = 1.38$ ,  $\eta_2 = 0.57$ ,  $\eta_3 = 0.47$  are QCD corrections [70], while  $x_i \equiv m_i^2 / M_W^2$ . The function  $S(x)$  was defined in Eq. (26), while

$$S(x, y) \equiv xy \left\{ \left[ \frac{1}{4} + \frac{3}{2(1-y)} - \frac{3}{4(1-y)^2} \right] \frac{\ln y}{y-x} + (y \leftrightarrow x) - \frac{3}{4(1-x)(1-y)} \right\} \quad . \quad (30)$$

Eq. (29) may then be rewritten (updating [71]) as

$$|\epsilon| = 4.39 A^2 B_K \eta [\eta_3 S(x_c, x_t) - \eta_1 S(x_c) + \eta_2 A^2 \lambda^4 (1 - \rho) S(x_t)] \quad . \quad (31)$$

Using the experimental values [47]  $|\epsilon| = (2.28 \pm 0.02) \times 10^{-3}$ ,  $f_K = 160$  MeV,  $\Delta m_K = 3.49 \times 10^{-15}$  GeV, and  $m_K = 0.4977$  GeV, the value  $B_K = 0.75 \pm 0.15$  [72], and the top quark mass  $\bar{m}_t(M_W) = 165 \pm 6$  GeV/ $c^2$ , we find that CP-violating  $K - \bar{K}$  mixing leads to the constraint

$$\eta(1 - \rho + 0.44) = 0.51 \pm 0.18 \quad , \quad (32)$$

where the term  $1 - \rho$  in parentheses corresponds to the loop diagram with two top quarks, and the term 0.44 corresponds to the additional contribution of charmed quarks. The major source of error on the right-hand side is the uncertainty in the parameter  $A \equiv V_{cb}/\lambda^2$ . Eq. (32) can be plotted in the  $(\rho, \eta)$  plane as a band bounded by hyperbolae with foci at  $(1.44, 0)$ .

#### D. Summary of parameter space

The constraints (22), (27), and (32) define the allowed region of parameters shown in Fig. 10. The boundaries shown are  $1\sigma$  errors, but are dominated by theoretical uncertainties in each case.

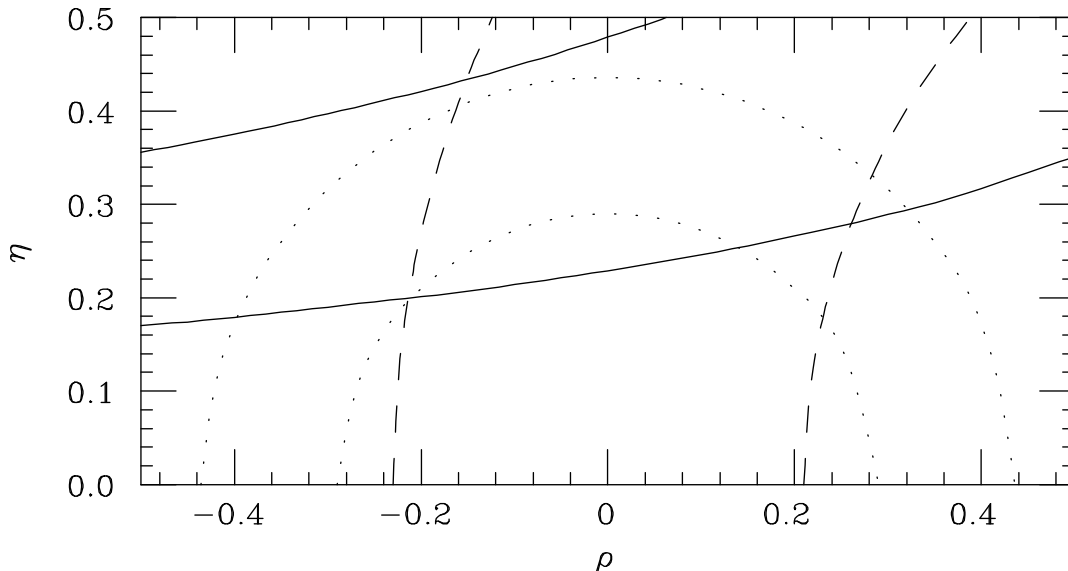


Figure 10: Region in the  $(\rho, \eta)$  plane allowed by constraints on  $|V_{ub}/V_{cb}|$  (dotted semi-circles),  $B^0 - \bar{B}^0$  mixing (dashed semicircles), and CP-violating  $K - \bar{K}$  mixing (solid hyperbolae).

A large region centered about  $\rho \simeq 0$ ,  $\eta \simeq 0.35$  is permitted. Nonetheless, it could be that the CP violation seen in kaons is due to an entirely different source, perhaps a superweak mixing of  $K^0$  and  $\bar{K}^0$  [69]. In that case one could probably still accommodate  $\eta = 0$ , and hence a real CKM matrix, by going slightly outside the  $1\sigma$  bounds based on  $|V_{ub}/V_{cb}|$  or  $B - \bar{B}$  mixing. In order to confirm the predicted nonzero value of  $\eta$ , we turn to other experimental possibilities.

### E. CP violation in $B$ meson decays

We have already mentioned the information provided by  $B^0 - \bar{B}^0$  mixing. The large value of  $\Delta m/\Gamma \simeq 0.7$  was an early hint, through graphs of the form of Fig. 8, that the top quark was very heavy. This large value also has another very important benefit: It makes possible a class of incisive studies of CP violation in neutral  $B$  meson decays [73].

By comparing rates decays for a state which is produced as  $B^0$  and one which is produced as a  $\bar{B}^0$  to final states which are eigenstates of CP, one can directly measure angles in the unitarity triangle of Fig. 7. Because of the interference between direct decays (e.g.,  $B^0 \rightarrow J/\psi K_S$ ) and those which proceed via mixing (e.g.,  $B^0 \rightarrow \bar{B}^0 \rightarrow J/\psi K_S$ ), these processes are described by time-dependent functions whose difference when integrated over all time is responsible for the rate asymmetry. Thus, if we define

$$C_f \equiv \frac{\Gamma(B_{t=0} \rightarrow f) - \Gamma(\bar{B}_{t=0} \rightarrow f)}{\Gamma(B_{t=0} \rightarrow f) + \Gamma(\bar{B}_{t=0} \rightarrow f)} \quad , \quad (33)$$

we have, in the limit of a single direct contribution to decay amplitudes,

$$A(J/\psi K_S, \pi^+ \pi^-) = -\frac{x_d}{1+x_d^2} \sin(2\beta, 2\alpha) \quad , \quad (34)$$

where  $x_d \equiv \Delta m(B^0)/\Gamma(B^0)$ . This limit is expected to be very good for  $J/\psi K_S$ , but some correction for penguin contributions (see Sec. 2 G) is probably needed for  $\pi^+ \pi^-$ . The value  $x_d \simeq 0.7$  is nearly optimum to maximize the coefficient of  $\sin(2\beta, 2\alpha)$ .



To see this behavior in more detail [74], we note that the time-dependent partial rates for a state which is initially  $B^0$  ( $\bar{B}^0$ ) to decay to a final state  $f$  may be written as

$$d\Gamma[B^0(\bar{B}^0) \rightarrow f]/dt \sim e^{-\Gamma t}[1 \mp \text{Im}\lambda_0 \sin(\Delta mt)] \quad , \quad (35)$$

where in order to obtain this simple result we neglect  $\Delta\Gamma/\Gamma$  in comparison with  $\Delta m/\Gamma$ . This step is justified for  $B$ 's, in contrast to the situation for  $K$ 's. The final states to which both  $B$  and  $\bar{B}$  can decay are only a small fraction of those to which  $B$  or  $\bar{B}$  normally decay, and so one should expect quite similar lifetimes for the two mass eigenstates. Integration of (35) gives

$$C_f = \frac{-x_d}{1+x_d^2} \text{Im}\lambda_0(f) \quad (36)$$

for the total asymmetry. For the CP-eigenstate final states mentioned,  $\lambda_0(J/\psi K_S) = -e^{-2i\beta}$  and  $\lambda_0(\pi^+\pi^-) = e^{2i\alpha}$ . The extra minus sign in the first relation is due to the odd CP of the  $J/\psi K_S$  final state.

The asymmetry (36) is suppressed both when  $\Delta m/\Gamma$  is very small and when it is very large (e.g., as is expected for  $B_s$ ). For  $B_s$ , in order to see an asymmetry, one must not integrate with respect to time. Experiments planned with detection of  $B_s$  as their focus will require precise vertex detection to measure mixing as a function of proper time. For  $B^0$ , on the other hand, the value of  $x/(1+x^2)$  for  $x = 0.7$  is 0.47, very close to its maximum possible value of 1/2 for  $x = 1$ .

When more than one eigenchannel contributes to a decay, there can appear terms of the form  $\cos(\Delta mt)$  as well as  $\sin(\Delta mt)$  in results analogous to Eqs. (35) [75]. These complicate the analysis somewhat, but information can be obtained from them [76] on the relative contributions of various channels to decays.

## F. Lifetime and mass differences for strange $B$ 's

The mixing between strange  $B$ 's due to diagrams like those in Fig. 8 is considerably enhanced relative to that between nonstrange  $B$ 's:

$$\frac{\Delta m_s}{\Delta m_d} = \frac{f_{B_s}^2 B_{B_s}}{f_B^2 B_B} \left| \frac{V_{ts}}{V_{td}} \right|^2 \simeq 17 - 52 \quad , \quad (37)$$

where we have taken the expected ranges of decay constant and CKM element ratios, and  $\Delta m_s$  refers to mixing between the  $B_s \equiv \bar{b}s$  and  $\bar{B}_s \equiv b\bar{s}$ . Alternatively, we may retrace the steps of Sec. 2 B, replacing appropriate quantities in Eq. (25), to derive an analogous expression for  $\Delta m_s$ , which we then evaluate directly. For  $V_{ts} = 0.040 \pm 0.004$ ,  $m_{B_s} = 5.37 \text{ GeV}/c^2$ ,  $f_{B_s} \sqrt{B_{B_s}} = 225 \text{ MeV}$ ,  $\eta_{B_s} = 0.6 \pm 0.1$ , and [40]  $\tau_{B_s} \equiv 1/\Gamma_s = 1.55 \pm 0.10 \text{ ps}$ , we find  $\Delta m_s/\Gamma_s = 22 \pm 6$ , with an additional 40% error associated with  $f_{B_s}^2 B_{B_s}$ . This result implies many particle-antiparticle oscillations in a decay lifetime, requiring good vertex resolution and highly time-dilated  $B_s$ 's for a measurement. The present experimental bound  $\Delta m_s > 9.2 \text{ ps}^{-1}$  based on combining ALEPH and DELPHI results [77] begins to restrict the parameter space in an interesting manner.

The large value of  $\Delta m_s$  entails a value of  $\Delta\Gamma_s$  between mass eigenstates of strange  $B$ 's which may be detectable. After all, the short-lived and long-lived neutral kaons differ in lifetime by a factor of 600. Strong interactions and the presence of key channels (e.g.,  $\pi\pi$ ) are a crucial effect in strange particle (e.g.,  $K^0$  and  $\bar{K}^0$ ) decays. While the  $b$  quark decays as if it is almost free, so that strong interactions here are much less important, it turns out that a corresponding difference in lifetimes for strange  $B$ 's of the order of 20% is not unlikely [78].

In the ratio  $\Delta m_s/\Delta\Gamma_s$ , uncertainties associated with the meson decay constants cancel out, and in lowest order (before QCD corrections are applied) one finds [79, 80]  $\Delta m_s/\Delta\Gamma_s \simeq \mathcal{O}(-[1/\pi][m_t^2/m_b^2]) \simeq -200$ . The sign indicates that the heavier state is expected to be the longer-lived one, as in the neutral kaon system. The top quark does not contribute to the width difference associated with the imaginary part of the graphs in Fig. 8, since no  $t\bar{t}$  pairs are produced in  $B_s$  decays.

Aside from small CP-violating effects, the mass eigenstates of strange  $B$ 's correspond to those  $B_s^{(\pm)}$  of even and odd CP. The decay of a  $\bar{B}_s$  meson via the quark subprocess  $b(\bar{s}) \rightarrow c\bar{c}s(\bar{s})$  gives rise to predominantly CP-even final states [81], so the CP-even eigenstate should have a greater decay rate. One calculation [78] gives

$$\frac{\Gamma(B_s^{(+)}) - \Gamma(B_s^{(-)})}{\bar{\Gamma}} \simeq 0.18 \frac{f_{B_s}^2}{(200 \text{ MeV})^2} \quad , \quad (38)$$

while a more recent estimate [82] is  $0.16_{-0.09}^{+0.11}$ . The lifetime difference between CP-even and CP-odd strange  $B$ 's thus can provide useful information on  $f_{B_s}$ , and hence indirectly on the weak interactions at short distances. One way to learn this lifetime difference [83] is to study angular distributions in  $B_s \rightarrow J/\psi + \phi \rightarrow e^+e^-K^+K^-$  (or  $\mu^+\mu^-K^+K^-$ ). The  $J/\psi$  and  $\phi$  are both spin-1 particles and hence can be produced in states of orbital angular momenta  $L = 0, 1$ , and 2 from the spinless  $B_s$  decay.  $L = 1$  corresponds to  $P = CP = -$ , while  $L = 0$  or 2 corresponds to  $P = CP = +$ . A simple transversity analysis [84] permits one to separate the two cases.

In the rest frame of the  $J/\psi$ , let the  $x$  axis be defined by the direction of the  $\phi$ , the  $x - y$  plane be defined by the kaons which are its decay products, and the  $z$  axis be the normal to that plane. Let the  $e^+$  (or  $\mu^+$ ) make an angle  $\theta$  with the  $z$  axis. Then the CP-even final states give rise to an angular distribution  $1 + \cos^2\theta$ , while the CP-odd state gives rise to  $\sin^2\theta$ . In case both CP eigenstates are present in  $B_s \rightarrow J/\psi\phi$ , one will see a gradual increase of the  $\sin^2\theta$  component relative to the  $1 + \cos^2\theta$  component. More likely (if predictions [81] are correct), the CP-even state will dominate, so that one will be measuring mainly the lifetime of this eigenstate when following the time-dependence of the decay. The average decay rate  $\bar{\Gamma} \equiv (\Gamma_+ + \Gamma_-)/2$  (the subscripts denote CP eigenvalues) is measured in flavor-tagged decays of  $B_s = \bar{b}s \rightarrow \bar{c} + \dots$  or  $\bar{B}_s = b\bar{s} \rightarrow c + \dots$

A recent analysis [85] of  $B \rightarrow J/\psi K^*$  has some bearing on the  $B_s \rightarrow J/\psi\phi$  partial-wave structure. The two processes are related by flavor SU(3), involving a substitution  $s \leftrightarrow d$  of the spectator quark. Thus, one expects the same partial waves in the two decays. The CLEO Collaboration has studied 146  $B \rightarrow J/\psi K^*$  decays in  $3.36 \times 10^6 B\bar{B}$  pairs produced at the Cornell Electron Storage Ring (CESR).

One can decompose the amplitude  $A$  for a spinless meson to decay to two vector mesons into three independent components [86], corresponding to linear polarization states of the vector mesons which are either longitudinal (0), or transverse to their directions of motion and parallel (||) or perpendicular ( $\perp$ ) to one another. The states 0 and || are P-even, while the state  $\perp$  is P-odd. Aside from the case of  $A_0$ , which is special for massive vector mesons, these arguments were advanced some time ago [87] to determine the parity of the neutral pion in its decays to two photons. Since  $J/\psi$  and  $\phi$  are both C-odd eigenstates, the properties under P are the same as those under CP.

A suitably normalized amplitude  $A_\perp$  thus can be expressed in terms of partial-wave amplitudes  $S$ ,  $P$ , and  $D$  as  $|A_\perp|^2 = |P|^2/(|S|^2 + |P|^2 + |D|^2)$ . In  $B_s \rightarrow J/\psi\phi$ ,  $|P|^2$  would correspond to a CP-odd final state and hence to the decay of the odd-CP eigenstate. The CLEO results [85] for the related process  $B \rightarrow J/\psi K^*$  are  $|A_\perp|^2 = 0.21 \pm 0.14$  from a fit to the transversity angle, and  $|A_\perp|^2 = 0.16 \pm 0.08 \pm 0.04$  from a fit to the

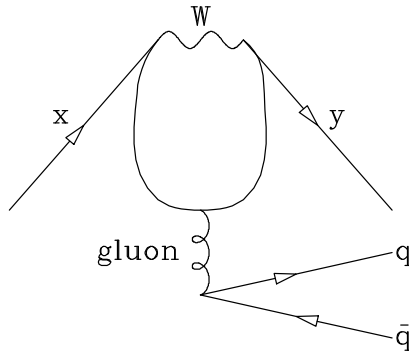


Figure 11: “Penguin” diagram describing transition of a quark  $x$  to another quark  $y$  with the same charge. The intermediate quarks have charge differing from  $Q(x) = Q(y)$  by one unit. Here  $q = (u, d, s)$ .

full angular distribution. This implies (via flavor SU(3)) that  $B_s \rightarrow J/\psi\phi$  is dominated by the CP-even final state, and thus the lifetime in this state measures approximately  $\tau(B_s^{(+)})$ . It will be interesting to see if any evidence for non-zero  $|P|^2$  can be gathered in  $B \rightarrow J/\psi K^*$ , in which case  $B_s \rightarrow J/\psi\phi$  should exhibit the time-variation in the transversity-angle distribution mentioned above [83].

### G. Processes dominated by penguin diagrams

Although the unitarity of the CKM matrix implies flavor conservation for charge-preserving electroweak interactions in lowest order, we have seen that loop diagrams can induce flavor-changing charge-preserving interactions in higher order. Another example of this phenomenon is provided by the “penguin” diagram [88] illustrated in Fig. 11. Although the penguin’s “leg” is a gluon in this illustration, it can also be a photon or  $Z$ . When the external quarks  $x$  and  $y$  have charge  $-1/3$ , the intermediate quarks have charge  $2/3$  and can include the top quark. Because of the top quark’s large mass, such penguin diagrams can be very important.

An example of a predicted penguin effect in  $s \rightarrow d$  transitions is a phase arising in the decays of neutral kaons to  $\pi\pi$ . This phase can lead to a “direct” contribution to the ratios for CP-violating and CP-conserving decays, in addition to that provided by the mixing parameter  $\epsilon$  measured earlier.

One may define

$$\eta_{+-} \equiv \frac{A(K_L \rightarrow \pi^+\pi^-)}{A(K_S \rightarrow \pi^+\pi^-)} ; \quad \eta_{00} \equiv \frac{A(K_L \rightarrow \pi^0\pi^0)}{A(K_S \rightarrow \pi^0\pi^0)} ; \quad (39)$$

the effect of “direct” decays then shows up in a parameter  $\epsilon'$  which causes  $\eta_{+-}$  and  $\eta_{00}$  to differ from one another:

$$\eta_{+-} = \epsilon + \epsilon' \quad ; \quad \eta_{00} = \epsilon - 2\epsilon' \quad . \quad (40)$$

Since  $\epsilon'$  and  $\epsilon$  are expected to have approximately the same phase (see, e.g., [5]), one expects

$$\begin{aligned} |\eta_{+-}| &\simeq |\epsilon|[1 + \text{Re}(\epsilon'/\epsilon)] \quad , \\ |\eta_{00}| &\simeq |\epsilon|[1 - 2\text{Re}(\epsilon'/\epsilon)] \quad , \end{aligned} \quad (41)$$

and hence

$$\left| \frac{\eta_{00}}{\eta_{+-}} \right|^2 = \frac{\Gamma(K_L \rightarrow 2\pi^0)}{\Gamma(K_S \rightarrow 2\pi^0)} / \frac{\Gamma(K_L \rightarrow \pi^+\pi^-)}{\Gamma(K_S \rightarrow \pi^+\pi^-)} = 1 - 6 \text{Re} \frac{\epsilon'}{\epsilon} \quad . \quad (42)$$

Present expectations [89] are that  $\epsilon'/\epsilon$  could be a few parts in  $10^4$  (but in any case  $\epsilon'/\epsilon \leq 10^{-3}$ ), requiring the ratio of ratios (42) to be measured to about one part in  $10^3$ . Experiments now in progress at Fermilab and CERN should have the required sensitivity. The previous results of these experiments are:

$$\text{E731 [90]} : \quad \text{Re}(\epsilon'/\epsilon) = (7.4 \pm 6.0) \times 10^{-4} \quad , \quad (43)$$

$$\text{NA31 [91]} : \quad \text{Re}(\epsilon'/\epsilon) = (23.0 \pm 6.5) \times 10^{-4} \quad , \quad (44)$$

leading to some question about whether a non-zero value has been observed. Because of the cancelling effects of gluonic and “electroweak” penguins (in which the curly line in Fig. 11 is a photon or  $Z$ ), the actual magnitude of  $\epsilon'/\epsilon$  is difficult to estimate, so that one’s best hope is for a non-zero value within the rather large theoretical range, thereby disproving the superweak model [69] of CP violation.

The contribution of the (gluonic) penguin diagram to the effective weak Hamiltonian may be written (for  $x, y$  equal to quarks of charge  $-1/3$ )

$$\begin{aligned} \mathcal{H}_W^{\text{penguin}} \simeq & \frac{G_F \alpha_s}{\sqrt{2} 6\pi} \left[ \xi_c \ln \frac{m_t^2}{m_u^2} + \xi_t \ln \frac{m_t^2}{m_u^2} \right] \\ & \left[ (\bar{y}_L \gamma^\mu \lambda^a x_L) (\bar{u} \gamma_\mu \lambda^a u + \bar{d} \gamma_\mu \lambda^a d + \dots) + \text{H.c.} \right] \quad , \quad (45) \end{aligned}$$

where  $\xi_i \equiv V_{ix} V_{iy}^*$ , and  $\lambda^a$  are color SU(3) matrices [ $a = (1, \dots, 8)$ ] normalized so that  $\text{Tr}(\lambda^a \lambda^b) = 2\delta^{ab}$ . The top quark is dominant in the flavor-changing processes  $b \rightarrow d$  and  $b \rightarrow s$  (with corrections due to charm which can be important in some cases [92]), while the charmed quark dominates the  $s \rightarrow d$  process. (The top quark plays a key role, however, in the electroweak penguin contribution to this process [89].) One may imitate the effect of an infrared cutoff for the gluonic penguin graph by using a constituent-quark mass  $m_u \sim 0.3 \text{ GeV}/c^2$ .

One can estimate the effect of Eq. (45) for the  $b \rightarrow sq\bar{q}$  penguin graph; one finds it is comparable to that of the  $b \rightarrow ud\bar{u}$  “tree” contribution  $(G_F/\sqrt{2})V_{ub}V_{ud}^*[\bar{u}\gamma_\mu(1 - \gamma_5)b][\bar{d}\gamma^\mu(1 - \gamma_5)u]$ . The penguin contribution to  $b \rightarrow dq\bar{q}$  and the  $b \rightarrow us\bar{u}$  tree contribution are both expected to be suppressed by approximately one power of the Wolfenstein parameter  $\lambda \sim 0.2$ , as one can see by comparing CKM elements. Thus,  $B^0 \rightarrow \pi^+\pi^-$  is expected to be dominated by the tree amplitude;  $B^0 \rightarrow K^+\pi^-$  is expected to be dominated by the penguin amplitude; and the rates of the two processes should be similar.

In Fig. 12 we show a contour plot of the significance of detection by the CLEO Collaboration [93] of the decays  $B^0 \rightarrow \pi^+\pi^-$  and  $B^0 \rightarrow K^+\pi^-$ . Evidence exists for a combination of  $B^0 \rightarrow K^+\pi^-$  and  $\pi^+\pi^-$  decays, generically known as  $B^0 \rightarrow h^+\pi^-$ . On the basis of  $2.4 \text{ fb}^{-1}$  of data, the most recent published result [94] is  $B(B^0 \rightarrow h^+\pi^-) = (1.8 \pm_{-0.5}^{+0.6} \pm_{-0.3}^{+0.2}) \times 10^{-5}$ . Although one still cannot conclude that either decay mode is nonzero at the  $3\sigma$  level, the most likely solution is roughly equal branching ratios (i.e., about  $10^{-5}$ ) for each mode. Only upper limits exist for other modes of two pseudoscalars [95], but these are consistent with predictions [96].

Penguin diagrams play a number of roles in  $B$  decays. We enumerate several of them; others are mentioned in [5].

1. The process  $B^+ \rightarrow K^0\pi^+$  is expected to be almost completely due to the penguin graph; one cannot write a corresponding tree graph for it. By comparison with the  $B^0 \rightarrow K^+\pi^-$  decay, where the penguin graph is expected to be the main contribution, one expects  $B(B^+ \rightarrow K^0\pi^+) \simeq 10^{-5}$ . The weak phase of the process (which changes sign under charge-conjugation) thus is expected to be  $\text{Arg}(V_{tb}^*V_{ts}) = \pi$ ,

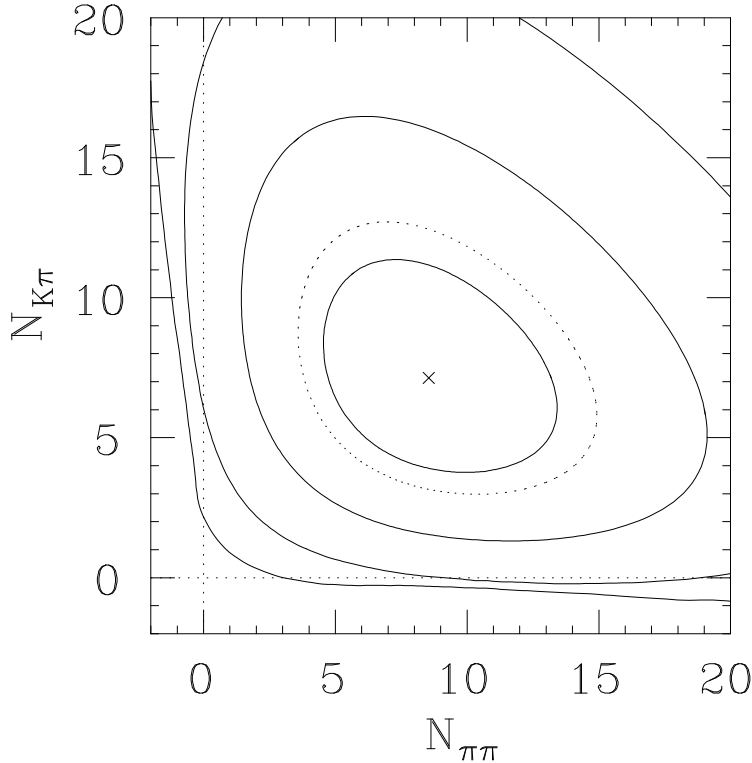


Figure 12: Contours of significance of detection of  $B^0 \rightarrow \pi^+\pi^-$  and  $B^0 \rightarrow K^+\pi^-$  by the CLEO Collaboration.

Table 3: Phases of amplitudes contributing to decays of  $B$  mesons to  $\pi\pi$  and  $K\pi$ . Here  $\Delta S$  refers to the change of strangeness in the process.

$ \Delta S $	“Tree”		“Penguin”	
	CKM elements	Phase	CKM elements	Phase
0	$V_{ub}^*V_{ud}$	$\gamma$	$V_{tb}^*V_{td}$	$-\beta$
1	$V_{ub}^*V_{us}$	$\gamma$	$V_{tb}^*V_{ts}$	$\pi$

so that the charge-conjugate process has the same weak phase. As a result, one turns out to be able to separate strong final-state interaction phases from weak phases and obtain estimates of quantities like the angle  $\gamma = \text{Arg}(V_{ub}^*)$  in Fig. 7 by comparing rates for  $B^+ \rightarrow (K^0\pi^+, K^+\pi^0, K^+\eta, K^+\eta')$  with the corresponding  $B^-$  rates [97]. One can also obtain this information by measuring the time-dependence in  $B^0(\bar{B}^0) \rightarrow \pi^+\pi^-$  and the rates for  $B^0 \rightarrow K^+\pi^-$ ,  $B^+ \rightarrow K^0\pi^+$ , and the charge-conjugate processes [98]. (The rates for  $B^+ \rightarrow K^0\pi^+$  and  $B^- \rightarrow \bar{K}^0\pi^-$  are expected to be equal because of the penguin dominance mentioned above.) The weak phases of the major amplitudes contributing to these decays are summarized in Table 3. The relative weak phase of tree and penguin amplitudes for strangeness-preserving decays is  $\gamma + \beta = \pi - \alpha$  (assuming the unitarity triangle to be valid), while the corresponding relative phase for strangeness-changing decays (aside from a sign) is just  $\gamma$ . As a result, one can measure both  $\alpha$  and  $\gamma$ .

2. A number of processes (in addition to the decay  $B^+ \rightarrow K^0\pi^+$  mentioned above) are dominated by penguin graphs. By comparing the rates for strangeness-preserving and strangeness-changing processes, one can measure the ratio  $|V_{td}/V_{ts}|$  [99]. Examples of useful ratios are  $B(B^+ \rightarrow \bar{K}^{*0}K^+)/B(B^+ \rightarrow \phi K^+)$  and  $B(B^+ \rightarrow \bar{K}^{*0}K^{*+})/B(B^+ \rightarrow \phi K^{*+})$ .

3. We mentioned in Sec. 2 E that the time-integrated rate asymmetry in  $B \rightarrow \pi^+\pi^-$  could provide information on the angle  $\alpha$  of the unitarity triangle. The most direct test is based on the assumption that the tree process  $\bar{b} \rightarrow \bar{u}u\bar{d}$  is the only direct contribution to this decay. However, “penguin pollution” [75] (due to the  $b \rightarrow d$  transition) makes the analysis less straightforward, even though the penguin amplitude is expected to be only about 0.2 of the tree amplitude. Ways to circumvent this difficulty include the detailed study of the isospin structure of the  $\pi\pi$  final state [76], and the use of flavor SU(3) to estimate penguin effects using  $B \rightarrow K\pi$ , where they are expected to be dominant [96, 98, 100].

## H. Rare kaon decays

We give a sample of processes influenced by loop diagrams in which the top quark plays a role. The present discussion is based on a recent discussion of  $K \rightarrow \pi\nu\bar{\nu}$  decays [101]. Details on other processes may be found in Refs. [5, 45, 70, 102, 103].

We are concerned with the subprocess  $s \rightarrow d\nu\bar{\nu}$ , which can proceed via loop diagrams involving exchange of a pair of  $W$ 's (a box diagram) or one  $W$  and one  $Z$  (an electroweak penguin). In each case results will be quoted for a sum over the three neutrino species.

1. The decay  $K^+ \rightarrow \pi^+\nu\bar{\nu}$  is predicted to have a branching ratio

$$B(K^+ \rightarrow \pi^+\nu\bar{\nu}) \simeq 10^{-11} A^4 |T(x_t)(1 - \rho - i\eta + [0.41 \pm 0.09])|^2 \quad , \quad (46)$$

where  $x_t \equiv m_t^2/M_W^2$ , and

$$T(x) \equiv \frac{x}{4} \left[ \left( \frac{3x-6}{(x-1)^2} \right) \ln x + \frac{x+2}{x-1} \right] \quad . \quad (47)$$

The term  $1 - \rho - i\eta$  in (46) is the contribution of the top quark, while the term in square brackets represents the contribution of charm, uncertain primarily because the charmed quark mass is not all that well known. Uncertainty in the Wolfenstein parameter  $A$  contributes a good deal to the error on the predicted branching ratio. The top quark's mass used to be a major source of error in this estimate, but is no longer. For the present value of  $m_t$ ,  $T(x_t) \simeq 3$ .

An experimentally measured branching ratio will define a band in the  $(\rho, \eta)$  plane whose boundaries are circles with centers at  $(1.41 \pm 0.09, 0)$ . Given the region of parameters already allowed in Fig. 10, such a measurement essentially specifies  $\rho$ . The predicted branching ratio is  $10^{-10}$ , give or take a factor of 2. The present experimental limit from an experiment (E787) at Brookhaven National Laboratory [104] is  $B(K^+ \rightarrow \pi^+\nu\bar{\nu}) < 2.4 \times 10^{-9}$  (90% c.l.).

2. The decay  $K_L \rightarrow \pi^0\nu\bar{\nu}$  is expected to be purely CP-violating [105]. The predicted branching ratio is

$$B(K_L \rightarrow \pi^0\nu\bar{\nu}) \simeq 4.4 \times 10^{-11} \eta^2 A^4 |T(x_t)|^2 \quad . \quad (48)$$

For the allowed range of  $A$  and  $\eta$ , one expects a branching ratio of  $2 \times 10^{-11}$ , give or take a factor of 2. While the present upper limit [106] of  $5.8 \times 10^{-5}$  (90% c.l.) is quite far from this, it represents a considerable advance from previous limits, and much improvement is expected in the next few years.

### 3. PRECISION ELECTROWEAK EXPERIMENTS

Tests of the electroweak theory have reached the precision that they are sensitive to the mass of the top quark. Indeed, the large top quark mass had been anticipated to some extent by these experiments. In this section we review the lowest-order theory, show how it is affected by the top quark in loop diagrams, and explore the sensitivity of precision electroweak measurements to further types of heavy particles which could shed light on the top quark's mass. We draw heavily on the discussion in Ref. [107], for which the present discussion serves in part as an update.

#### A. Lowest-order formalism

In order to construct a renormalizable theory of the weak interactions, it was proposed quite early [108] to regard the four-fermion interaction as the limit at zero momentum transfer of a process in which an intermediate vector boson (now called  $W$ ) was exchanged, so that one identifies  $G_F/\sqrt{2} = g^2/8M_W^2$ . The Fermi coupling constant is well known:  $G_F = 1.16639(2) \times 10^{-5} \text{ GeV}^{-2}$ . However, neither the coupling constant  $g$  nor the  $W$  mass  $M_W$  were known when this proposal was made. Searches for  $W$ 's as light as a couple of  $\text{GeV}/c^2$  were undertaken in the early 1960's.

If  $W^\pm$  exchange is to be described by a gauge interaction, the simplest group containing charged  $W$ 's is  $SU(2)$ , which also contains a  $W^0$ . But one cannot identify the  $W^0$  with a photon. Aside from the fact that the symmetry must be badly broken, so that the photon remains massless while the charged  $W$ 's become very heavy, there are two other difficulties. First, the charged  $W$ 's couple to matter with a  $V - A$  interaction [109], i.e., to left-handed particles, while the photon couples via a  $V$  interaction, i.e., to both left-handed and right-handed particles. Second, if the photon really were identified with  $W^0$  all the charges of particles would have to be half-integer, just like values of  $J_3$ , the third component of angular momentum.

The solution [6] is to add an  $SU(2)$  singlet  $B$  to the theory, with another coupling constant  $g'$ . The photon can then be one mixture of the  $B$  and the  $W^0$ , while there will be another neutral particle which is the orthogonal mixture:

$$\begin{aligned} \text{Photon} : \quad & A = B \cos \theta + W^0 \sin \theta \quad (m = 0) \quad ; \\ \text{New} \quad & : \quad Z = -B \sin \theta + W^0 \cos \theta \quad (m \neq 0) \quad . \end{aligned} \quad (49)$$

The  $W^0$  couples to the third component  $I_{3L}$  of the  $SU(2)$ . The subscript " $L$ " stands for "left-handed" and refers to the fact that all three components of the  $SU(2)$ , both the charged  $W$ 's and the  $W^0$ , couple only to left-handed particles or right-handed antiparticles. The  $B$  couples to a new quantum number "weak hypercharge," invented to account for the difference between electromagnetic charge and  $I_{3L}$ :

$$Q_{\text{em}} = I_{3L} + \frac{Y_W}{2} \quad . \quad (50)$$

Once the interaction Lagrangian is expressed in terms of the photon and  $Z$ , one finds that the electron charge  $e$  is related to the other parameters in the theory by  $e = g \sin \theta = g' \cos \theta$ , so that

$$\frac{1}{e^2} = \frac{1}{g^2} + \frac{1}{g'^2} \quad ; \quad M_W = \left( \frac{\pi \alpha}{\sqrt{2} G_F} \right)^{1/2} / \sin \theta \quad . \quad (51)$$

Moreover, the  $Z$  mass is related to the  $W$  mass:

$$M_Z = \frac{M_W}{\cos \theta} \quad ; \quad \frac{G_F}{\sqrt{2}} = \frac{g^2 + g'^2}{8M_Z^2} \quad . \quad (52)$$

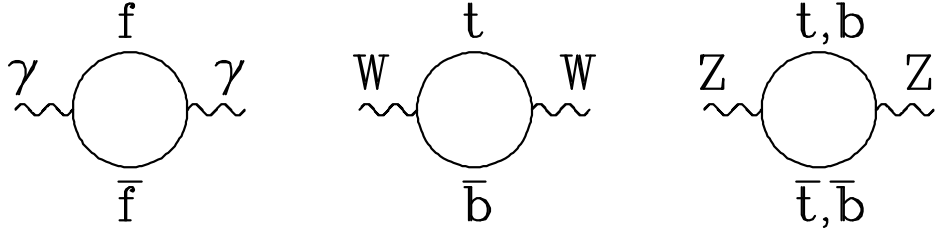


Figure 13: Loop diagrams with virtual fermions leading to important vacuum polarization effects. (a) Photons (all fermions  $f$  below the top quark are important); (b)  $W$ ; (c)  $Z$ .

## B. Effects in loop diagrams

The effects of fermions in loop diagrams, as shown in Fig. 13, are seen in several ways in the electroweak interactions.

The photon vacuum polarization effects shown in Fig. 13(a) lead to an effective fine structure constant  $\alpha(q^2)$  at an invariant momentum scale  $q^2$  which is related to the usual  $\alpha \simeq 1/137.036$  at  $q^2 = 0$  by

$$\alpha^{-1}(q) = \alpha^{-1}[1 - \Pi_{\gamma\gamma}(q^2)] \quad ; \quad \Pi_{\gamma\gamma} = \frac{\alpha}{3\pi} \sum_f Q_f^2 \left[ -\frac{5}{3} + \ln \frac{q^2}{m_f^2} \right] \quad . \quad (53)$$

The quantity  $\Pi_{\gamma\gamma}$  can be evaluated in part using data on  $e^+e^- \rightarrow$  hadrons; several recent precise determinations [110] lead to  $\alpha^{-1}(M_Z) \simeq 128.9 \pm 0.1$ . This quantity is scheme-dependent; one also sees it quoted in as  $127.9 \pm 0.1$  in the  $\overline{\text{MS}}$  scheme [111].

If we had used  $\alpha^{-1} = 137.036$ , the expressions we have written for the  $W$  and  $Z$  masses would imply, using the latest value [7]  $\sin^2 \theta = 0.23165$ , that  $M_W = 77.5 \text{ GeV}/c^2$  and  $M_Z = 88.4 \text{ GeV}/c^2$ . The use of the correct value of  $\alpha^{-1}(M_Z)$  changes these predictions to  $M_W = 79.86 \text{ GeV}/c^2$ ,  $M_Z = 91.11 \text{ GeV}/c^2$ . These values are to be compared with the experimental ones  $M_W = 80.34 \pm 0.10 \text{ GeV}/c^2$  (see below) and  $M_Z = 91.1863 \pm 0.0020 \text{ GeV}/c^2$  (see [7], [112] and [113]). The use of the correct value of  $\alpha$  considerably improves the predictions, but the experimental ratio  $M_W/M_Z$  is higher than predicted. The major part of the reason may be traced to the effect of the very heavy top quark in the loop diagrams of Figs. 13(b) and 13(c).

Both vector and axial-vector currents enter in the couplings of  $W$  and  $Z$  to fermions; the axial-vector currents are not conserved when the fermions have mass. Moreover, even the vector currents are not conserved when the fermions have unequal masses [as in Fig. 13(b)]. The result is the appearance of contributions to  $\Pi$  for the  $W$  and  $Z$  which are quadratic in fermion masses. No such contributions appear in  $\Pi_{\gamma\gamma}$ , as a result of electromagnetic gauge invariance and current conservation.

The low-energy limits of  $W$  and  $Z$  exchange are now described by

$$\frac{G_F}{\sqrt{2}} = \frac{g^2}{8M_W^2} \quad , \quad \frac{G_F}{\sqrt{2}}\rho = \frac{g^2 + g'^2}{8M_Z^2} \quad , \quad (54)$$

where the parameter  $\rho$ , which receives contributions from quark loops to  $W$  and  $Z$  self-energies, is dominated by the top [114]:

$$\rho \simeq 1 + \frac{3G_F m_t^2}{8\pi^2 \sqrt{2}} \quad , \quad (55)$$



Consequently, if we define  $\theta$  by means of the precise measurement at LEP of  $M_Z$ ,

$$M_Z^2 = \frac{\pi\alpha}{\sqrt{2}G_F\rho\sin^2\theta\cos^2\theta} \quad , \quad (56)$$

then  $\theta$  will depend on  $m_t$ , and so will  $M_W$  in Eq. (51). The ratio  $M_W/M_Z = \sqrt{\rho}\cos\theta$  then may be used to extract a value  $\sqrt{\rho} = 1.0050 \pm 0.0013$ , implying  $m_t = 179(1 \pm 0.13)$  GeV/ $c^2$ . We shall see that the inclusion of other electroweak data does not greatly alter this simple result.

In order to display dependence of electroweak observables on such quantities as the top quark and Higgs boson masses  $m_t$  and  $M_H$ , we choose to expand the observables about “nominal” values calculated for specific  $m_t$  and  $M_H$ . We thereby bypass a discussion of “direct” radiative corrections which are independent of  $m_t$ ,  $M_H$ , and new particles. We isolate the dependence on  $m_t$ ,  $M_H$ , and new physics arising from “oblique” corrections [115], associated with loops in the  $W$  and  $Z$  propagators like those shown in Figs. 13(b,c).

For  $m_t = 175$  GeV,  $M_H = 300$  GeV, the measured value of  $M_Z$  leads to a nominal expected value of  $\sin^2\theta_{\text{eff}} = 0.2315$ . In what follows we shall interpret the effective value of  $\sin^2\theta$  as that measured via leptonic vector and axial-vector couplings:  $\sin^2\theta_{\text{eff}} \equiv (1/4)(1 - [g_V^\ell/g_A^\ell])$ . We have corrected the nominal value of  $\sin^2\theta_{\overline{\text{MS}}} \equiv \hat{s}^2$  as quoted by DeGrassi, Kniehl, and Sirlin [116] for the difference [117]  $\sin^2\theta_{\text{eff}} - \hat{s}^2 = 0.0003$  and for the recent change in the evaluation of  $\alpha(M_Z)$  [110].

Defining the parameter  $T$  by  $\Delta\rho \equiv \alpha T$ , we find

$$T \simeq \frac{3}{16\pi\sin^2\theta} \left[ \frac{m_t^2 - (175 \text{ GeV})^2}{M_W^2} \right] - \frac{3}{8\pi\cos^2\theta} \ln \frac{M_H}{300 \text{ GeV}} \quad . \quad (57)$$

The weak mixing angle  $\theta$ , the  $W$  mass, and other electroweak observables depend on  $m_t$  and  $M_H$ .

The weak charge-changing and neutral-current interactions are probed under a number of different conditions, corresponding to different values of momentum transfer. For example, muon decay occurs at momentum transfers small with respect to  $M_W$ , while the decay of a  $Z$  into fermion-antifermion pairs imparts a momentum of nearly  $M_Z/2$  to each member of the pair. Small “oblique” corrections [115], logarithmic in  $m_t$  and  $M_H$ , arise from contributions of new particles to the photon,  $W$ , and  $Z$  propagators. Other (smaller) “direct” radiative corrections are important in calculating actual values of observables.

We may then replace (54) by

$$\frac{G_F}{\sqrt{2}} = \frac{g^2}{8M_W^2} \left( 1 + \frac{\alpha S_W}{4\sin^2\theta} \right) \quad , \quad \frac{G_F\rho}{\sqrt{2}} = \frac{g^2 + g'^2}{8M_Z^2} \left( 1 + \frac{\alpha S_Z}{4\sin^2\theta\cos^2\theta} \right) \quad , \quad (58)$$

where  $S_W$  and  $S_Z$  are coefficients representing variation with momentum transfer. Together with  $T$ , they express a wide variety of electroweak observables in terms of quantities sensitive to new physics. (The presence of such corrections was noted quite early by Veltman [118].) The Peskin-Takeuchi [115] variable  $U$  is equal to  $S_W - S_Z$ , while  $S \equiv S_Z$ .

Expressing the “new physics” effects in terms of deviations from nominal values of top quark and Higgs boson masses, we have the expression (57) for  $T$ , while contributions of Higgs bosons and of possible new fermions  $U$  and  $D$  with electromagnetic charges  $Q_U$  and  $Q_D$  to  $S_W$  and  $S_Z$ , in a leading-logarithm approximation, are [119]

$$S_Z = \frac{1}{6\pi} \left[ \ln \frac{M_H}{300 \text{ GeV}/c^2} + \sum N_C \left( 1 - 4\overline{Q} \ln \frac{m_U}{m_D} \right) \right] \quad , \quad (59)$$

$$S_W = \frac{1}{6\pi} \left[ \ln \frac{M_H}{300 \text{ GeV}/c^2} + \sum N_C \left( 1 - 4Q_D \ln \frac{m_U}{m_D} \right) \right] . \quad (60)$$

The expressions for  $S_W$  and  $S_Z$  are written for doublets of fermions with  $N_C$  colors and  $m_U \geq m_D \gg m_Z$ , while  $\bar{Q} \equiv (Q_U + Q_D)/2$ . The sums are taken over all doublets of new fermions. In the limit  $m_U = m_D$ , one has equal contributions to  $S_W$  and  $S_Z$ . For a single Higgs boson and a single heavy top quark, Eqs. (59) and (60) become

$$S_Z = \frac{1}{6\pi} \left[ \ln \frac{M_H}{300 \text{ GeV}/c^2} - 2 \ln \frac{m_t}{175 \text{ GeV}/c^2} \right] ,$$

$$S_W = \frac{1}{6\pi} \left[ \ln \frac{M_H}{300 \text{ GeV}/c^2} + 4 \ln \frac{m_t}{175 \text{ GeV}/c^2} \right] , \quad (61)$$

where the leading-logarithm expressions are of limited validity for  $M_H$  and  $m_t$  far from their nominal values. A degenerate heavy fermion doublet with  $N_c$  colors thus contributes  $\Delta S_Z = \Delta S_W = N_c/(6\pi)$ . For example, in a minimal dynamical symmetry-breaking (“technicolor”) scheme about which we shall have more to say presently, with a single doublet of  $N_c = 4$  fermions, one will have  $\Delta S = 2/(3\pi) \simeq 0.2$ . This will turn out to be marginally acceptable, while many non-minimal schemes, with large numbers of doublets, will be seen to be ruled out.

### C. Analysis of present data

We shall discuss a number of observables, including neutrino deep inelastic scattering, direct  $W$  mass measurements, direct measurements of a number of  $Z$  properties, and parity violation in atoms.

Among the first pieces of evidence for neutral currents was the presence of muonless events in neutrino deep inelastic scattering [120]. The ratios of neutrino and antineutrino neutral-current (NC) to charged-current (CC) cross sections,  $R_\nu$  and  $R_{\bar{\nu}}$ , are predicted to be [121]

$$R_\nu \equiv \frac{\sigma_{NC}(\nu N)}{\sigma_{CC}(\nu N)} = \rho^2 \left[ \frac{1}{2} - x + \frac{5}{9}x^2(1+r) \right] ,$$

$$R_{\bar{\nu}} \equiv \frac{\sigma_{NC}(\bar{\nu} N)}{\sigma_{CC}(\bar{\nu} N)} = \rho^2 \left[ \frac{1}{2} - x + \frac{5}{9}x^2\left(1 + \frac{1}{r}\right) \right] , \quad (62)$$

where  $x \equiv \sin^2 \theta$  and  $r \equiv \sigma_{CC}(\bar{\nu} N)/\sigma_{CC}(\nu N)$ . These expressions are proportional to  $\rho^2$  since they involve neutral current *cross sections* (squares of amplitudes).

The resulting plot of  $R_\nu$  vs.  $R_{\bar{\nu}}$  as a parametric function of  $\sin^2 \theta$  is shown in Fig. 14. One gets a “nose-like” curve. The experimental rate for  $\bar{\nu} N \rightarrow \bar{\nu} + \dots$  (the plotted point is based on Ref. [122]) is about as low as it can be, while the rate for  $\nu N \rightarrow \nu + \dots$  is very sensitive to  $\sin^2 \theta$  and provides a good measure of it. It turns out that the  $x$  and  $\rho$  dependences combine in such a way that  $R_\nu$  actually depends on  $m_t$  and  $M_H$  in very much the same way as does  $M_W$ . As a result, measurements of  $R_\nu$  are often quoted as effective measurements of  $M_W$ , which is what we shall do here.

Averaging a new measurement [122] with previous determinations [123, 124], one finds a result equivalent to [7, 125]  $M_W = 80.306 \pm 0.218 \text{ GeV}/c^2$  when one takes into account the measured value of  $M_Z$ . [A somewhat different average was quoted in [122], implying  $M_W = 80.220 \pm 0.208 \text{ GeV}/c^2$ .]

Direct measurements of the  $W$  mass have been presented by the CDF and D0 Collaborations [126, 127]. These use kinematic fitting to the sharp Jacobian peak in

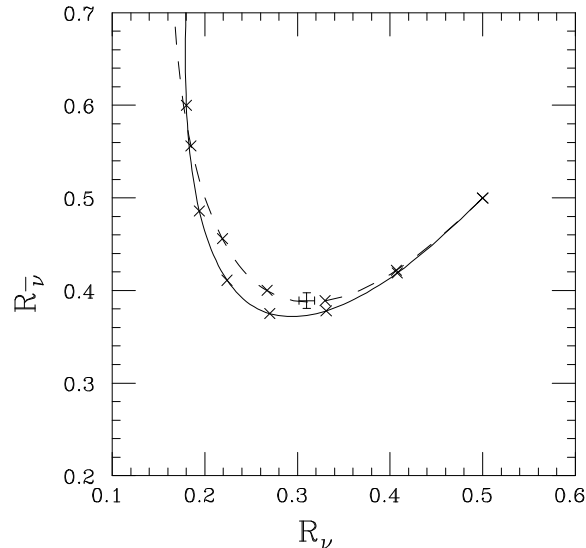


Figure 14: Ratios  $R_{\nu}$  and  $R_{\bar{\nu}}$  plotted against one another for varying values of  $\sin^2 \theta$  and  $\rho = 1$ . The  $\times$  marks denote units of 0.1 in  $\sin^2 \theta$ , starting at the point (0.5,0.5) for  $\sin^2 \theta = 0$ . The dashed line corresponds to  $r = 1/3$ , which would be appropriate if the nucleon had no antiquarks but were composed only of valence quarks. The solid line corresponds to  $r = 0.4$  (approximately the measured value). Plotted point illustrates measured values.

Table 4: Recent direct measurements of the  $W$  mass.

Collaboration	$M_W$ (GeV/ $c^2$ )
CDF (Run 1A)	$80.41 \pm 0.18$
D0 (Run 1A)	$80.35 \pm 0.27$
D0 (Run 1B)	$80.38 \pm 0.17$
LEP	$80.3 \pm 0.4 \pm 0.1$
UA2	$80.36 \pm 0.37$
Average	$80.356 \pm 0.125$

$\bar{p}p \rightarrow W + \dots \rightarrow \ell\nu_{\ell} + \dots$ , where  $\ell = (e, \mu)$ . Now, for the first time, it is possible as a result of the increased energy at LEP to directly measure a point on the excitation curve in  $e^+e^- \rightarrow W^+W^-$  [128], yielding a surprisingly accurate value for only a few dozen events. These results are compared with an earlier determination by the UA2 Collaboration [129] in Table 4. (See also Ref. [113].)

The  $W$  width  $\Gamma_W$  is an interesting quantity (see also Ref. [113]). A popular way of measuring it which is sometimes quoted as giving the total width is to measure the *ratio* of signals  $\sigma(\bar{p}p \rightarrow W + \dots \rightarrow \ell\nu_{\ell} + \dots)/\sigma(\bar{p}p \rightarrow Z + \dots \rightarrow \ell^+\ell^- + \dots)$ . In fact, however, since one needs to combine the standard model prediction for  $\Gamma(W \rightarrow \ell\nu)$  with this ratio in order to extract  $\Gamma_W$ , what one actually ends up measuring is the *branching ratio*  $B(W \rightarrow \ell\nu_{\ell})$ .

The standard model predicts [130]

$$B(W \rightarrow \ell\nu_{\ell}) \simeq \frac{1}{3 + 6[1 + (\alpha_s(M_W)/\pi)]} = 0.1084 \pm 0.0002 \quad (63)$$

if the  $W \rightarrow t\bar{b}$  channel is closed and there are no unanticipated channels other than

Table 5: Determinations at LEP of  $\sin^2 \theta_{\text{eff}}$ 

Observable	Name	Value	Error
$A_{FB}^\ell$	Forward-backward asymmetry	0.23085	0.00056
$A_\tau$	See notes (a,b)	0.23240	0.00085
$A_e$	See notes (a,b)	0.23264	0.00096
$\langle Q_{FB} \rangle$	F-B charge asymm., light quarks	0.23200	0.00100
$A_{FB}^c$	F-B charm asymmetry	0.23155	0.00112
$A_{FB}^b$	F-B bottom asymmetry	0.23246	0.00041
$\sin^2 \theta_{\text{eff}}^{\text{LEP}}$	LEP Average	0.23200	0.00027

(a)  $A_f \equiv 2g_V^f g_A^f / [(g_V^f)^2 + (g_A^f)^2]$

(b)  $A_\tau, A_e$  extracted from angular dependence of  $\tau$  polarization

the three species of  $\ell\nu_\ell$  and the lighter-quark channels. The world average [113] is  $0.110 \pm 0.003$ . On the other hand, a cruder but less theory-dependent measurement of the total width [131] makes use of the different dependence on  $\Gamma_W$  of charged lepton pair production on and off the  $W$  peak, and leads to  $\Gamma_W = 2.11 \pm 0.28 \pm 0.26$  GeV in accord with the standard model prediction [113] of  $2.077 \pm 0.014$  GeV. The “oblique” corrections mentioned above turn out not to affect the  $W$  width [130].

A number of measurements of  $Z$  properties have become possible as a result of the huge statistics amassed at the LEP  $e^+e^-$  Collider in the reaction  $e^+e^- \rightarrow Z \rightarrow \dots$ . The ability of the SLC Collider at Stanford to polarize electron beams longitudinally has permitted useful information to be obtained at that machine despite a much lower collision rate. The numbers we shall quote are those contained in the latest version of the LEP Electroweak Working Group document [7], which should be consulted for further references.

The mass of the  $Z$ , now measured to be  $M_Z = 91.1863 \pm 0.0020$  GeV/ $c^2$ , can serve an input to the electroweak theory when combined with  $G_F$  and  $\alpha(M_Z)$  to predict all other observables as functions of  $m_t$  and  $M_H$ . Deviations of observables from “nominal” values predicted for specific choices of  $m_t$  and  $M_H$  can be described as linear functions of the parameters  $S$ ,  $T$ , and  $U$  mentioned above. Every observable is a homogeneous function of degree 0, 1, or 2 of the factor  $\rho = \rho^{\text{nominal}}(1 + \alpha T)$  and of  $\sin^2 \theta(S, T)$ . Thus, every observable will define a band in the  $S - T$  plane (assuming for present purposes that  $S_W = S_Z$ , i.e.,  $U = 0$ ).

Other measured  $Z$  parameters [7] include the total width  $\Gamma_Z = 2.4946 \pm 0.0027$  GeV, the hadron production cross section  $\sigma_h^0 = 41.508 \pm 0.056$  nb, and  $R_\ell \equiv \Gamma_{\text{hadrons}}/\Gamma_{\text{leptons}} = 20.778 \pm 0.029$ , which may be combined to obtain the  $Z$  leptonic width  $\Gamma_{\ell\ell}(Z) = 83.91 \pm 0.11$  MeV.

A number of determinations of  $\sin^2 \theta$  are obtained from asymmetries measured at LEP. These are summarized in Table 5.

The LEP average,  $\sin^2 \theta_{\text{eff}}^{\text{LEP}} = 0.23200 \pm 0.00027$ , is to be compared with that based on the left-right asymmetry parameter  $A_{LR}$  measured with polarized electrons at SLC [132]:  $\sin^2 \theta_{\text{eff}}^{\text{SLC}} = 0.23061 \pm 0.00047$ . The  $\chi^2$  for the average in Table 5 is 6.3 for 5 degrees of freedom, while it rises to 12.8 for 6 degrees of freedom when the SLC value is added.

Parity violation in atoms, stemming from the interference of  $Z$  and photon exchanges between the electrons and the nucleus, provides further information on electroweak couplings. The most precise constraint at present arises from the measure-

Table 6: Electroweak observables described in fit.

Quantity	Experimental value	Theoretical value
$Q_W$ (Cs)	$-71.0 \pm 1.8$ <sup>a)</sup>	$-73.2$ <sup>b)</sup> $- 0.80S - 0.005T$
$Q_W$ (Tl)	$-115.0 \pm 4.5$ <sup>c)</sup>	$-116.8$ <sup>d)</sup> $- 1.17S - 0.06T$
$M_W$ (GeV)	$80.341 \pm 0.104$ <sup>e)</sup>	$80.35$ <sup>f)</sup> $- 0.29S + 0.45T$
$\Gamma_{\ell\ell}(Z)$ (MeV)	$83.91 \pm 0.11$ <sup>g)</sup>	$83.90 - 0.18S + 0.78T$
$\sin^2 \theta_{\text{eff}}$	$0.23200 \pm 0.00027$ <sup>h)</sup>	$0.2315$ <sup>i)</sup> $+ 0.0036S - 0.0026T$
$\sin^2 \theta_{\text{eff}}$	$0.23061 \pm 0.00047$ <sup>j)</sup>	$0.2315$ <sup>i)</sup> $+ 0.0036S - 0.0026T$

<sup>a)</sup> Weak charge in cesium [133]

<sup>b)</sup> Calculation [135] incorporating atomic physics corrections [134]

<sup>c)</sup> Weak charge in thallium [138, 139] (see text)

<sup>d)</sup> Calculation [140] incorporating atomic physics corrections [141]

<sup>e)</sup> Average of direct measurements and indirect information

from neutral/charged current ratio in deep inelastic neutrino scattering [122, 123, 124]

<sup>f)</sup> Including perturbative QCD corrections [116]

<sup>g)</sup> LEP average [7]

<sup>h)</sup> From leptonic asymmetries at LEP [7]

<sup>i)</sup> As calculated [116] with correction for relation between  $\sin^2 \theta_{\text{eff}}$  and  $\hat{s}^2$  [117]

<sup>j)</sup> From left-right asymmetry in annihilations at SLC [132]

ment of the *weak charge* (the coherent vector coupling of the  $Z$  to the nucleus),  $Q_W = \rho(Z - N - 4Z \sin^2 \theta)$ , in atomic cesium [133], with the result  $Q_W(\text{Cs}) = -71.04 \pm 1.58 \pm 0.88$ . The first error is experimental, while the second is theoretical [134]. The prediction [135]  $Q_W(\text{Cs}) = -73.20 \pm 0.13$  is insensitive to standard-model parameters [135, 136, 137] once  $M_Z$  is specified; discrepancies are good indications of new physics. Recently the weak charge has also been measured in atomic thallium. Averaging determinations by the Seattle [138] and Oxford [139] in a manner described in more detail in [107], we find  $Q_W(\text{Tl}) = -115.0 \pm 4.5$ , to be compared with a prediction [140, 141, 142] of  $-116.8$ .

We have performed a fit to the electroweak observables listed in Table 6. The “nominal” values (including [116]  $\sin^2 \theta_{\text{eff}} = 0.2315$ ) are calculated for  $m_t = 175$  GeV and  $M_H = 300$  GeV. We use  $\Gamma_{\ell\ell}(Z)$ , even though it is a derived quantity, because it has little correlation with other variables in our fit. It is mainly sensitive to the axial-vector coupling  $g_A^\ell$ , while asymmetries are mainly sensitive to  $g_V^\ell$ .

In order to focus on electroweak parameters and avoid the use of highly correlated measurements, we omit several quantities from the fit which are normally included in complete analyses. (1) The total width  $\Gamma_{\text{tot}}(Z)$  is omitted since it is highly correlated with  $\Gamma_{\ell\ell}(Z)$  and mainly provides information on the value of the strong fine-structure constant  $\alpha_s$ . With  $\alpha_s = 0.12 \pm 0.01$ , the observed total  $Z$  width is consistent with predictions. For the same reason, we omit the quantity  $R_\ell$ . (2) The invisible width of the  $Z$  is compatible with three species of neutrinos. It would provide information on  $\rho/\rho^{\text{nominal}} = 1 + \alpha T$  but is less useful as a source of that information than the leptonic width, and is highly correlated with it. (3) The experimental situation regarding the partial width  $\Gamma(Z \rightarrow b\bar{b})$  has changed recently [143]. We omit it from the fit while discussing it separately below.

Each observable in Table 6 specifies a band in the  $S - T$  plane with different

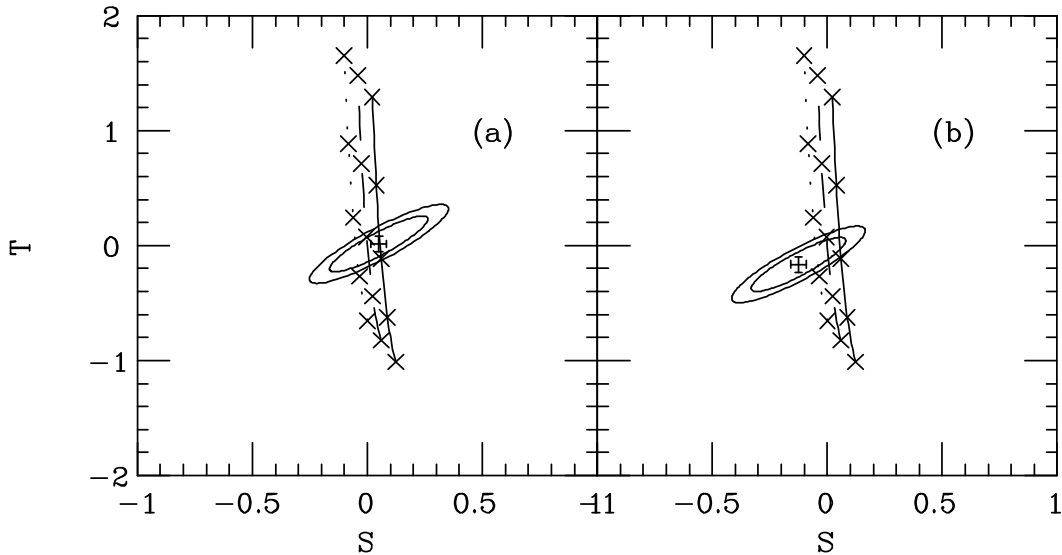


Figure 15: Allowed ranges of  $S$  and  $T$  at 68% (inner ellipses) and 90% (outer ellipses) confidence levels, corresponding to  $\chi^2 = 2.3$  and 4.6 above the minimum (crosses at center of ellipses). Dotted, dashed, and solid lines correspond to standard model predictions for  $M_H = 100, 300, 1000$  GeV. Symbols  $\times$ , from bottom to top, denote predictions for  $m_t = 100, 140, 180, 220,$  and  $260$  GeV. (a) Fit including APV experiments with present errors; (b) errors on APV experiments reduced by a factor of 4, with present central values of  $Q_W$  retained.

slope, as seen from the ratios of coefficients of  $S$  and  $T$ . Parity violation in atomic cesium and thallium is sensitive almost entirely to  $S$  [135, 137]. The impact of  $\sin^2 \theta_{\text{eff}}$  determinations on  $S$  is considerable. The leptonic width of the  $Z$  is sensitive primarily to  $T$ . The  $W$  mass specifies a band of intermediate slope in the  $S - T$  plane; here we assume  $S_W = S_Z$ . Strictly speaking, the ratio  $R_\nu$  specifies a band with slightly more  $T$  and less  $S$  dependence than  $M_W$  [115, 135]; we have ignored this difference here.

The resulting constraints on  $S$  and  $T$  are shown in Fig. 15(a). A top quark mass of  $175 \pm 6$  GeV/ $c^2$  (the CDF and D0 average), corresponding as we noted in Sec. 2 to  $\bar{m}_t(M_W) = 165 \pm 6$  GeV/ $c^2$ , is compatible with all Higgs boson masses between 100 and 1000 GeV/ $c^2$ , as seen by the curved lines intersecting the error ellipses. The centers of the ellipses lie at  $S = 0.05, T = 0.01$ , indicating that the fit is very comfortable with the nominal values chosen for  $m_t$  and  $M_H$ .

Independently of the standard model predictions, values of  $S$  between  $-0.3$  and  $0.3$  are permitted at the 90% confidence level. The values from atomic parity violation,  $S = -2.7 \pm 2.3$  [133] based on cesium and  $S = -1.5 \pm 3.8$  based on thallium [138, 139], have an average  $S = -2.4 \pm 2.0$ . The value of  $S$  is now known much more precisely than specified by these experiments. On the other hand, since the weak charge  $Q_W$  provides unique information on  $S$ , its determination with a factor of four better accuracy than present levels could have a noticeable effect on global fits, as shown in Fig. 15(b).

In contrast to many fits in the literature (see, e.g., [144, 145, 146]), ours does not exhibit a preference for any particular Higgs boson mass in the absence of separate information about  $m_t$ . We show curves of  $\chi^2$  as a function of  $m_t$  for several values of  $M_H$  in Fig. 16.

The minima of the  $\chi^2$  curves are nearly identical (slightly above 8 for the six data points in Table 6, i.e., for 5 degrees of freedom) for all three choices of  $M_H$ . When the value  $\bar{m}_t(M_W) = 165 \pm 6$  GeV/ $c^2$  (delimited by the horizontal band) is selected, some

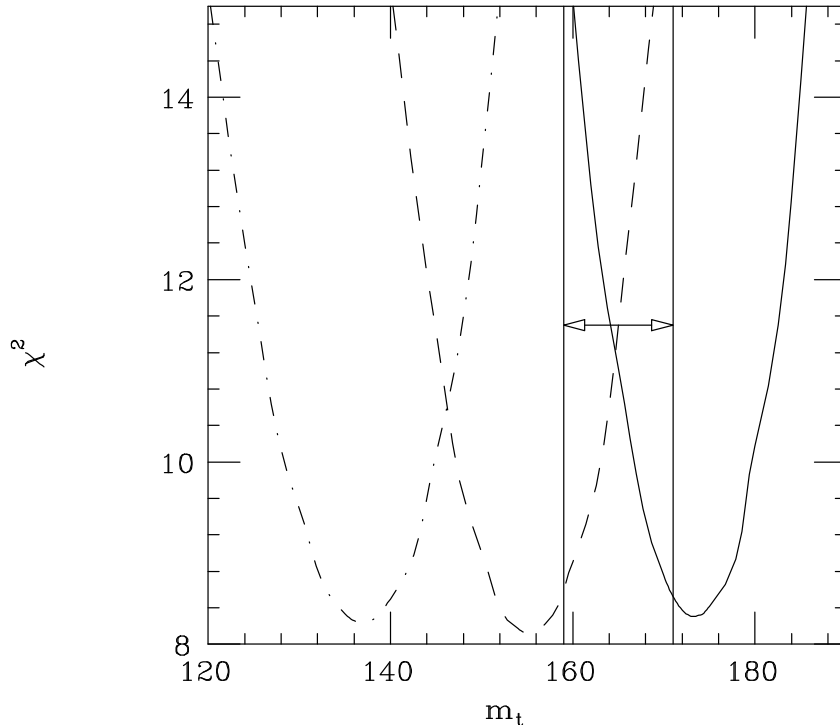


Figure 16: Values of  $\chi^2$  for fits to the data in Table 6, as function of  $m_t$  for several values of  $M_H$ . Dot-dashed, dashed, and solid curves correspond to  $M_H = 100, 300,$  and  $1000 \text{ GeV}/c^2$ , respectively. Horizontal bands denote the  $1\sigma$  limits for  $\bar{m}_t(M_W) = 165 \pm 6 \text{ GeV}/c^2$ .

preference arises for a Higgs boson mass in the range between 300 and 1000  $\text{GeV}/c^2$ . To see this more clearly, we include  $m_t$  in the fit in Fig. 17.

The favored value of  $M_H$  in the fit based on the data in Table 6 and the top quark mass mentioned above is  $M_H = (560 \times 1.5^{\pm 1}) \text{ GeV}/c^2$ . (See Fig. 17(a).) This is considerably higher than most other determinations (see, e.g., [144, 145, 146]). The experimental average of the two last rows in Table 6,  $\sin^2 \theta_{\text{eff}} = 0.23165 \pm 0.00024$  is slightly above our “nominal” value of  $\sin^2 \theta_{\text{eff}} = 0.2315$ ; a discrepancy in this direction tends to push the Higgs boson mass up from its nominal value of 300  $\text{GeV}/c^2$ . To accentuate this effect we explore the effect of omitting the SLC data on  $A_{LR}$  (the last row in Table 6). The small upward change in  $\sin^2 \theta_{\text{eff}}$ , by  $+0.00035$ , leads the favored  $M_H$  to increase by a factor of 1.5, to  $(820 \times 1.7^{\pm 1}) \text{ GeV}/c^2$ . (See Fig. 17(b).) The  $\chi^2$ , incidentally, drops by more than 6.

An effect which leads us to obtain a larger  $M_H$  than some other fits is that our “nominal”  $\sin^2 \theta_{\text{eff}} = 0.2315$  is slightly below theirs. For example [7], the fitted value  $\sin^2 \theta_{\text{eff}} = 0.2318 \pm 0.0002$  is quoted for  $m_t = 177 \pm 7 \text{ GeV}/c^2$  when  $M_H = 300 \text{ GeV}/c^2$ .

A further possible reason for the discrepancy between our fits and others is that the others incorporate  $R_\ell \equiv \Gamma(Z \rightarrow \text{hadrons})/\Gamma(Z \rightarrow \ell^+\ell^-)$ , whose experimental value of  $20.778 \pm 0.029$  is somewhat above the nominal value (20.757 in Ref. [7]). We have chosen to omit this quantity since it depends on  $\alpha_s$ . Experimental determinations of  $\alpha_s(M_Z)$  may be converging rapidly enough that one can trust them; the value [147]  $\alpha_s(M_Z) = 0.118 \pm 0.003$  was quoted recently. The quantity  $\rho$  cancels in  $R_\ell$ . Aside from its dependence on  $\alpha_s$  (we find  $\partial R_\ell/\partial \alpha_s = 6.7$ ),  $R_\ell$  provides a measure of  $x \equiv \sin^2 \theta$ ; we find  $\partial R/\partial x = -17.5$ . Thus a high  $R_\ell$  implies a low  $\sin^2 \theta$ . Low experimental values of  $\sin^2 \theta$  push  $M_H$  down.

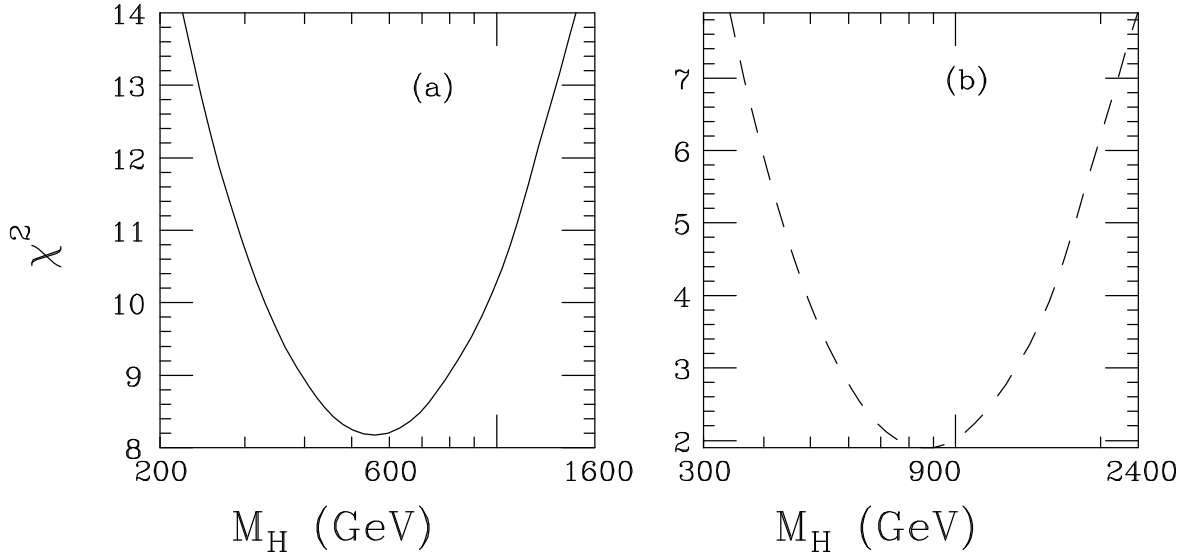


Figure 17: Values of  $\chi^2$  for fits to the data in Table 6 and the value  $\bar{m}_t(M_W) = 165 \pm 6 \text{ GeV}/c^2$ , as function of  $M_H$ . (a) SLC data (last row of Table 6) included (6 d.o.f.); (b) SLC data omitted (5 d.o.f.).

Another possibility is that some fits allow a separate parameter to describe  $A_{FB}^b$ . This quantity, as shown by the last row of Table 5, has a small quoted error. If it is omitted, the LEP average becomes  $\sin^2 \theta_{\text{eff}} = 0.23163 \pm 0.00037$  with  $\chi^2 = 4.0$  for 4 d.o.f., while if the SLC result is added to this sample, one finds  $\sin^2 \theta_{\text{eff}} = 0.23124 \pm 0.00029$  with  $\chi^2 = 6.9$  for 5 d.o.f. This low value again favors low  $M_H$ .

In any event the difference between Figs. 17(a) and (b) shows the pitfalls of drawing a conclusion about  $M_H$  when its value is so sensitive to a single datum. One is really only determining  $\log M_H$ , whose value is affected by less than  $1\sigma$  by including or dropping the SLC data.

#### D. The decay $Z \rightarrow b\bar{b}$

We now return to the question of the  $Z \rightarrow b\bar{b}$  branching ratio, which has engaged considerable theoretical attention in the past couple of years [148]. We first discuss the calculation of  $\Gamma(Z \rightarrow f\bar{f})$  for any fermion  $f$ .

The interaction Lagrangian for a  $Z$  and a fermion described by the Dirac field  $\psi$  is

$$\mathcal{L}_{\text{int}} = -\sqrt{g^2 + g'^2} \bar{\psi} \gamma^\mu Z_\mu (I_{3L} \mathcal{P}_L - Q \sin^2 \theta) \psi \quad , \quad (64)$$

where  $\mathcal{P}_L \equiv (1 - \gamma_5)/2$ . As an example, for a  $b$  quark with  $I_{3L} = -(1/2)$ , the axial and vector coupling constants (in a convenient normalization) are  $g_A = 1/4$ ,  $g_V = -(1/4) + (1/3) \sin^2 \theta$ . The  $Z$  partial width is then

$$\begin{aligned} \Gamma(Z \rightarrow f\bar{f}) &= \frac{\sqrt{2} G_F M_Z^3 \rho}{3\pi} N_c \left(1 - \frac{4m_f^2}{M_Z^2}\right)^{1/2} \\ &\times \left[ g_A^2 \left(1 - \frac{4m_f^2}{M_Z^2}\right) + g_V^2 \left(1 + \frac{2m_f^2}{M_Z^2}\right) \right] \quad . \end{aligned} \quad (65)$$

For a massless neutrino  $g_V = -g_A = 1/4$ , so

$$\Gamma(Z \rightarrow \nu\bar{\nu}) = \frac{G_F M_Z^3 \rho}{12\pi\sqrt{2}} = 166 \text{ MeV} \times \rho \quad . \quad (66)$$



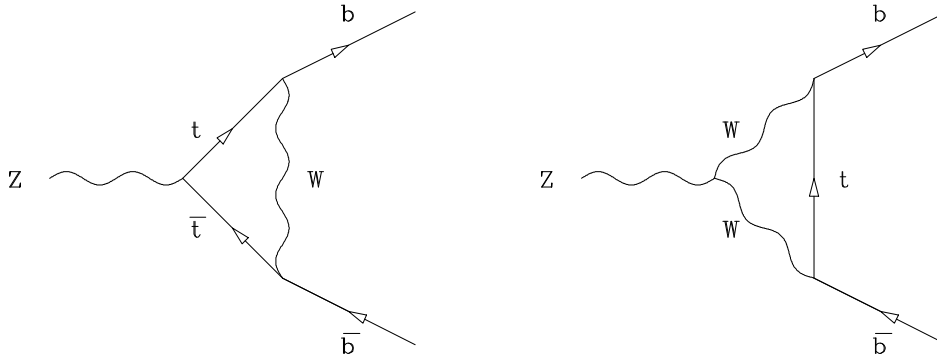


Figure 18: Examples of graphs contributing to  $\Gamma(Z \rightarrow b\bar{b})$ .

As mentioned, the fact that the invisible width of the  $Z$  is about 1/2 GeV leads one to conclude that there are three species of light neutrinos.

A calculation of  $\Gamma(Z \rightarrow d\bar{d}) \equiv \Gamma_d$ , for which  $g_A^2 = 1/16 = 0.0625$  and  $g_V^2 = 0.0299$ , gives  $(368 \text{ MeV})(\rho)(1 + [\alpha_s/\pi])$ , or, with  $\rho \simeq 1.01$  and  $1 + (\alpha_s/\pi) = 1.04$ , about 387 MeV. When compared with [7]  $\Gamma_h \equiv \Gamma(Z \rightarrow \text{hadrons}) = 1743.6 \pm 2.5 \text{ MeV}$ , this gives  $R_d^0 \equiv \Gamma(Z \rightarrow d\bar{d})/\Gamma(Z \rightarrow \text{hadrons}) \simeq 0.222$ . More precise calculations (see, e.g., [148]) give  $R_d^0 \simeq 0.221$ . We distinguish between  $R_q^0 \equiv \Gamma(Z \rightarrow q\bar{q})/\Gamma(Z \rightarrow \text{hadrons})$  and what is actually measured at the  $Z$  peak,  $R_q \equiv \sigma(e^+e^- \rightarrow q\bar{q})/\sigma(e^+e^- \rightarrow \text{hadrons})$ . As a result of a small photon contribution,  $R_b^0 = R_b + 0.0003$  [149].

The non-zero  $b$  mass must be taken into account in  $Z \rightarrow b\bar{b}$ . The predominance of  $g_A^2$  over  $g_V^2$  for the  $Zb\bar{b}$  coupling (in a ratio of about 2 to 1) means that the kinematic factor  $\beta^3 \simeq 0.980$  for axial couplings, where  $\beta = [1 - (4m_b^2/M_Z^2)]^{1/2}$ , has an appreciable effect. The corresponding kinematic factor for vector couplings,  $\beta(3 - \beta^2)/2$ , is nearly 1. Thus there is an overall reduction in  $R_b/R_d$  by about 1.3% just due to  $m_b$ , leading to the kinematically corrected prediction [150]  $R_{b \text{ kin}}^0 = 0.2183 \pm 0.0001$ .

The top quark affects  $\Gamma(Z \rightarrow b\bar{b})$  through graphs like those shown in Fig. 18. (In 't Hooft – Feynman gauge one must also include contributions of charged Higgs bosons, replacing  $W$  in all possible ways.) Contributions quadratic in  $m_t$  appear [151], as in the  $\rho$  parameter, so that  $R_b^0/R_{b \text{ kin}}^0 = 1 - aG_F m_t^2$ , where  $a$  is a dimensionless constant. For the observed value of the top quark mass the vertex-corrected standard-model prediction is  $R_b^0 = 0.2158$  [7], amounting to an additional correction of  $-1.2\%$ .

Until this past summer, results from the LEP and SLD groups seemed to indicate a value of  $R_b$  noticeably above the standard-model prediction. More recently [143], the ALEPH Collaboration has analyzed the full LEP I data set using two different methods. Using a lifetime tag, they find  $R_b = 0.2169 \pm 0.0011 \pm 0.0017$ , while using five mutually exclusive hemisphere tags they find  $R_b = 0.2158 \pm 0.0009 \pm 0.0011$ . The current LEP average [7], incorporating some new results from other LEP groups and from SLD [152], is  $R_b^0 = 0.2178 \pm 0.0011$ . These results are in accord with standard model predictions. They do not yet conclusively confirm the  $-1.2\%$  effect due to top-quark graphs like those in Fig. 18, but at least indicate that  $R_b < R_d$ .

Table 7: Final states of a  $t\bar{t}$  pair as function of decays of the  $W$  bosons in  $t \rightarrow W + b$ . Here  $\cancel{E}_T$  stands for “missing transverse energy,” while  $j$  stands for “jet”.

$W^+ \rightarrow$	1/9	1/9	1/9	2/3
$W^- \rightarrow$	$e\nu$	$\mu\nu$	$\tau\nu$	$u\bar{d}' + c\bar{s}'$
1/9 $e\nu$	$ee\cancel{E}_T$ +2j	$e\mu\cancel{E}_T$ +2j	$e\tau\cancel{E}_T$ +2j	$e\cancel{E}_T$ +4j
1/9 $\mu\nu$	$e\mu\cancel{E}_T$ +2j	$\mu\mu\cancel{E}_T$ +2j	$\mu\tau\cancel{E}_T$ +2j	$\mu\cancel{E}_T$ +4j
1/9 $\tau\nu$	$e\tau\cancel{E}_T$ +2j	$\mu\tau\cancel{E}_T$ +2j	$\tau\tau\cancel{E}_T$ +2j	$\tau\cancel{E}_T$ +4j
2/3 $\bar{u}d' + \bar{c}s'$	$e\cancel{E}_T$ +4j	$\mu\cancel{E}_T$ +4j	$\tau\cancel{E}_T$ +4j	6j

## 4. TOP QUARK OBSERVATION AT THE TEVATRON

### A. Production and decay

Quite some time ago [153, 154] it was realized that the Fermilab Tevatron would be able to produce top quarks heavy enough to decay to  $W + b$ . An estimate [154] in 1984 predicted  $\sigma(\bar{p}p \rightarrow t\bar{t} + \dots) \sim 10 \text{ pb}(m_t/150 \text{ GeV}/c^2)^{-5}$  at c.m. energy  $\sqrt{s} = 2 \text{ TeV}$ . The major subprocesses contributing to  $t\bar{t}$  production ( $q$  and  $g$  stand for quark and gluon) are  $q\bar{q} \rightarrow g^* \rightarrow t\bar{t}$  and  $gg \rightarrow t\bar{t}$  (via  $t$  exchange or a gluon in the direct channel). The  $q\bar{q}$  subprocess is dominant for the actual situation, so one has to know the distribution of quarks and antiquarks inside the nucleon. This information is provided, for example, by deep inelastic scattering [155]. We shall quote more precise predictions presently.

The decay of the top quark for  $m_t > M_W + m_b$  is essentially 100% to  $W + b$  unless other channels (like  $H^+ + b$ , where  $H^+$  is a charged Higgs boson) exist. We have already mentioned that this expectation is confirmed [2], though not yet with overwhelming accuracy. Assuming that only the  $W + b$  channel is significant, the decays of a  $t\bar{t}$  pair then may be decomposed according to Table 7. We have used the shorthand  $d'$  and  $s'$  for the linear combinations (3) and (4) of  $d$  and  $s$  which couple to  $u$  and  $c$  via  $W$ .

Energy balance in Tevatron collisions can only be checked in the transverse direction since particles can escape undetected at small angles relative to the beam. Large missing transverse energy serves as a signature of neutrino production in  $W$  leptonic decay. One always expects at least two jets of hadrons associated with the two  $b$  quarks in  $t\bar{t}$  decays. If one or two  $W$ 's decays hadronically a total of 4 or 6 jets should then be produced.

All the channels in Table 7 except for those with one or two  $\tau$  leptons have now been studied. These include dileptons (about 5%), leptons + jets (about 30%), and jets (about 45%). A start is even being made on channels with one  $\tau$  and one  $e$  or  $\mu$ . Thus a large fraction of the  $t\bar{t}$  channels are seen.

### B. Recent CDF and D0 analyses

We summarize in this subsection some results which were presented at the 1996 Warsaw Conference by the CDF and D0 Collaborations [26]. For CDF results, in addition to those presented at Warsaw, one may consult Refs. [156] for details. As an example of how one exploits the possibilities of Table 7, we now give some details of the CDF analyses.

Table 8: CDF top quark events in different channels based on an integrated luminosity of  $110 \text{ pb}^{-1}$ . Only the statistical error is shown for the channels with  $\tau$ . Acceptances were calculated for  $m_t = 175 \text{ GeV}/c^2$ .

Channel	$N_{\text{data}}$	$N_{\text{background}}$	$\sigma(t\bar{t})$ (pb)
Dilepton	10	$2.1 \pm 0.4$	$9.3_{-3.4}^{+4.4}$
$\ell + j$ (SVX)	34	$7.96 \pm 1.37$	$6.8_{-1.8}^{+2.3}$
$\ell + j$ (SLT)	40	$24.3 \pm 3.5$	$8.0_{-3.6}^{+4.4}$
Hadronic	192	$137 \pm 11$	$10.7_{-4.0}^{+7.6}$
$\tau + (e, \mu)$	4	$2.0 \pm 0.35$	$15.6_{-13.2}^{+18.6}$
Total			$7.5_{-1.6}^{+1.9}$

1. In the *dilepton* sample, where  $\ell = e$  or  $\mu$ , one asks that the leptons have opposite charges, demands missing transverse energy ( $\cancel{E}_T$ ) as a signature of one or more neutrinos, and requires two jets (signatures of the two  $b$  quarks). As a result, 7 events with  $e\mu$ , two with  $\mu\mu$ , and one with  $ee$  were found. Six “tagged” jets in a total of 4 events were identified as  $b$ ’s after the fact, but  $b$  identification was not required *a priori*.

2. In the *lepton + jets* sample, with  $\ell = e$  or  $\mu$ , one again asks for  $\cancel{E}_T$ , at least three observed jets, and at least one identified  $b$  quark. The  $b$  quark can be identified by its displaced vertex, since the average  $b$  lifetime is 1.5 to 1.6 ps, using the silicon vertex detector (“SVX”). Alternatively, its semileptonic decay, with a branching ratio of about 10.5% to each of  $e + \dots$  and  $\mu + \dots$ , gives rise to a soft lepton tag (“SLT”). One sees 34 SVX events and 40 SLT events.

3. In the *6 jets* sample, one asks to see at least 5 of them, requiring a  $b$  to be tagged via the SVX. Here 192 events are seen.

In Table 8 we summarize the CDF measurements in different channels. The CDF cross sections in various channels average to a value  $\sigma_{\text{CDF av.}}(p\bar{p} \rightarrow t\bar{t} + \dots) = 7.5_{-1.6}^{+1.9}$  pb at  $\sqrt{s} = 1.8 \text{ TeV}$ .

The corresponding D0 results make use of dilepton events, lepton + jets events with kinematic discrimination, and lepton + jets events with a soft muon “tag” associated with the semileptonic decay  $b \rightarrow c\mu^- \bar{\nu}_\mu$ . The results, based on the full 1992–5 sample with  $100 \text{ pb}^{-1}$  of integrated luminosity, are shown in Table 9. The column labeled “expected” refers to the number of events anticipated for a top quark with mass  $m_t = 180 \text{ GeV}/c^2$  based on cross sections of Ref. [157]. The D0 top quark cross sections are  $4.7 \pm 3.2$  pb in the dilepton channel,  $4.6 \pm 5.1$  pb in the hadron channel,  $4.2 \pm 2.0$  pb in the lepton + jets channel with kinematic discrimination, and  $7.0 \pm 3.3$  pb in the lepton + jets/tag channel.

Combining all CDF and D0 cross section determinations, one finds

$$\sigma(p\bar{p} \rightarrow t\bar{t} + \dots) = 6.4_{-1.2}^{+1.3} \text{ pb} \quad (\sqrt{s} = 1.8 \text{ TeV}) \quad . \quad (67)$$

This is to be compared with theoretical estimates such as

$$\sigma_{\text{Theory}}(p\bar{p} \rightarrow t\bar{t} + \dots) = \left\{ \begin{array}{l} 4.84_{-0.69}^{+0.73} \text{ pb} \quad [158] \\ 4.75_{-0.62}^{+0.73} \text{ pb} \quad [159] \end{array} \right\} \quad . \quad (68)$$

Table 9: D0 top quark events in different channels based on an integrated luminosity of  $100 \text{ pb}^{-1}$ .

Channel	$N_{\text{expected}}$	$N_{\text{background}}$	$N_{\text{data}}$
$e\mu$	$1.7 \pm 0.3$	$0.4 \pm 0.1$	3
$ee$	$0.9 \pm 0.1$	$0.7 \pm 0.2$	1
$\mu\mu$	$0.5 \pm 0.1$	$0.5 \pm 0.3$	1
$e + \text{jets}$	$6.5 \pm 1.4$	$3.8 \pm 1.4$	10
$\mu + \text{jets}$	$6.4 \pm 1.5$	$5.4 \pm 2.0$	11
$e + \text{jets/tag}$	$2.4 \pm 0.4$	$1.4 \pm 0.4$	5
$\mu + \text{jets/tag}$	$2.8 \pm 0.9$	$1.1 \pm 0.2$	6
Total	$21.2 \pm 3.8$	$13.4 \pm 3.0$	37

### C. Mass

The most precise CDF value of the top quark mass [26] comes from a combined analysis including (a) 34 events with a lepton, jets, and at least one SVX tag (leading to  $m_t = 177 \pm 7 \text{ GeV}/c^2$ ), (b) a more refined analysis of the same sample, weighting events in terms of the quality of information they provide, leading to the value  $174 \pm 8 \text{ GeV}/c^2$ , (c) the dilepton sample, leading to  $160 \pm 28 \text{ GeV}/c^2$  and  $162 \pm 22 \text{ GeV}/c^2$  in two different analyses (the second using the average  $M_{\ell b}^2$  of the lepton and  $b$ ), and (d) the multijet sample, leading to  $187 \pm 15 \text{ GeV}/c^2$ . The resulting mass plot is shown in Fig. 19.

The CDF Collaboration has also presented distributions in top quark transverse momentum and in  $m_{t\bar{t}}$ , the effective mass of the  $t\bar{t}$  system [156]. These data are in accord with standard model expectations.

The D0 top quark mass obtained from the lepton + jets sample is  $169 \pm 11 \text{ GeV}/c^2$ , while  $158 \pm 26 \text{ GeV}/c^2$  is obtained from the dilepton sample. The mass distribution from the lepton + jets sample (before a  $1 \text{ GeV}/c^2$  jet energy correction has been applied) is shown in Fig. 20. The world average of  $175 \pm 6 \text{ GeV}/c^2$  is based on all the CDF and D0 determinations.

In Fig. 21 we plot the expected top quark cross section [158] as a function of  $m_t$  at the c.m. energies  $\sqrt{s} = 1.8$  and 2 TeV. Also shown are the individual CDF and D0 mass and cross section points. It is clear there is satisfactory agreement with the standard model, though there would be room, if one so chose, for an additional 50% extra contribution to the cross section from some non-standard process.

### D. Decays

The branching ratio of the top quark to  $W + b$  can be measured relative to all  $W + q$  decays by comparing double  $b$  tags with single  $b$  tags [2]. The result is

$$\frac{B(t \rightarrow W + b)}{B(t \rightarrow W + q)} = 0.94 \pm 0.27 \pm 0.13 \quad , \quad (69)$$

implying  $V_{tb} = 0.97 \pm 0.15 \pm 0.07$  in accord with standard-model expectations.

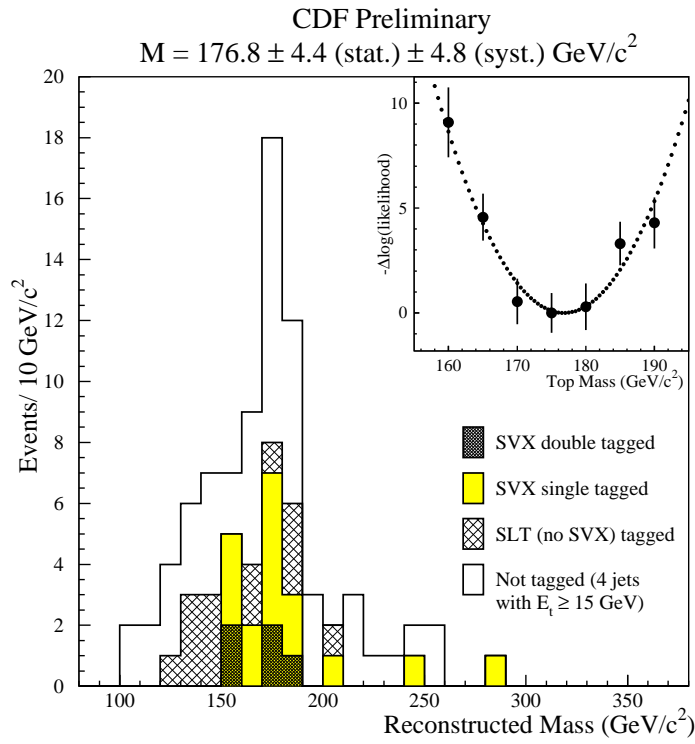


Figure 19: CDF top quark mass distributions as of July 1996.

### DØ Mass Fit preliminary

**2D** fit to 32 events (**LB** sample)  
 constrain signal by PR fit  
 $m_{top} = 168 \pm 8(stat.), \chi^2 = 21.7/22$

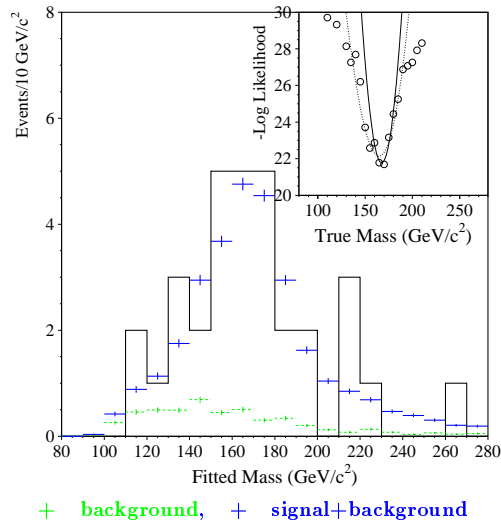


Figure 20: DØ top quark mass distribution from lepton + jets sample as of July 1996. A correction of +1 GeV/c<sup>2</sup> must be applied for the energy scale.

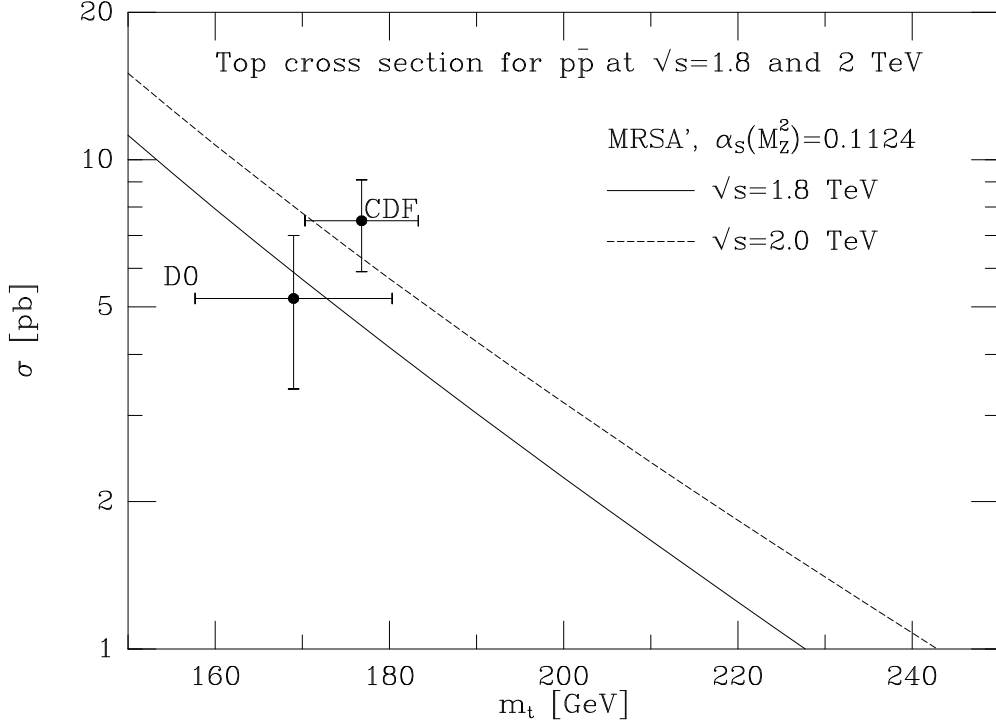


Figure 21: Top quark cross section prediction as a function of  $m_t$ .

## 5. TOP QUARK PRODUCTION IN ELECTRON-POSITRON COLLISIONS

### A. Excitation curve

Eventually it will become possible to produce top quarks in pairs in high-energy electron-positron annihilations. Accordingly, we discuss the production of pairs of arbitrary fermions  $f$  via virtual photons ( $\gamma^*$ ) and  $Z$ 's ( $Z^*$ ) in the direct channel. These results will be of use in Sec. 6 when we discuss exotic quarks and leptons.

Define  $x \equiv \sin^2 \theta$ ,  $s \equiv E_{c.m.}^2$ , and  $r \equiv [s/(s - m_Z^2)x(1 - x)]$ . Then far from the  $Z$  pole, where the  $Z$  width can be neglected, the contribution of a virtual photon and  $Z$  in the direct channel to the cross section for production of a fermion with electric charge  $Q_f$  and axial and vector  $Z$  couplings  $g_A = -(1/2)I_{3L}^f$  and  $g_V = (1/2)I_{3L}^f - Q_f x$  is

$$\sigma(e^+e^- \rightarrow f\bar{f}) = \sigma_\gamma \left\{ Q_f^2 - 2rQ_f g_V^e g_V^f + r^2[(g_V^e)^2 + (g_A^e)^2][(g_V^f)^2 + \frac{\beta^2}{K_V}(g_A^f)^2] \right\} , \quad (70)$$

where

$$\sigma_\gamma \equiv \frac{4\pi\alpha^2}{3s} N_c \beta K_V , \quad \beta \equiv \left( 1 - \frac{4m_f^2}{s} \right)^{1/2} , \quad K_V \equiv \frac{3 - \beta^2}{2} , \quad (71)$$

and  $N_c$  is the number of colors of fermions. For quarks ( $N_c = 3$ ) the cross section should be multiplied by an additional correction factor of  $1 + (\alpha_s/\pi) \approx 1.04$ . The values of  $\sigma/\sigma_0$  far above pair production threshold, where  $\sigma_0 \equiv \sigma(e^+e^- \rightarrow \gamma^* \rightarrow \mu^+\mu^-)$ , are compared in Table 10 for various fermion species  $f$  when the energy is far below the  $Z$  pole (where only the virtual photon dominates) and when it is far above the  $Z$  (where the interference in vector contributions of the photon and  $Z$  is possible). All the cross sections far above the  $Z$  are enhanced relative to the values they would have due to the virtual photon alone.

Table 10: Cross sections  $\sigma$  [in units of  $\sigma_0 \equiv \sigma(e^+e^- \rightarrow \gamma^* \rightarrow \mu^+\mu^-)$ ] for  $e^+e^-$  production of pairs of fermions  $f\bar{f}$  via virtual photons and  $Z$ 's in the direct channel. Here  $t$ -channel exchanges are neglected for  $e$  and  $\nu_e$ . Values of  $g_V^f$  are quoted for  $x = 0.2315$ . QCD corrections to quark production have been neglected.

Fermion $f$	$Q_f$	$g_V^f$	$g_A^f$	$\sigma/\sigma_0$ far below $Z$	$\sigma/\sigma_0$ far above $Z$
$u$	2/3	0.0957	-1/4	4/3	1.80
$d$	-1/3	-0.1728	1/4	1/3	0.92
$e^-$	-1	-0.0185	1/4	1	1.13
$\nu_e$	0	1/4	-1/4	0	0.25

The predicted top quark cross section, shown in Fig. 22, is composed of incoherent contributions corresponding to vector and axial-vector couplings to the top. The vector part involves  $\gamma^* - Z^*$  interference. These contributions have rather different energy dependence as a result of different kinematic factors. The vector contribution peaks around  $E_{\text{c.m.}} = 410$  GeV, while the axial vector contribution peaks around 550 GeV. At 410 GeV, the axial contribution is only 5% of the total, rising to about 25% asymptotically. The sum of the two contributions peaks around 420 GeV at a value of about 0.7 pb.

## B. Sensitivity to interactions

The top quark mass is too large to permit the formation of  $t\bar{t}$  bound states or top mesons ( $t$  quarks bound to light antiquarks). The top quark decays to  $W + b$  with a partial width of about 1.4 GeV, as noted in the Introduction. This is considerably larger than the spacings between quarkonium levels shown in Figs. 3 and 4. Nonetheless one can learn some things about the top-antitop interaction by studying the shape of the threshold function and how it is distorted in comparison with the lowest-order prediction in Fig. 22 [160, 161]. One probably sees a vestige of the  $1S$  level as a slight threshold enhancement with respect to the free-quark behavior, while Higgs interactions [161] can alter the threshold shape considerably.

## 6. SPECULATIONS ON SOURCE OF TOP QUARK MASS

### A. Mass matrix lore

In Sec. 2 A we saw that the  $3 \times 3$  quark mass matrices  $\mathcal{M}_{U,D}$  were diagonalized by separate unitary transformations  $L_{U,D}$  and  $R_{U,D}$  on left- and right-handed quarks. The CKM matrix  $V = L_U^\dagger L_D$  carries no information about the transformations  $R_{U,D}$ . As a result, separate unitary transformations can be performed on right-handed  $U$  and  $D$  quarks, as long as corresponding redefinitions of the mass matrix are made. Moreover, the simultaneous transformations  $L_U^\dagger \rightarrow L_U^\dagger A$  and  $L_D \rightarrow A^\dagger L_D$ , with  $AA^\dagger = 1$ , also leave  $V$  unchanged. Thus there is considerable freedom in the choice of basis for mass matrices, which has led to a large folklore. We shall barely scratch the surface.

An early observation [162, 163] was the relation between the Cabibbo angle and the ratio of  $d$  and  $s$  masses:  $\sin \theta_c \simeq (m_d/m_s)^{1/2}$ . This result can be obtained with a correction term  $-(m_u/m_c)^{1/2}$  if one postulates a zero in the upper-left corner of the

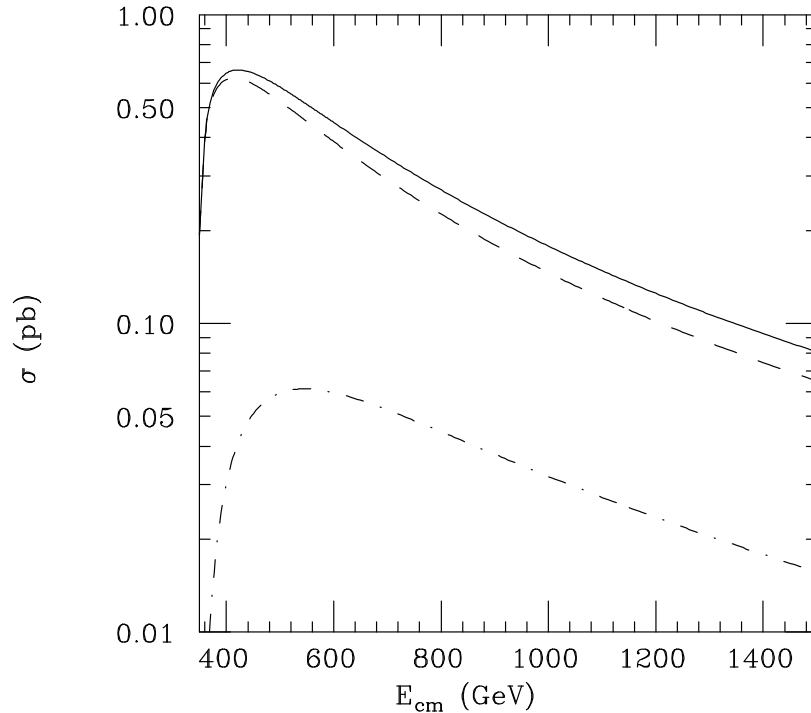


Figure 22: Cross section prediction for  $e^+e^- \rightarrow (\gamma^*, Z^*) \rightarrow t\bar{t}$  as a function of  $E_{\text{c.m.}}$ . Solid line: full cross section; dashed line: contribution of vector couplings of  $t$ ; dot-dashed line: contribution of axial coupling of  $t$ .)

mass matrices for two families of quarks:

$$\mathcal{M}_Q = \begin{bmatrix} 0 & a \\ a & b \end{bmatrix} \quad , \quad (72)$$

where  $a \ll b$ . Since the determinant of this matrix is  $-a^2$  while its trace is  $b$ , its eigenvalues are approximately  $-a^2/b$  and  $b$ , corresponding to the eigenvectors  $[1, -a/b]$  and  $[a/b, 1]$ , respectively. We then identify

$$\begin{aligned} a_U &= \sqrt{-m_u m_c} \quad , \quad b_U = m_c \quad , \\ a_D &= \sqrt{-m_d m_s} \quad , \quad b_D = m_s \quad . \end{aligned} \quad (73)$$

The CKM matrix may be computed from the scalar product of the appropriate eigenvectors  $U_i$  and  $D_j$  via [164]  $V_{ij} = U_i^\dagger \cdot D_j$ . For example,

$$V_{us} = \left[ 1, -\sqrt{\frac{-m_u}{m_c}} \right] \cdot \left[ \sqrt{\frac{-m_d}{m_s}} \right. \\ \left. 1 \right] = \sqrt{\frac{-m_d}{m_s}} - \sqrt{\frac{-m_u}{m_c}} \quad . \quad (74)$$

The negative sign of a quark mass is no cause for concern; it can always be changed by redefining  $q \rightarrow \gamma_5 q$ . The relative phases of the two terms on the right-hand side of (74) can be adjusted by an *ansatz* regarding the phases of terms in the mass matrices. For  $m_s/m_d \simeq 20$  [165], the observed value  $V_{us} \simeq 0.22$  is obtained for a relative phase of the two terms close to  $90^\circ$ .

The crucial role of zeroes in mass matrices for three-family models was first exploited by Fritzsch [166], explored in some detail by Ramond and his group [167], and has been reviewed recently by Branco *et al.* [168]. These zeroes go under the rubric of



Table 11: Quark mass ratios contributing to CKM matrix elements in one basis for quark mass matrices. Here the symbol  $q$  stands for  $m_q$ .

CKM element	Quark mass ratios	Magnitudes of ratios
$V_{us}, V_{cd}$	$(d/s)^{1/2}, (u/c)^{1/2}$	0.22, 0.06
$V_{cb}, V_{ts}$	$s/b, c/t$	0.03, 0.007
$V_{ub}$	$(ds)^{1/2}/b, (s/b)(u/c)^{1/2}, (uc)^{1/2}/t$	0.007, 0.002, 0.0004
$V_{td}$	$(ds)^{1/2}/b, (c/t)(d/s)^{1/2}, (uc)^{1/2}/t$	0.007, 0.002, 0.0004

“texture zeroes.” A “democratic” basis has also been proposed [169], which explains the hierarchies  $m_u, m_c \ll m_t$  and  $m_d, m_s \ll m_b$  by perturbing around matrices of the form

$$\mathcal{M} = \frac{1}{3} \begin{bmatrix} 1 & 1 & 1 \\ 1 & 1 & 1 \\ 1 & 1 & 1 \end{bmatrix} \quad (75)$$

with eigenvectors

$$\frac{1}{\sqrt{2}} \begin{bmatrix} 1 \\ -1 \\ 0 \end{bmatrix}, \quad \frac{1}{\sqrt{6}} \begin{bmatrix} 1 \\ 1 \\ -2 \end{bmatrix}, \quad \frac{1}{\sqrt{3}} \begin{bmatrix} 1 \\ 1 \\ 1 \end{bmatrix}, \quad (76)$$

corresponding to eigenvalues 0, 0, 1. By means of a unitary transformation one can end up with a matrix  $\mathcal{M}$  consisting of all zeroes except for a 1 in the lower right-hand corner.

A curious basis choice seems to be encountered in several quite different approaches [164, 170]:

$$\mathcal{M} = \begin{bmatrix} 0 & \alpha p & \alpha \\ \alpha p & \beta & \beta q \\ \alpha & \beta q & \gamma \end{bmatrix}, \quad (77)$$

where  $p$  and  $q$  are numbers of order 1. For  $\alpha \ll \beta \ll \gamma$  the eigenvectors and eigenvalues of this matrix are easy to compute. The CKM elements and the quark mass ratios which contribute to them (with phases which must be adjusted by hand) are summarized in Table 11. The magnitudes of the mass ratios appear to be appropriate for the sizes of the CKM elements. No insight is present in these models (nor in most others) regarding the choice of relative phases, however.

## B. A two-family fable

Perhaps one of the least popular ideas these days is the notion that quarks are somehow composite objects. Nonetheless, an exercise (perhaps no more than a fable, as applied to quarks) shows the potential insight a composite model can provide into the interplay between masses and mixing [164, 171].

The exercise is based on states for which there are experimental candidates: the charmed-strange baryons known as  $\Xi_c$  illustrated in Fig. 5. These are interesting because no two quarks in them have the same mass. They consist of  $csq$ , where  $q = u$  or  $d$ .

The lowest charmed-strange baryon, now called  $\Xi_c$  [47] and denoted in Fig. 5 by  $\Xi_c^a$  (originally  $A$  in Ref. [172]), has its light quarks  $s$  and  $q$  in a state primarily of zero spin and flavor SU(3) antisymmetry. The total spin of the  $\Xi_c^a$  is 1/2.

A candidate for an excited version of the  $\Xi_c$ , which we label as  $\Xi_c^s$  in Fig. 5 (originally  $S$  in Ref. [172]), has been claimed by the WA89 Collaboration at CERN [173]. It lies 95 MeV/ $c^2$  above the  $\Xi_c^a$  and decays to it by photon emission. It, too, has total spin equal to 1/2, but its light quarks are coupled up primarily to a state of spin 1 and flavor SU(3) symmetry. This state is on shaky ground as it has only been reported in conference proceedings and is not confirmed by experiments at the CLEO detector at Cornell.

Finally, the Cornell experiments just mentioned *do* see a candidate for a  $\Xi_c^*$  state at higher mass [32], which fits well with the assignment of a state of total spin 3/2 (originally  $S^*$  in Ref. [172]). This state decays to  $\Xi_c^a + \pi$ . The light quarks, of course, have to be in a pure spin-1 state here.

The masses of many hadrons can be described in terms of sums of constituent-quark masses and hyperfine-interaction terms inversely proportional to quark masses [174]. Thus, for example, for a  $\Xi_c$ , one will have

$$M \simeq m_c + m_s + m_q + a \left( \frac{\sigma_q \cdot \sigma_s}{m_q m_s} + \frac{\sigma_q \cdot \sigma_c}{m_q m_c} + \frac{\sigma_s \cdot \sigma_c}{m_s m_c} \right) \quad (78)$$

We note that  $m_q < m_s \ll m_c$ . Now, when  $m_c \rightarrow \infty$ , this mass operator is diagonal in the basis labeled by  $S_{sq}$ :

$$\begin{bmatrix} S_{sq} = 0 \\ S_{sq} = 1 \end{bmatrix} \leftrightarrow \begin{bmatrix} \Xi_c^a \\ \Xi_c^s \end{bmatrix} \quad \text{for } J = 1/2 \text{ states} \quad . \quad (79)$$

When  $m_c \neq \infty$ , however, this is only an approximate basis: The mass eigenstates are mixed. Moreover, *changing  $m_q$  changes the mixing angle*. We suggest this as a paradigm for the CKM rotation. In an attempt to construct a realistic two-family model [164, 171], specific relations among parameters are necessary in order to ensure that the  $J = 3/2$  state lies much higher in mass than the  $J = 1/2$  ones, and in order to obtain the appropriate “texture” zero in the upper left-hand corner of the  $2 \times 2$  mass matrix for the  $J = 1/2$  states. The three-family model constructed in Ref. [164] from similar arguments leads to the mass matrix (77) with  $p = q = \sqrt{2}$ .

### C. Is the top quark special?

The top quark is heavier, *so far*, than any other known fermion. We do not know if this is merely because it is near the limit of what one can produce via the strong interactions at present energies (this is certainly true), or something more fundamental. Many suggestions have been made about the crucial role played by its large mass. We have mentioned already the contribution of  $m_t$  to loop diagrams in particle-antiparticle mixing (Sec. 2) and in precise electroweak physics (Sec. 3). Here we mention some roles of a more fundamental nature which a heavy top might play.

Veltman [175] proposed that the top quark plays a crucial role in the cancellation of quadratic divergences in the effective Higgs potential, leading to the mass relation  $12m_t^2 = 3M_H^2 + 3m_Z^2 + 6M_W^2$  in the limit that other quark masses are neglected. This implies that the Higgs boson lies slightly below  $2m_t$  in mass, as if it were a  $t\bar{t}$  bound state. In the limit in which the electroweak couplings  $g$  and  $g'$  vanish,  $M_H \rightarrow 2m_t$  and the binding energy vanishes.

Nambu [176], drawing in part on his pioneering work with Jona-Lasinio [177], notes that in many dynamical symmetry breaking schemes, in which a condensate of fermion pairs  $\langle f\bar{f} \rangle \neq 0$  leads to chiral symmetry breaking, there exist in the spectrum

Table 12: Analogy between states in Nambu-Jona-Lasinio (NJL) model and dynamic symmetry breaking (DSB) in electroweak interactions

State in NJL model	Role	State in DSB scheme	Role
Pions	Nambu-Goldstone bosons of spont. broken chiral symm.	Higgs bosons $\phi^\pm$ and $(\phi^0 - \bar{\phi}^0)/\sqrt{2}$	Provide longitudinal components of $W$ and $Z$ bosons
Nucleon	Constituent of pion	Top quark	Constituent of Higgs boson?
$\sigma$	Weakly bound nucleon-antinucleon state	Higgs boson $(\phi^0 + \bar{\phi}^0)/\sqrt{2}$	Preserves unitarity in scatt. of longit. $W$ 's and $Z$ 's

not only a zero-mass pseudoscalar boson, but the fermion  $f$  and a scalar excitation “ $\sigma$ ” at  $m_\sigma = 2m_f$ . The analogies suggested by this observation are shown in Table 12.

Bardeen, Hill, and Lindner [178] emulate the Nambu-Jona-Lasinio model with a new interaction to generate the Higgs boson out of  $t\bar{t}$ . A nonzero condensate  $\langle t\bar{t} \rangle \neq 0$  develops, leading to electroweak symmetry breaking. The new interactions are needed both to bind  $t\bar{t}$  and to communicate the effects of the nonzero condensate to the other fermions.

In contrast to the above approach, Gérard and Weyers [179] introduce no new interaction. The Higgs field  $\phi$  initially has  $m_\phi^2 > 0$ ; its coupling to  $t\bar{t}$  turns an effective Higgs potential with upward curvature at  $\phi = 0$  into one with negative curvature, so that a non-zero value of  $\langle \phi \rangle$  develops, triggering electroweak symmetry breaking. This scheme only is self-consistent for a narrow range of Higgs boson masses around  $85 \text{ GeV}/c^2$ , and thus makes a very specific prediction.

Some versions of supersymmetry, described in more detail in Ref. [180] and by Graham Ross at this Institute [1], have two Higgs doublets with  $m^2$  values which are the same at some very large (unification) mass scale  $\mu$ . One doublet ( $\phi_1$ ) interacts with down-type quarks and charged leptons, while the other ( $\phi_2$ ) interacts with up-type quarks (including the top quark) and perhaps neutrinos. As a result of the strong coupling of  $\phi_2$  with the top quark,  $m^2(H_2)$  (where  $H_2$  is the neutral scalar object in the complex doublet  $\phi_2$ ) evolves toward a negative value as  $\mu$  is lowered, triggering electroweak symmetry breaking.

A scheme known as “reduction of coupling constants” [181] (see also [182]) or “gauge – Yukawa unification” [183] notes the presence of special relations for the renormalization-group behavior of coupling constants when gauge couplings  $g$  and Yukawa couplings  $g_Y$  are related. In contrast to supersymmetry, these schemes do not necessarily entail any extended symmetries. They posit a special role for finiteness in perturbation theory to each order.

## D. Technicolor

The electroweak dynamical symmetry breaking scheme described in Table 12 makes use of the top quark to form a fermion condensate which breaks the symmetry. One can also postulate some *new* fermion which binds with its antiparticle under some new superstrong force to form the pseudo-Nambu-Goldstone bosons which are

needed to make the  $W$  and  $Z$  massive. This is the essence of the scheme [184, 185] which has come to be known as “technicolor.”

Suppose the  $u$  and  $d$  quark were massless. The pion would be a massless quark-antiquark bound state in QCD. Its coupling to the  $W$  via the divergence of the axial current would give the  $W$  a mass  $M_W = gF_\pi/2 \simeq 30 \text{ MeV}/c^2$ , where we use the normalization  $F_\pi = 93 \text{ MeV}$  here. In order to generate a  $W$  with mass  $M_W = gv/2 = 80.34 \text{ GeV}/c^2$ , noting that  $g^2/4\pi \simeq 1/30$ , we need instead some fermion-antifermion pair with a decay constant  $v = 246 \text{ GeV}$ . Thus, one needs an interaction which becomes strong at a mass scale roughly  $246/0.093 = 2650$  times as high as the QCD scale. This is the postulated technicolor interaction. The fermions responding to this interaction are known as *technifermions*.

The  $Z - \gamma - \gamma$  vertex described by a triangle diagram like that in Fig. 2 will be anomaly-free if the sum over technifermions  $F$  of  $Q_F^2 I_{3L}^F$  vanishes. The simplest way in which this can be realized is with a single doublet with  $Q_F = \pm 1/2$ . The doublet may come in  $N_T$  different “technicolors.” This is “minimal technicolor.” It works fine for the masses of the  $W$  and  $Z$ .

An extension of technicolor to the description of quark and lepton masses immediately runs into difficulty. A new interaction (“extended technicolor” [186]) is needed to communicate the effects of  $\langle \bar{F}F \rangle \neq 0$  to the ordinary quarks and leptons. This interaction has the potential for introducing flavor-changing neutral currents and steps must be taken to prevent them. The biggest mass (top) naturally poses the biggest problem for this theory.

## E. Quark-lepton pattern and new physics

Returning again to Fig. 1, we see that the up-type quarks are less “dense” than the down-type quarks or charged leptons on a logarithmic plot. Moreover, their center of gravity is higher. This suggests that the down-type quarks and charged leptons are being pushed down in mass by mixing with heavier extra levels with  $Q = \pm 1/3$  and  $Q = \pm 1$ .

The situation with the neutrinos is even more extreme. They appear to be very light if not massless. (Oscillation results, which would require non-zero masses, are not yet conclusive.) A popular way to understand such light masses is the “seesaw” mechanism [187] involving mixing with other very heavy neutrinos. The neutrino mass matrix may be written in terms of left-handed states in a basis  $(\nu_L, \nu_L^c)$  as

$$\mathcal{M}_\nu = \begin{bmatrix} 0 & m_D \\ m_D & M \end{bmatrix}, \quad (80)$$

where  $m_D$  stands for a Dirac mass, and  $M$  is a large Majorana mass. The eigenvalues of this matrix are approximately  $-m_D^2/M$  and  $M$ , corresponding to the eigenvectors  $[1, -m_D/M]$  and  $[m_D/M, 1]$ .

Thus, the large top quark mass could be telling us that at higher masses one expects more matter which is *not* like the top quark: quarks of charge  $-1/3$  or new leptons. What can serve as the source for these new forms of matter? We seek the answer in several schemes for quark-lepton unification.

## F. Quark-lepton unity

The “grand unification” of strong and electroweak interactions in a larger symmetry, and the identification of quarks and leptons as objects related to one another under this symmetry, involves such groups as  $SU(5)$  [188],  $SO(10)$  [189], and  $E_6$  [190].

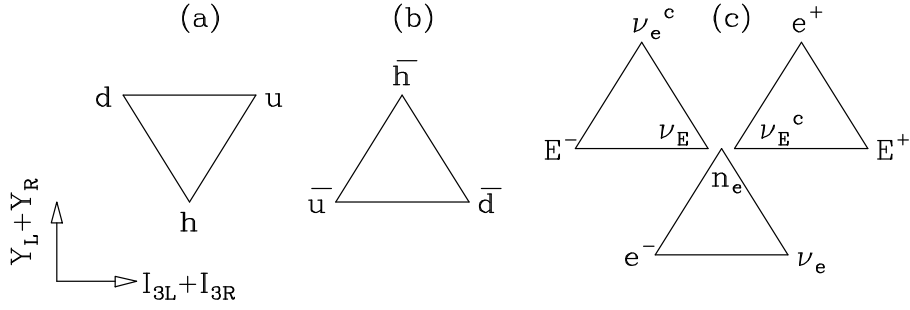


Figure 23: Left-handed fermions belonging to the **27**-plet of  $E_6$ . (a) Quarks [triangle denotes  $\mathbf{3}$  of  $SU(3)_L$ ]; (b) antiquarks [triangle denotes  $\mathbf{3}^*$  of  $SU(3)_R$ ]; (c) leptons [triangles denote  $\mathbf{3}^*$ 's of  $SU(3)_L$ ; they are arranged in a  $\mathbf{3}$  of  $SU(3)_R$ ].

One forms a  $5 \times 5$  matrix of  $SU(5)$  by simply putting the  $3 \times 3$  matrices of color  $SU(3)$  in the upper left-hand corner and the  $2 \times 2$  matrices of  $SU(2)_L$  in the lower right. The miracle of  $SU(5)$  is that it also possesses a  $U(1) \sim \text{diag}(2, 2, 2, -3, -3)$  which is just right for weak hypercharge!

Within  $SU(5)$  a specific choice of representations ( $\mathbf{5}^* + \mathbf{10}$ ) is required for the left-handed fermions in order to accommodate the known states and to eliminate anomalies. This choice is automatic if left-handed fermions are assigned to the **16**-dimensional spinor multiplet of  $SO(10)$ ; the additional state is a right-handed neutrino. Thus, we have the decomposition

$$[SO(10)] \quad \mathbf{16}_L = \mathbf{5}_L^* + \mathbf{10}_L + \mathbf{1}_L \quad [SU(5)] \quad . \quad (81)$$

The right-handed neutrino can acquire a large Majorana mass without violating the  $SU(3)_c \times SU(2)_L \times U(1)$  symmetry of the standard model. Anomalies are not present in  $SO(10)$ , as long as matter belongs to complete multiplets.

The group  $E_6$  contains  $SO(10)$ . Its lowest-dimensional representation (**27**) contains the **16** of  $SO(10)$ , as well as **10**- and **1**-dimensional (“exotic”) representations of  $SO(10)$ . These, in turn, have the following  $SU(5)$  decompositions:

$$[SO(10)] \quad \mathbf{10}_L = \mathbf{5}_L + \mathbf{5}_L^* \quad [SU(5)] \quad ; \quad [SO(10)] \quad \mathbf{1}_L = \mathbf{1}_L \quad [SU(5)] \quad . \quad (82)$$

There has been some interest in  $E_6$  as a result of its appearance in certain versions of superstring theories [191, 192].

### G. The $E_6$ zoo

One way to illustrate the particle content of the **27**-plet of  $E_6$  is via the decomposition [193]  $E_6 \rightarrow SU(3)_c \times SU(3)_L \times SU(3)_R$ , whereby

$$\mathbf{27}_L = (\mathbf{3}_c, \mathbf{3}_L, \mathbf{1}_R) + (\mathbf{3}_c^*, \mathbf{1}_L, \mathbf{3}_R^*) + (\mathbf{1}_c, \mathbf{3}_L^*, \mathbf{3}_R) \quad . \quad (83)$$

The left-handed fermions can then be plotted in a space (Fig. 23) in which the  $x$ -axis is  $I_{3L} + I_{3R}$ , while the  $y$ -axis is  $Y_L + Y_R$ . The electric charge of particles is  $Q_{\text{em}} = I_{3L} + I_{3R} + (Y_L + Y_R)/2$ . (I thank Graham Ross for reminding me of the utility of this picture.) The new particles [beyond those in the **16** of  $SO(10)$ ] consist of  $h$  (an isosinglet  $Q = -1/3$  quark),  $E^\pm$  (a weak isodoublet charged lepton),  $\nu_E$  and  $\nu_E^c$  (a weak isodoublet Dirac neutrino, or else two Majorana neutrinos each belonging to a weak

Table 13: Cross sections  $\sigma$  [in units of  $\sigma_0 \equiv \sigma(e^+e^- \rightarrow \gamma^* \rightarrow \mu^+\mu^-)$ ] for  $e^+e^-$  production of pairs of exotic fermions  $f\bar{f}$  via virtual photons and  $Z$ 's in the direct channel. The  $\nu_E$  is assumed to be a Dirac neutrino. Values of  $g_V^f$  are quoted for  $x = 0.2315$ . QCD corrections to  $h$  quark production have been neglected.

Fermion	$Q_f$	$g_V^f$	$g_A^f$	$\sigma/\sigma_0$ far below $Z$	$\sigma/\sigma_0$ far above $Z$
$h$	$-1/3$	0.0772	0	$1/3$	0.35
$E^-$	$-1$	$-0.2685$	0	1	1.20
$\nu_E$	0	$1/2$	0	0	0.50

isodoublet), and an “inert” isosinglet Majorana neutrino  $n_e$ . By “weak isodoublet” or “weak isosinglet” we mean behavior under  $SU(2)_L$ .

Another way to visualize the additional states in  $E_6$  is to note that the standard-model fermions belonging to  $(\mathbf{16}, \mathbf{5}^*)$  of  $(SO(10), SU(5))$  are a column vector consisting of  $(\bar{d}_1, \bar{d}_2, \bar{d}_3, e^-, \nu_e)$ . Then since  $SU(5)$  contains all the standard-model generators, equal  $SU(5)$  representations have equal standard-model transformation properties. (We are not considering “flipped”  $SU(5)$  models in which the electric charge lies outside  $SU(5)$  [194].) Thus, in  $(\mathbf{10}, \mathbf{5}^*) = (\bar{h}_1, \bar{h}_2, \bar{h}_3, E^-, \nu_E)$ , one identifies the  $\bar{h}_i$  states as a color-triplet of isosinglet  $Q = 1/3$  antiquarks, and  $(E^-, \nu_E)$  as a weak isodoublet of leptons. In the charge-conjugate representation  $(\mathbf{10}, \mathbf{5}) = (h_1, h_2, h_3, E^+, \nu_E^c)$ , the  $Q = -1/3$  quarks  $h$  are then weak *isosinglets*, while  $E^+, \nu_E^c$  are a weak *isodoublet*. Such fermions are not encountered in the standard model. Neither is the  $(\mathbf{1}, \mathbf{1})$  consisting of the single state  $n_e$ , which is a weak isosinglet.

One can calculate the cross sections for  $e^+e^- \rightarrow (\gamma^*, Z^*) \rightarrow f\bar{f}$  for the new fermions, in the manner leading to Table 10. In computing the values of  $g_V$  and  $g_A$  for  $E^-$  and a Dirac neutrino  $\nu_E$  both left-handed and right-handed states have the same value of  $I_{3L}$ :  $-1/2$  for  $E^-$  and  $+1/2$  for  $\nu_E$ . The results are shown in Table 13.

All of these states are produced exclusively via the vector current, and hence their maximum cross section is expected to occur very close to threshold. If one is sufficiently far from the  $Z$  pole, this maximum occurs at  $E_{c.m.} \simeq 1.18E_{th}$ . Closer to the  $Z$  pole, the maximum occurs even lower [195].

The new fermions in  $E_6$  are marginally consistent with the constraints on the parameters  $S$  and  $T$  mentioned in Sec. 3. The parameter  $T$  describes the effects of mass difference between  $I_{3L} = +1/2$  and  $I_{3L} = -1/2$  fermions. Recalling  $\rho/\rho^{\text{nominal}} = 1 + \alpha T$ , a more precise expression for  $\Delta\rho$  than that given in terms of  $m_t$  is [196]

$$\Delta\rho = \frac{N_c G_F}{8\sqrt{2}\pi^2} \left( m_1^2 + m_2^2 - \frac{4m_1^2 m_2^2}{m_1^2 - m_2^2} \ln \frac{m_1}{m_2} \right) . \quad (84)$$

The  $E_6$  fermions thus make a significant contribution to  $\Delta\rho$  only when  $m(E^-) \neq m(\nu_E)$ . The exotic quarks do not contribute because they are isosinglets.

The parameter  $S$  arises as a result of  $W^0 - B$  mixing [115]. Consequently, it receives no contribution in  $E_6$  from the isosinglet  $h$  quarks. There are two doublets  $(E^-, \nu_E)$  and  $(E^+, \nu_E^c)$  of leptons per family, leading to a contribution  $\Delta S = 2(1/6\pi) \simeq 0.1$  per family. One can just barely tolerate three families.

## H. Extended gauge structure

At any given mass scale, there is an interplay between the fermion spectrum and

the subgroup of any grand unified theory (GUT) which remains unbroken at that mass scale. If a fermion is heavy, no GUT subgroup which relies on that fermion for anomaly cancellation should be unbroken far below that fermion's mass. Let us recapitulate how this works in several of the unified gauge groups we have mentioned.

1. In  $SU(5)$  we need a  $\mathbf{5}^*$  and a  $\mathbf{10}$  to avoid anomalies in  $I_{3L}Q^2$ .
2. In  $SO(10) \rightarrow SU(5) \times U(1)_\chi$  (the notation is that of Refs. [192] and [197]), the  $U(1)_\chi$  symmetry is anomalous (the sum of  $Q_\chi I_{3L}^2$  is non-zero) unless the  $\nu_L^c$  is light.
3. In  $SO(10) \rightarrow SO(6) \times SO(4)$  (which is the same as  $SU(4) \times SU(2)_L \times SU(2)_R$ ), the subsequent symmetry breakdowns are  $SU(4) \rightarrow SU(3)_C \times U(1)_{B-L}$  and  $SU(2)_R \rightarrow U(1)_R$ . Each of these  $U(1)$ 's separately is anomalous unless the  $\nu_L^c$  is light. However, one can write the electric charge as

$$Q = I_{3L} + I_{3R} + \frac{B-L}{2} = I_{3L} + \frac{Y_W}{2} \quad (85)$$

Since  $I_{3L}(\nu_L^c) = -1/2$  while  $(-L/2)(\nu_L^c) = +1/2$ , one has  $(Y_W/2)(\nu_L^c) = 0$ , and the  $Y_W$  anomaly is insensitive to  $\nu_L^c$ .

4. In  $E_6 \rightarrow SO(10) \times U(1)_\psi$  (see, again, [192, 197]) the cancellation of the  $U(1)_\psi$  anomaly requires the entire  $\mathbf{27}$ -plet to be light.

One may conjecture that the converse is also true: If an extended set of fermions is found to be light, there may exist an extended gauge structure for which this set of fermions provides the required anomaly cancellation. Thus, the search for new fermions may have bearing on extended gauge structures. One can also directly search for new gauge bosons (see, e.g., Ref. [198]) in lepton pair production, identifying them via characteristic forward-backward asymmetries [199, 200].

## I. An unusual event

The CDF Collaboration [201] has reported one event with an electron-positron pair, two photons, and missing energy ( $e^+e^- \gamma\gamma \cancel{E}_T$ ), produced in proton-antiproton collisions at  $E_{\text{c.m.}} = 1.8$  TeV. Popular interpretations of this event have appeared within the context of supersymmetry [202], involving the production of a pair of selectrons ( $\tilde{e}^+\tilde{e}^-$ ) or a pair of charginos ( $\chi^+\chi^-$ ) which then decay to  $e^+e^-$  and radiatively-decaying neutral superpartners. An interpretation has also appeared in one non-supersymmetric model [203].

The  $E_6$  scenario mentioned above can interpret this event in the following way [195]:

$$\bar{p}p \rightarrow Z_I + \dots \rightarrow E^+E^- + \dots \quad (86)$$

followed by the chain

$$E^- \rightarrow e^- W_I^{(*)} \rightarrow e^- \bar{N}_e \bar{n}_e \rightarrow e^- \gamma n_e \bar{n}_e \quad (87)$$

and its charge-conjugate for  $E^+$  decay. The  $n_e$  state is allowed to be stable as long as its mass satisfies cosmological bounds (typically less than a few tens of eV). The  $Z_I$  is a neutral gauge boson with mass greater than present limits [198] of a few hundred GeV. The  $W_I$  belongs to a subgroup  $SU(2)_I$  of  $E_6$  along with the  $Z_I$  [204]; it occurs in the decomposition  $E_6 \rightarrow SU(2)_I \times SU(6)$ , where the  $SU(6)$  breaks subsequently to the standard  $SU(5)$  GUT. The  $W_I$  is probably virtual, as indicated by the asterisk in parentheses. The neutral nature of all three bosons in  $SU(2)_I$  is a key feature permitting the flavor of  $E^-$  to be passed on to the electron.

How does one tell the difference between these scenarios? Supersymmetry has superpartners of the gauge bosons known as ‘‘gauginos,’’ and very specific relations between couplings involving superpartners and ordinary couplings.  $E_6$  has exotic fermions

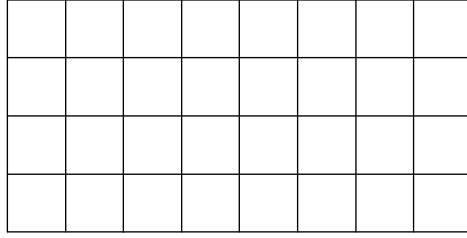


Figure 24: Part of a familiar pattern.

but they are not superpartners of Higgs bosons [despite a superficial resemblance; both belong to  $\mathbf{10}$ 's of  $\text{SO}(10)$ .] A typical reaction expected in  $E_6$  is  $e^+e^- \rightarrow \nu_E \bar{\nu}_E$ , followed by  $\nu_E \rightarrow \nu_e \bar{N}_1 N_2$ , with one of the exotic neutrinos  $\bar{N}_1$  decaying radiatively to  $\bar{N}_2 + \gamma$ .

A feature common to both scenarios is that in addition to the  $e^+e^- \gamma \cancel{E}_T$  event, one should also see in  $\bar{p}p$  collisions some diphoton events with missing transverse energy and *without* charged lepton pairs. Searches for such events have been performed in the CDF data [205]. Of all events with two photons and missing transverse energy, the event  $e^+e^- \gamma \cancel{E}_T$  has the highest  $\cancel{E}_T$ . Thus, there are no indications yet of non-standard behavior in the diphoton events with  $\cancel{E}_T$  but without  $e^+e^-$ .

There is still a need for extensive discussions of standard-model backgrounds to this event, such as multiple interactions, radiative production of  $W$  pairs, effects of cracks in the detector, and so on. One cannot conclude anything from a single event, but it can point the way to searches for related phenomena.

## 7. CONCLUSIONS

We have discussed the top quark mass more from the standpoint of what it does than where it comes from. It participates in a crucial way in loop diagrams, leading to mixing of neutral kaons and  $B$  mesons, thereby accounting for CP violation in the kaon system and predicting appreciable CP-violating effects for  $B$ 's. It also affects electroweak observables, to the extent that its mass could be anticipated to within a few tens of  $\text{GeV}/c^2$  before it was discovered.

The origin of the top quark mass, on the other hand, is related to the origin of *all* the quark masses, which also is linked to the curious pattern of weak charge-changing couplings expressed by the Cabibbo-Kobayashi-Maskawa (CKM) matrix. We have presented a *potpourri* of ideas about these questions while not finding any of them particularly conclusive. The best we can do is to note some overall patterns suggested by the quark and lepton masses in Fig. 1, which may indicate that we are not yet in possession of the complete experimental picture. At the very least, this is certainly the case for neutrinos, where we don't even know if they have masses. But there could be more. I leave you with the following exercise in pattern recognition: What familiar pattern do you see in Fig. 24?

One can re-express the pattern as shown in Fig. 25; perhaps it suggests something at this point.

Finally, when one adds variety to the pattern, it becomes recognizable as the periodic table of the elements (Fig. 26).

The variety of the pattern of the elementary particles laid the foundations of the quark model and our understanding of the fundamental strong interactions. Will there be a similar advance for quarks and leptons? The pattern of quarks and leptons has been quite regular up to now, just as if the periodic table of the elements consisted





Figure 25: Part of a familiar pattern, expressed differently.

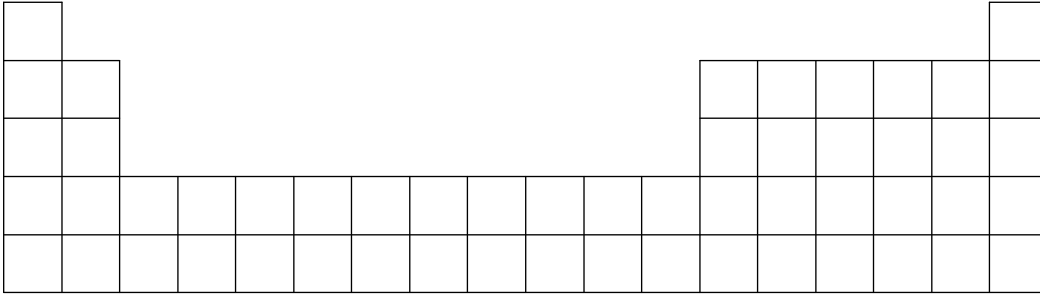


Figure 26: A larger part of a familiar pattern.

only of rows of equal length and were missing hydrogen, helium, the transition metals, the lanthanides, and the actinides. Whether one discovers superpartners of the known states, or variety such as predicted in extended gauge structures, the new states could help us to make sense of the pattern of the masses of the more familiar ones. In this sense the top quark mass may not be the end of a story, but just the beginning.

## ACKNOWLEDGMENTS

I would like to thank Jim Amundson, Isi Dunietz, Aaron Grant, Michael Gronau, Oscar Hernández, Nahmin Horowitz, Mike Kelly, Harry Lipkin, David London, Bill Marciano, Alex Nippe, Sheldon Stone, Tatsu Takeuchi, and Mihir Worah for enjoyable collaborations on some of the topics mentioned in these lectures. In addition I am grateful to Gideon Alexander, Guido Altarelli, Alain Blondel, Keith Ellis, Paul Frampton, Henry Frisch, Michaelangelo Mangano, Paolo Nason, Matthias Neubert, Steve Pollock, Graham Ross, Chris Sachrajda, Bob Sachs, Pat Sandars, Michael Schmitt, Jack Steinberger, Sam Ting, Tini Veltman, Petr Vogel, Brian Webber, Larry Willets, Bruce Winstein, and Lincoln Wolfenstein for fruitful discussions, and to the CERN Theory Group for its hospitality during the preparation of this report. Finally, I wish to thank the organizers of the Summer Institute and all of my other hosts in Cargèse for making this first visit such an enjoyable one. Parts of the research described here were performed at the Aspen Center for Physics, the Fermilab Theory Group, the Institute for Nuclear Theory at the University of Washington, and the Technion. This work was supported in part by the United States Department of Energy under Grant No. DE FG02 90ER40560.

## References

- [1] G. Ross, lectures at this Institute.
- [2] T. J. LeCompte, Top decay physics at CDF and measurement of the CKM element  $V_{tb}$ , Fermilab report FERMILAB-CONF-96-021-E, Jan., 1996, presented at 2nd Rencontres du Vietnam, *Physics at the Frontiers of the Standard Model*, Ho Chi Minh City, Vietnam, 21 – 28 Oct., 1995.
- [3] N. Cabibbo, *Phys. Rev. Lett.* 10:531 (1963).
- [4] M. Kobayashi and T. Maskawa, *Prog. Theor. Phys.* 49:652 (1973).
- [5] J. L. Rosner, Present and future aspects of CP violation, Enrico Fermi Institute Report No. 95-36 [hep-ph/9506364], lectures given at the VIII J. A. Swieca Summer School, *Particles and Fields*, Rio de Janeiro, February, 1995, proceedings to be published by World Scientific.
- [6] S. L. Glashow, *Nucl. Phys.* 22:579 (1961); S. Weinberg, *Phys. Rev. Lett.* 19:1264 (1967); A. Salam, in *Proceedings of the Eighth Nobel Symposium*, edited by N. Svartholm (Almqvist and Wiksell, Stockholm; Wiley, New York, 1978), p. 367.
- [7] LEP Electroweak Working Group, CERN report LEPEWWG/96-02, July 30, 1996, presented at XXVIII International Conference on High Energy Physics, Warsaw, July 25–31, 1996.
- [8] Y. Hara, *Phys. Rev.* 134:B701 (1964); Z. Maki and Y. Ohnuki, *Prog. Theor. Phys.* 32:144 (1964); B. J. Bjorken and S. L. Glashow, *Phys. Lett.* 11:255 (1964).
- [9] M. Gell-Mann and M. Lévy, *Nuovo Cim.* 19:705 (1960).
- [10] S. L. Glashow, J. Iliopoulos, and L. Maiani, *Phys. Rev. D* 2:1285 (1970).
- [11] C. Bouchiat, J. Iliopoulos, and Ph. Meyer, *Phys. Lett.* 38B:519 (1972). See also H. Georgi and S. L. Glashow, *Phys. Rev. D* 6:429 (1972); D. J. Gross and R. Jackiw, *ibid.* 6:477 (1972).
- [12] For more details see, e.g., V. L. Fitch and J. L. Rosner, Elementary particle physics in the second half of the twentieth century, in *Twentieth Century Physics*, edited by L. M. Brown, A. Pais, and B. Pippard (AIP/IOP, New York and Bristol, 1995), ch. 9.
- [13] W. Pauli, Zur älteren und neueren Geschichte des Neutrinos, in *Collected Scientific Papers*, R. Kronig and V. F. Weisskopf, eds., Interscience, New York, 1964, v. 2, p. 1313.
- [14] See, e.g., L. M. Brown, in *Twentieth Century Physics*, L. M. Brown, A. Pais, and B. Pippard, eds., AIP/IOP, New York and Bristol, 1995, ch. 5.
- [15] S. H. Neddermeyer and C. D. Anderson, *Phys. Rev.* 51:884 (1937). See also J. C. Street and E. C. Stevenson, *Phys. Rev.* 51:1005 (1937); Y. Nishina, M. Takeuchi, and T. Ichimaya, *Phys. Rev.* 52:1198 (1937).
- [16] G. Danby *et al.*, *Phys. Rev. Lett.* 9:36 (1962).
- [17] J. J. Aubert *et al.*, *Phys. Rev. Lett.* 33:1404 (1974).

- [18] J.-E. Augustin *et al.*, *Phys. Rev. Lett.* 33:1406 (1974).
- [19] E. G. Cazzoli *et al.*, *Phys. Rev. Lett.* 34:1125 (1975); G. Goldhaber *et al.*, *Phys. Rev. Lett.* 37:255 (1976); I. Peruzzi *et al.*, *Phys. Rev. Lett.* 37:569 (1976).
- [20] M. Perl *et al.*, *Phys. Rev. Lett.* 35:1489 (1975); *Phys. Lett.* 63B:466 (1976); *Phys. Lett.* 70B:487 (1977).
- [21] H. Harari, in *Proceedings of the 1975 International Symposium on Lepton and Photon Interactions at High Energies*, Stanford University, Aug. 21–27, 1975, W. T. Kirk, ed., SLAC, Stanford, CA, (1975), p. 317.
- [22] S. W. Herb *et al.*, *Phys. Rev. Lett.* 39:252 (1977); W. R. Innes *et al.*, *Phys. Rev. Lett.* 39:1240, 1640(E) (1977).
- [23] S. Behrends *et al.* (CLEO Collaboration), *Phys. Rev. Lett.* 50:881 (1983).
- [24] F. Abe *et al.* (CDF Collaboration), *Phys. Rev. Lett.* 73:225 (1994); *Phys. Rev. D* 50:2966 (1995); *Phys. Rev. Lett.* 74:2626 (1995); S. Abachi *et al.* (D0 Collaboration), *Phys. Rev. Lett.* 74:2632 (1995).
- [25] Fermilab E-872, R. Ramieka, spokesperson. See B. Lundberg *et al.*, Measurement of  $\tau$  lepton production from the process  $\nu_\tau + N \rightarrow \tau$ , Fermilab proposal P-872, Jan., 1994.
- [26] P. Tipton, Plenary talk, XXVIII International Conference on High Energy Physics, Warsaw, July 25–31, 1996; CDF Collaboration, presented by R. Hughes, reports PA-05-052, PA05-053, and PA08-108; D0 Collaboration, presented by A. Zieminski, reports PA05-027, PA05-028, and PA05-029.
- [27] M. Jezabek, J. H. Kühn, and T. Teubner, *Zeit. Phys. C* 56:653 (1992).
- [28] Mark III Collaboration, R. M. Baltrusaitis *et al.*, *Phys. Rev. Lett.* 52:2126 (1984).
- [29] See, e.g., W. Kwong and J. L. Rosner, *Phys. Rev. D* 38:279 (1988); W. Buchmüller and S. Cooper, Upsilon spectroscopy, in *High-Energy Electron-Positron Physics*, A. Ali and P. Söding, eds., World Scientific, Singapore (1988), p. 412.
- [30] C. Quigg and J. L. Rosner, *Phys. Lett.* 71B:153 (1977); *Comments on Nucl. and Part. Phys.* 8:11 (1978); *Phys. Rep.* 56:167 (1979).
- [31] A. Martin, *Phys. Lett.* 93B:338 (1980); *ibid.* 100B:511 (1981).
- [32] CLEO Collaboration, P. Avery *et al.*, *Phys. Rev. Lett.* 75:4364 (1995); L. Gibbons *et al.*, *Phys. Rev. Lett.* 77:810 (1996).
- [33] CLEO Collaboration, report PA01-078, presented by R. Kutschke at XXVIII International Conference on High Energy Physics, Warsaw, July 25–31, 1996. We thank J. Yelton for communicating this result to us.
- [34] M. Neubert, lectures at this Institute. See also M. Neubert, CERN report CERN-TH/96-55 [hep-ph/9604412], to be published in *Int. J. Mod. Phys. A*.
- [35] N. Gray, D. J. Broadhurst, W. Grafe, and K. Schilcher, *Zeit. Phys. C* 48:673 (1990), and references therein.

- [36] A. Ali and D. London, DESY report DESY 96-140 [hep-ph/9607392], presented at High Energy Physics International Euroconference on QCD (QCD 96), Montpellier, France, July 4 – 12, 1996.
- [37] L.-L. Chau and W.-Y. Keung, *Phys. Rev. Lett.* 53:1802 (1984); H. Harari and M. Leurer, *Phys. Lett. B* 181:123 (1986); J. D. Bjorken and I. Dunietz, *Phys. Rev. D* 36:2109 (1987).
- [38] L. Wolfenstein, *Phys. Rev. Lett.* 51:1945 (1983).
- [39] See, e.g., M. Bourquin *et al.*, *Zeit. Phys. C* 21:27 (1983); H. Leutwyler and M. Roos, *Zeit. Phys. C* 25:91 (1984); J. F. Donoghue, B. R. Holstein, and S. W. Kliment, *Phys. Rev. D* 35:934 (1987); F. J. Gilman, K. Kleinknecht, and B. Renk, in Review of particle properties, Particle Data Group, *Phys. Rev. D* 54:94 (1996).
- [40] T. Browder and K. Honscheid, *Prog. Nucl. Part. Phys.* 35:81 (1995).
- [41] L. Gibbons, Plenary talk, XXVIII International Conference on High Energy Physics, Warsaw, July 25–31, 1996.
- [42] L.-L. Chau and W.-Y. Keung, *Phys. Rev. Lett.* 53:1802 (1984); M. Gronau and J. Schechter, *ibid.* 54:385 (1985); M. Gronau, R. Johnson, and J. Schechter, *Phys. Rev. D* 32:3062 (1985); C. Jarlskog, in *Physics at LEAR with Low Energy Antiprotons*, proceedings of the workshop, Villars-sur-Ollon, Switzerland, 1987, edited by C. Amsler *et al.* (Harwood, Chur, Switzerland, 1988), p. 571; J. D. Bjorken and I. Dunietz, *Phys. Rev. D* 36:2109 (1987).
- [43] Y. Nir and H. Quinn, *Ann. Rev. Nucl. Part. Sci.* 42:211 (1992).
- [44] T. P. Cheng and L. F. Li, *Gauge Theory of Elementary Particles* (Oxford University Press, 1984).
- [45] J. L. Rosner, in *Testing the Standard Model* (Proceedings of the 1990 Theoretical Advanced Study Institute in Elementary Particle Physics), edited by M. Cvetič and P. Langacker (World Scientific, Singapore, 1991), p. 91.
- [46] T. Inami and C. S. Lim, *Prog. Theor. Phys.* 65:297 (1981); *ibid.* 65:1772(E) (1981).
- [47] Particle Data Group, *Phys. Rev. D* 54:1 (1996).
- [48] A. Abada *et al.*, *Nucl. Phys.* B376:172 (1992).
- [49] A. Buras, M. Jamin, and P. H. Weisz, *Nucl. Phys.* B347:491 (1990).
- [50] UA1 Collaboration, C. Albajar *et al.*, *Phys. Lett. B* 186:237, 247 (1987); *ibid.* 197:565(E) (1987).
- [51] ARGUS Collaboration, H. Albrecht *et al.*, *Phys. Lett. B* 192:245 (1987).
- [52] ALEPH Collaboration, D. Buskulic *et al.*, *Phys. Lett. B* 313:498 (1993); DELPHI Collaboration, P. Abreu *et al.*, *Phys. Lett. B* 338:409 (1994); OPAL Collaboration, R. Akers *et al.*, *Phys. Lett. B* 327:411 (1994); *ibid.* 336:585 (1994). For a compilation of the many new LEP results presented in 1996 see Ref. [41].

- [53] CDF Collaboration, F. Abe *et al.*, Fermilab report FERMILAB-CONF-95-231-E, July, 1995, contributed to *LP95: Proceedings of the International Symposium on Lepton and Photon Interactions (IHEP)*, 10–15 August 1995, Beijing, People’s Republic of China, Z.-P. Zheng and H.-S. Chen, eds., World Scientific, Singapore, 1996; report PA08-032, presented by P. Sphicas at XXVIII International Conference on High Energy Physics, Warsaw, July 25–31, 1996.
- [54] SLD Collaboration, reports PA08-026A, PA08-026B, and PA08-027/028, presented by D. Su at XXVIII International Conference on High Energy Physics, Warsaw, July 25–31, 1996.
- [55] C. Zeitnitz, invited talk at the 4th International Workshop on *B*-Physics at Hadron Machines (BEAUTY 96), Rome, June 17–21, 1996, proceedings to be published in *Nucl. Instr. Meth.* A slightly different average was presented in Ref. [41]:  $\Delta m_d = 0.464 \pm 0.017 \text{ ps}^{-1}$ .
- [56] CERN WA75 Collaboration, S. Aoki *et al.*, *Prog. Theor. Phys.* 89:131 (1993); CLEO Collaboration, D. Acosta *et al.*, *Phys. Rev. D* 49:5690 (1994); F. Muheim and S. Stone, *Phys. Rev. D* 49:3767 (1994); BES Collaboration, J. Z. Bai *et al.*, *Phys. Rev. Lett.* 74:4599 (1995); F. Muheim, parallel session on *B* physics, in *The Albuquerque Meeting: DPF 94* (Division of Particles and Fields Meeting, American Physical Society, Albuquerque, NM, August 2–6, 1994), ed. by S. Seidel (World Scientific, River Edge, NJ, 1995); Fermilab E653 Collaboration, K. Kodama *et al.*, *Phys. Lett. B* 382:299 (1996).
- [57] ARGUS Collaboration, H. Albrecht *et al.*, *Phys. Lett. B* 219:121 (1989); D. Bortoletto, Ph. D. Thesis, Syracuse University, 1989; D. Bortoletto and S. L. Stone, *Phys. Rev. Lett.* 65:2951 (1990); CLEO Collaboration, D. Bortoletto *et al.*, *Phys. Rev. D* 45:2212 (1992); J. L. Rosner, *Phys. Rev. D* 42:3732 (1990); in *Research Directions for the Decade* (Proceedings of the 1990 DPF Snowmass Workshop), edited by E. L. Berger (World Scientific, Singapore, 1991), p. 255; M. Paulini *et al.*, in *Proceedings of the Joint International Symposium and Europhysics Conference on High Energy Physics*, S. Hegarty, K. Potter, and E. Quercigh, eds., World Scientific, Singapore (1992), p. 592; CLEO Collaboration, A. Bean *et al.*, *Phys. Rev. Lett.* 70:2681 (1993).
- [58] G. Martinelli, Plenary talk, XXVIII International Conference on High Energy Physics, Warsaw, July 25–31, 1996.
- [59] Mark III Collaboration, J. Adler *et al.*, *Phys. Rev. Lett.* 60:1375 (1988); *ibid.* 63:1658(E) (1989).
- [60] J. Z. Bai *et al.* (BEPC Collaboration), SLAC report SLAC-PUB-7147, 1996.
- [61] J. Amundson *et al.*, *Phys. Rev. D* 47:3059 (1993); J. L. Rosner, *The Fermilab Meeting – DPF 92* (Division of Particles and Fields Meeting, American Physical Society, Fermilab, 10–14 November, 1992), ed. by C. H. Albright *et al.* (World Scientific, Singapore, 1993), p. 658.
- [62] See, e.g., A. Duncan *et al.*, *Phys. Rev. D* 51:5101 (1995); UKQCD Collaboration, C. R. Allton *et al.*, *Nucl. Phys. B* 437:641 (1995); MILC Collaboration, C. Bernard *et al.*, report WASH-U-HEP-96-31, June, 1996 [hep-lat/9608092], presented at Lattice 96: 14th International Symposium on Lattice Field Theory, St. Louis, MO, 4–8 June 1996; G. Martinelli, Ref. [58].

- [63] B. Grinstein, *Phys. Rev. Lett.* 71:3067 (1993).
- [64] J. H. Christenson, J. W. Cronin, V. L. Fitch, and R. Turlay, *Phys. Rev. Lett.* 13:138 (1964).
- [65] *CP Violation*, edited by C. Jarlskog (World Scientific, Singapore, 1989).
- [66] M. Gell-Mann and A. Pais, *Phys. Rev.* 97:1387 (1955).
- [67] T. D. Lee, R. Oehme and C. N. Yang, *Phys. Rev.* 106:340 (1957); B. L. Ioffe, L. B. Okun' and A. P. Rudik, *Zh. Eksp. Teor. Fiz.* 32:396 (1957) [Sov. Phys. – JETP 5:328 (1957)].
- [68] K. Lande, E. T. Booth, J. Impeduglia, and L. M. Lederman, *Phys. Rev.* 103:1901 (1956).
- [69] L. Wolfenstein, *Phys. Rev. Lett.* 13:562 (1964).
- [70] A. J. Buras, M. Jamin, and P. H. Weisz, *Nucl. Phys.* B347:491 (1990); S. Herrlich and U. Nierste, *Nucl. Phys.* B419:292 (1994); *Phys. Rev. D* 52:6505 (1995).
- [71] C. Hamzaoui, J. L. Rosner, and A. I. Sanda, in *Proceedings of the Workshop on High Sensitivity Beauty Physics at Fermilab*, Fermilab, Nov. 11–14, 1987, edited by A. J. Slaughter, N. Lockyer, and M. Schmidt (Fermilab, Batavia, IL, 1988), p. 97; J. L. Rosner, A. I. Sanda, and M. P. Schmidt, *ibid.*, p. 165.
- [72] See, e.g., the following sources quoted by [36]: S. Sharpe, *Nucl. Phys. B (Proc. Suppl.)* 34:403 (1994); J. Bijnens and J. Prades, *Nucl. Phys.* B444:523 (1995); A. Soni, Brookhaven National Laboratory report BNL-62284 [hep-lat/9510036]; JLQCD Collaboration, S. Aoki *et al.*, *Nucl. Phys. B (Proc. Suppl.)* 47:465 (1996); APE Collaboration, M. Crisafulli *et al.*, *Phys. Lett. B* 369:325 (1996). Our quoted error reflect a somewhat more generous spread in values obtained by different means.
- [73] For discussions with references to earlier literature see, e.g., I. I. Bigi and A. I. Sanda, *Nucl. Phys.* B281:41 (1987); I. Dunietz, *Ann. Phys. (N.Y.)* 184:350 (1988); M. B. Wise, in *Particles and Fields 3* (Proceedings of the 1988 Banff Summer Institute on Particles and Fields), edited by A. N. Kamal and F. C. Khanna (World Scientific, Singapore, 1989), p. 124; I. I. Bigi, V. A. Khoze, N. G. Uraltsev, and A. I. Sanda, in Ref. [65], p. 175; J. L. Rosner, in *Testing the Standard Model* (Proceedings of the 1990 Theoretical Advanced Study Institute in Elementary Particle Physics), edited by M. Cvetič and P. Langacker (World Scientific, Singapore, 1991), p. 91; Y. Nir and H. R. Quinn, *Ann. Rev. Nucl. Part. Sci.* 42:211 (1992); B. Winstein and L. Wolfenstein, *Rev. Mod. Phys.* 65:1113 (1993).
- [74] I. Dunietz and J. L. Rosner, *Phys. Rev. D* 34:1404 (1986); I. Dunietz, Ref. [73].
- [75] D. London and R. Peccei, *Phys. Lett. B* 223:257 (1989); M. Gronau, *Phys. Rev. Lett.* 63:1451 (1989); B. Grinstein, *Phys. Lett. B* 229:280 (1989); M. Gronau, *Phys. Lett. B* 300:163 (1993).
- [76] M. Gronau and D. London, *Phys. Rev. Lett.* 65:3381 (1990).
- [77] ALEPH and DELPHI Collaborations, presented at XXVIII International Conference on High Energy Physics, Warsaw, July 25–31, 1996; L. Gibbons, Ref. [41].

- [78] I. I. Bigi *et al.*, in *B Decays*, edited by S. Stone (World Scientific, Singapore, 1994), p. 132.
- [79] I. Dunietz, *Phys. Rev. D* 52:3048 (1995).
- [80] T. E. Browder and S. Pakvasa, *Phys. Rev. D* 52:3123 (1995).
- [81] R. Aleksan, A. Le Yaouanc, L. Oliver, O. Pène, and J. C. Raynal, *Phys. Lett. B* 316:567 (1993).
- [82] M. Beneke, G. Buchalla, and I. Dunietz, *Phys. Rev. D* 54:4419 (1996); M. Beneke, SLAC report SLAC-PUB-96-7258, presented at XXVIII International Conference on High Energy Physics, Warsaw, July 25–31, 1996.
- [83] A. S. Dighe, I. Dunietz, H. J. Lipkin, and J. L. Rosner, *Phys. Lett. B* 369:144 (1996). See also R. Fleischer and I. Dunietz, Univ. of Karlsruhe report TTP 96-07 [hep-ph/9605220] (unpublished); A. Dighe, I. Dunietz, and R. Fleischer, in preparation.
- [84] H. J. Lipkin, in *Proceedings of the SLAC Workshop on Physics and Detector Issues for a High-Luminosity Asymmetric B Factory*, edited by David Hitlin, published as SLAC, LBL and Caltech reports SLAC-373, LBL-30097 and CALT-68-1697, 1990, p. 49; I. Dunietz *et al.*, *Phys. Rev. D* 43:2193 (1991); I. Dunietz, Appendix in *B Decays*, edited by S. Stone (World Scientific, Singapore, 1994), p. 550.
- [85] CLEO Collaboration, CLEO-CONF-96-22, report PA05-074, presented by R. Kutschke at XXVIII International Conference on High Energy Physics, Warsaw, July 25–31, 1996.
- [86] J. L. Rosner, *Phys. Rev. D* 42:3732 (1990).
- [87] L. D. Landau, *Dokl. Akad. Nauk SSSR* 60:207 (1948); C. N. Yang, *Phys. Rev.* 77:242,722 (1950). See also N. P. Chang and C. A. Nelson, Jr., *Phys. Rev. Lett.* 40:1617 (1978); *Phys. Rev. D* 20:2923 (1979).
- [88] J. Ellis, M. K. Gaillard, and D. V. Nanopoulos, *Nucl. Phys.* B100:313 (1975); *ibid.* B109:213 (1976); A. I. Vainshtein, V. I. Zakharov, and M. A. Shifman, *Pis'ma Zh. Eksp. Teor. Fiz.* 22:123 (1975) [*JETP Lett.* 22:55 (1975)]; *Zh. Eksp. Teor. Fiz.* 72:1275 (1977) [*Sov. Phys. – JETP* 45:670 (1977)]; J. Ellis, M. K. Gaillard, D. V. Nanopoulos, and S. Rudaz, *Nucl. Phys.* B131:285 (1977); *ibid.* B132:541(E) (1978).
- [89] M. B. Wise, in *Particles and Fields 3* (Proceedings of the 1988 Banff Summer Institute on Particles and Fields), edited by A. N. Kamal and F. C. Khanna (World Scientific, Singapore, 1989), p. 124; J. M. Flynn and L. Randall, *Phys. Lett. B* 224:221 (1989); G. Buchalla, A. J. Buras, and M. Harlander, *Nucl. Phys.* B337:313 (1990); A. J. Buras, M. Jamin, and M. E. Lautenbacher, *Nucl. Phys.* B408:209 (1993); M. Ciuchini, E. Franco, G. Martinelli, and L. Reina, *Phys. Lett. B* 301:263 (1993); S. Bertolini, talk given at Workshop on *K* Physics, Orsay, France, 30 May – 4 June 1996, INFN (Trieste) report SISSA-110-96-EP [hep-ph/9607312]; A. J. Buras, Plenary talk, XXVIII International Conference on High Energy Physics, Warsaw, July 25–31, 1996.

- [90] Fermilab E731 Collaboration, L. K. Gibbons *et al.*, *Phys. Rev. Lett.* 70:1203 (1993).
- [91] CERN NA31 Collaboration, G. D. Barr *et al.*, *Phys. Lett. B* 317:233 (1993).
- [92] A. J. Buras and R. Fleischer, *Phys. Lett. B* 341:379 (1995).
- [93] CLEO Collaboration, M. Battle *et al.*, *Phys. Rev. Lett.* 71:3922 (1993).
- [94] CLEO Collaboration, D. M. Asner *et al.*, *Phys. Rev. D* 53:1039 (1996).
- [95] CLEO Collaboration, P. Gaidarev, *Bull. Am. Phys. Soc.* 40:923 (1995).
- [96] M. Gronau, J. L. Rosner, and D. London, *Phys. Rev. Lett.* 73:21 (1994); O. F. Hernandez, D. London, M. Gronau, and J. L. Rosner, *Phys. Lett. B* 333:500 (1994); M. Gronau, O. F. Hernández, D. London, and J. L. Rosner, *Phys. Rev. D* 50:4529 (1994).
- [97] M. Gronau and J. L. Rosner, *Phys. Rev. D* 53:2516 (1996).
- [98] M. Gronau and J. L. Rosner, *Phys. Rev. Lett.* 76:1200 (1996); A. S. Dighe, M. Gronau, and J. L. Rosner, *Phys. Rev. D* 54:3309 (1996); A. S. Dighe and J. L. Rosner, *Phys. Rev. D* 54:4677 (1996).
- [99] M. Gronau and J. L. Rosner, *Phys. Lett. B* 376:205 (1996).
- [100] J. Silva and L. Wolfenstein, *Phys. Rev. D* 49:R1151 (1994); F. DeJongh and P. Sphicas, *Phys. Rev. D* 53:4930 (1996).
- [101] G. Buchalla and A. J. Buras, hep-ph/9607447. See also G. Buchalla and A. J. Buras, *Nucl. Phys. B* 412:106 (1994).
- [102] C. O. Dib, Ph.D. Thesis, Stanford University, 1990, SLAC Report SLAC-364, April, 1990 (unpublished).
- [103] B. Winstein and L. Wolfenstein, *Rev. Mod. Phys.* 65:1113 (1993).
- [104] Brookhaven E787 Collaboration, S. Adler *et al.*, *Phys. Rev. Lett.* 76:1421 (1996).
- [105] M. K. Gaillard and B. W. Lee, *Phys. Rev. D* 10:897 (1974).
- [106] Fermilab E799 Collaboration, M. Weaver *et al.*, *Phys. Rev. Lett.* 72:3758 (1994).
- [107] J. L. Rosner, *Phys. Rev. D* 53:2724 (1996).
- [108] The earliest such proposals were made by H. Yukawa, *Proc. Phys. Math. Soc. Jap.* 17:48 (1935), and O. Klein, in *Les Nouvelles Théories de la Physique*, Paris, Inst. de Coöperation Intellectuelle (1939), p. 81. For others (in the 1950's) see Ref. [12].
- [109] R. P. Feynman and M. Gell-Mann, *Phys. Rev.* 109:193 (1958); E. C. G. Sudarshan and R. E. Marshak, *Phys. Rev.* 109:1860 (1958).



- [110] S. Eidelman and F. Jegerlehner, Paul Scherrer Institute report PSI-PR-95-1, January, 1995; H. Burkhardt and B. Pietrzyk, *Phys. Lett. B* 356:398 (1995). Both sets of authors quote  $\alpha^{-1}(M_Z) = 128.89 \pm 0.09$ . Values differing only slightly from this are obtained by A. D. Martin and D. Zeppenfeld, *Phys. Lett. B* 345:558 (1995) [ $\alpha^{-1}(M_Z) = 128.99 \pm 0.06$ ] and by M. Swartz, SLAC report SLAC-PUB-95-7001, Sept. 1995, submitted to *Phys. Rev. D* [ $\alpha^{-1}(M_Z) = 128.96 \pm 0.06$ ].
- [111] A. Sirlin, *Phys. Rev. Lett.* 72:1786 (1994).
- [112] A. Pich, lectures at this Institute.
- [113] D. Treille, lectures at this Institute.
- [114] M. Veltman, *Nucl. Phys.* B123:89 (1977).
- [115] M. Peskin and T. Takeuchi, *Phys. Rev. Lett.* 65:964 (1990); *Phys. Rev. D* 46:381 (1992), and references therein.
- [116] G. DeGrassi, B. A. Kniehl, and A. Sirlin, *Phys. Rev. D* 48:3963 (1993).
- [117] P. Gambino and A. Sirlin, *Phys. Rev. D* 49:1160 (1994).
- [118] M. Veltman, *Phys. Lett. B* 91:95 (1980).
- [119] D. C. Kennedy and P. G. Langacker, *Phys. Rev. Lett.* 65:2967 (1990); *ibid.* 66:395(E) (1991).
- [120] F. J. Hasert *et al.*, *Phys. Lett. B* 46:138 (1973); *Nucl. Phys.* B73:1 (1974); A. Benvenuti *et al.*, *Phys. Rev. Lett.* 32:800 (1974); B. Aubert *et al.*, *Phys. Rev. Lett.* 32:1454 (1974).
- [121] C. H. Llewellyn Smith, *Nucl. Phys.* B228:205 (1983).
- [122] CCFR Collaboration, FERMILAB-CONF-96/227-E, presented by K. S. McFarland at XXXI Rencontres de Moriond, March, 1996.
- [123] CDHS Collaboration, H. Abramowicz *et al.*, *Phys. Rev. Lett.* 57:298 (1986); A. Blondel *et al.*, *Zeit. Phys. C* 45:361 (1990).
- [124] CHARM Collaboration, J. V. Allaby *et al.*, *Phys. Lett. B* 177:446 (1986); *Zeit. Phys. C* 36:611 (1987).
- [125] A. Blondel, Plenary talk, XXVIII International Conference on High Energy Physics, Warsaw, July 25–31, 1996.
- [126] CDF Collaboration, F. Abe *et al.*, *Phys. Rev. Lett.* 75:11 (1995); *Phys. Rev. D* 52:4784 (1995).
- [127] D0 Collaboration, report PA07-038, presented by A. Zieminski at XXVIII International Conference on High Energy Physics, Warsaw, July 25–31, 1996.
- [128] ALEPH, DELPHI, L3, and OPAL Collaborations, presented at XXVIII International Conference on High Energy Physics, Warsaw, July 25–31, 1996. For a compilation of the results see Ref. [125].
- [129] UA2 Collaboration, J. Alitti *et al.*, *Phys. Lett. B* 276:354 (1992).

- [130] J. L. Rosner, M. P. Worah, and T. Takeuchi, *Phys. Rev. D* 49:1363 (1994).
- [131] CDF Collaboration, F. Abe *et al.*, *Phys. Rev. Lett.* 74:341 (1995).
- [132] SLD Collaboration, report PA07-063, presented by D. Su at XXVIII International Conference on High Energy Physics, Warsaw, July 25–31, 1996.
- [133] M. C. Noecker, B. P. Masterson, and C. E. Wieman, *Phys. Rev. Lett.* 61:310 (1988).
- [134] V. A. Dzuba, V. V. Flambaum, and O. P. Sushkov, *Phys. Lett. A* 141:147 (1989); S. A. Blundell, W. R. Johnson, and J. Sapirstein, *Phys. Rev. Lett.* 65:1411 (1990); *Phys. Rev. D* 45:1602 (1992).
- [135] W. Marciano and J. L. Rosner, *Phys. Rev. Lett.* 65:2963 (1990); *ibid.* 68:898(E) (1992).
- [136] J. L. Rosner, *Phys. Rev. D* 42:3107 (1990).
- [137] P. G. H. Sandars, *J. Phys. B* 23:L655 (1990).
- [138] P. A. Vetter, D. M. Meekhof, P. K. Majumder, S. K. Lamoreaux, and E. N. Fortson, *Phys. Rev. Lett.* 74:2658 (1995).
- [139] N. H. Edwards, S. J. Phipp, P. E. G. Baird, and S. Nakayama, *Phys. Rev. Lett.* 74:2654 (1995).
- [140] P. G. H. Sandars and B. W. Lynn, *J. Phys. B* 27:1469 (1994).
- [141] V. A. Dzuba, V. V. Flambaum, P. G. Silvestrov, and O. P. Sushkov, *J. Phys. B* 20:3297 (1987).
- [142] A. C. Hartley, E. Lindroth, and A. M. Mårtensson-Pendrill, *J. Phys. B* 23:3417 (1990); A. C. Hartley and P. G. H. Sandars, *J. Phys. B* 23:4197 (1990).
- [143] ALEPH Collaboration, reports PA10-014 and PA10-015, presented by J. Carr at XXVIII International Conference on High Energy Physics, Warsaw, July 25–31, 1996.
- [144] P. Langacker, M. Luo, and A. K. Mann, *Rev. Mod. Phys.* 64:87 (1992).
- [145] J. Ellis, G. Fogli, and E. Lisi, CERN report CERN-TH/96-216 [hep-ph/9608239] (unpublished).
- [146] W. de Boer, A. Dabelstein, W. Hollik, W. Mösle, and U. Schwickerath, Karlsruhe Univ. report IEKP-KA/96-08 [hep-ph/9609209] (unpublished).
- [147] M. Schmelling, Plenary talk, XXVIII International Conference on High Energy Physics, Warsaw, July 25–31, 1996.
- [148] See, e.g., R. S. Chivukula, in *The Albuquerque Meeting: DPF 94* (Division of Particles and Fields Meeting, American Physical Society, Albuquerque, NM, August 2–6, 1994), ed. by S. Seidel (World Scientific, River Edge, NJ, 1995), p. 273; T. Takeuchi, A. K. Grant, and J. L. Rosner, *ibid.*, p. 1231; A. K. Grant, *Phys. Rev. D* 51:207 (1995).

- [149] ALEPH, DELPHI, L3, and OPAL Collaborations, LEP Heavy Flavor Working Group, D. Abbaneo *et al.*, CERN report CERN-PPE/96-017, Feb. 1996, submitted to *Nucl. Inst. Meth.*
- [150] J. Steinberger, seminar at CERN, August 27, 1996; ALEPH Collaboration, A. O. Bazarko *et al.* [hep-ex/9609005], presented at *The Minneapolis Meeting: DPF 96* (Division of Particles and Fields Meeting, American Physical Society, Minneapolis, MN, 10–15 August, 1996), to be published.
- [151] J. Bernabeu, A. Pich, and A. Santamaria, *Phys. Lett. B* 200:569 (1988); B. A. Kniehl and J. H. Kühn, *Phys. Lett. B* 224:229 (1989); K. G. Chetyrkin and J. H. Kühn, *Phys. Lett. B* 248:359 (1990); G. Altarelli and R. Barbieri, *Phys. Lett. B* 253:161 (1991); K. G. Chetyrkin, J. H. Kühn, and A. Kwiatkowski, *Phys. Lett. B* 282:221 (1992). For a recent discussion see A. K. Grant, *Phys. Rev. D* 51:207 (1995).
- [152] SLD Collaboration, Measurement of  $R_b$  at SLD, report PA10-23, presented by D. Su at XXVIII International Conference on High Energy Physics, Warsaw, July 25–31, 1996.
- [153] E. Eichten, I. Hinchliffe, K. Lane, and C. Quigg, *Rev. Mod. Phys.* 56:579 (1984); *ibid.* 58:1065(E) (1986).
- [154] J. L. Rosner, *Phys. Lett.* 146B:108 (1984).
- [155] J. Feltesse, lectures at this Institute.
- [156] CDF Collaboration, Fermilab reports FERMILAB-CONF-96-118-E, March, 1996 (presented by P. Azzi), and FERMILAB-CONF-96-146-E, June, 1996 (presented by A. Barbaro-Galtieri), at XXXI Rencontre de Moriond, *QCD and High-Energy Hadronic Interactions*, Les Arcs, France, 23–30 March 1996.
- [157] E. Laenen *et al.*, *Phys. Lett. B* 321:254 (1994).
- [158] R. K. Ellis, W. J. Stirling, and B. Webber, to be published by Cambridge University Press (1996). I thank R. K. Ellis for updating the plot of Fig. 21.
- [159] S. Catani, M. L. Mangano, P. Nason, and L. Trentadue, *Phys. Lett. B* 378:329 (1996).
- [160] W. Kwong, *Phys. Rev. D* 43:1488 (1991).
- [161] M. E. Peskin and M. J. Strassler, *Phys. Rev. D* 43:1500 (1991).
- [162] R. Gatto, G. Sartori, and M. Tonin, *Phys. Lett.* 28B:128 (1968); N. Cabibbo and L. Maiani, *ibid.* 28B:131 (1968); R. J. Oakes, *ibid.* 29B:683 (1969).
- [163] S. Weinberg, in *A Festschrift for I. I. Rabi*, *Trans. N. Y. Acad. Sci. Ser. II* 38 (1977); F. Wilczek and A. Zee, *Phys. Lett.* 70B:418 (1977); *ibid.* 72B:504(E) (1978); H. Fritzsch, *ibid.* 70B:436 (1977).
- [164] J. L. Rosner and M. P. Worah, *Phys. Rev. D* 46:1131 (1992).
- [165] H. Leutwyler, lectures at this Institute.
- [166] H. Fritzsch, *Phys. Lett.* 85B:81 (1979); *Nucl. Phys.* B155:189 (1979).

- [167] H. Arason *et al.*, *Phys. Rev. D* 46:3945 (1992); H. Arason, D. J. Castano, E. J. Piard, and P. Ramond, *Phys. Rev. D* 47:232 (1992); P. Ramond, R. G. Roberts, and G. G. Ross, *Nucl. Phys. B* 406:19 (1993); D. J. Castano, E. J. Piard, and P. Ramond, *Phys. Rev. D* 49:4882 (1994); T. Blazek, M. Carena, S. Raby, and C. Wagner, Ohio State Univ. report OHSTPY-HEP-T-96-014 [hep-ph/9608273], and references therein.
- [168] G. C. Branco, W. Grimus, and L. Lavoura, *Phys. Lett. B* 380:119 (1996); G. C. Branco, D. Emmanuel-Costa, and J. I. Silva-Marcos, report [hep-ph/9608477] (unpublished).
- [169] H. Harari, H. Haut and J. Weyers, *Phys. Lett.* 78B:459 (1978); Y. Nambu, in *New Theories in Physics* (23–27 May, 1988, Kazimierz, Poland), Z. Ajduk, S. Pokorski, and A. Trautman, eds., World Scientific, Singapore, 1989, p. 1; in *Strong Coupling Gauge Theories and Beyond*, Proceedings of the Second International Workshop, Nagoya, Japan, 1990, T. Muta and K. Yamawaki, eds., World Scientific, Singapore (1991), p. 3; Enrico Fermi Institute Report No. 92-03, in *Proceedings of the Workshop on Electroweak Symmetry Breaking*, Hiroshima, 1991, p. 1; Enrico Fermi Institute Report No. 92-37, Spontaneous symmetry breaking and the origin of mass, invited talk at Int. Conf. on Fluid Mech. and Theor. Phys. in honor of Professor Chou Pei-Yuan’s 90th Birthday, 1992; P. Kaus and S. Meshkov, *Mod. Phys. Lett. A* 3:1251 (1988); *ibid.* 4:603(E) (1989); *Phys. Rev. D* 42:1863 (1990). See also the second of Refs. [168].
- [170] K. Matumoto and T. Matsuoka, *Prog. Theor. Phys.* 83:373 (1990); *ibid.* 84:53 (1990); K. Matumoto, *ibid.* 84:185,787 (1990); *ibid.* 85:1149 (1991); second of Refs. [168].
- [171] J. L. Rosner, *Prog. Theor. Phys.* 66:1421 (1981).
- [172] M. K. Gaillard, B. W. Lee, and J. L. Rosner, *Rev. Mod. Phys.* 47:277 (1975).
- [173] WA89 Collaboration, S. Paul *et al.*, *Nucl. Phys. A* 585:183c (1995). See, however, CLEO Collaboration, report PA01-079, presented by R. Kutschke at XXVIII International Conference on High Energy Physics, Warsaw, July 25–31, 1996.
- [174] A. De Rújula, H. Georgi, and S. L. Glashow, *Phys. Rev. D* 12:147 (1975); S. Gasiorowicz and J. L. Rosner, *Am. J. Phys.* 49:954 (1981).
- [175] M. Veltman, in *Proc. Int. Symp. on Lepton and Photon Interactions at High Energies (Fermilab, August 23–29, 1979)*, T. B. W. Kirk and H. D. I. Abarbanel, eds., Fermilab, Batavia, IL (1979), p. 529; *Acta Physica Polonica B* 12:437 (1981).
- [176] Y. Nambu, Ref. [169].
- [177] Y. Nambu and G. Jona-Lasinio, *Phys. Rev.* 122:345 (1961); *ibid.* 124:246 (1961).
- [178] W. A. Bardeen, C. T. Hill, and M. Lindner, *Phys. Rev. D* 41:1647 (1990).
- [179] J.-M. Gérard and J. Weyers, *Phys. Lett.* 146B:411 (1984); J. P. Fatelo, J.-M. Gérard, T. Hambye, and J. Weyers, *Phys. Rev. Lett.* 74:492 (1995); M. Chaichian, P. Chiappetta, J.-M. Gérard, R. Gonzalez Felipe, and J. Weyers, *Phys. Lett. B* 365:141 (1996), and references therein.

- [180] L. Hall, The heavy top quark and supersymmetry, lectures given at the 1995 SLAC Summer Institute, July 10–21, 1995, report LBL-38110 [hep-ph/9605258].
- [181] R. Oehme, Enrico Fermi Institute Report No. 95-47 [hep-th/9511006], and references therein.
- [182] W. Marciano, *Phys. Rev. Lett.* 62:2793 (1989); *Phys. Rev. D* 41:219 (1990).
- [183] J. Kubo *et al.*, Max-Planck-Institut report MPI-PHT-95-132 [hep-ph/9512400], and references therein.
- [184] L. Susskind, *Phys. Rev. D* 20:2619 (1979).
- [185] S. Weinberg, *Phys. Rev. D* 13:974 (1976); *ibid.* 19:1277 (1979).
- [186] For a review see E. Farhi and L. Susskind, *Phys. Rep.* 74:277 (1981).
- [187] M. Gell-Mann, P. Ramond, and R. Slansky, in *Supergravity*, edited by P. van Nieuwenhuizen and D. Z. Freedman (North-Holland, Amsterdam, 1979), p. 315; T. Yanagida, in *Proc. Workshop on Unified Theory and Baryon Number in the Universe*, edited by O. Sawada and A. Sugamoto (KEK Report No. 79-18, Tsukuba, Japan, 1979).
- [188] H. Georgi and S. L. Glashow, *Phys. Rev. Lett.* 32:438 (1974).
- [189] H. Georgi in *Proceedings of the 1974 Williamsburg DPF Meeting*, ed. by C. E. Carlson (New York, AIP, 1975) p. 575; H. Fritzsch and P. Minkowski, *Ann. Phys. (N.Y.)* 93:193 (1975).
- [190] F. Gürsey, P. Ramond, and P. Sikivie, *Phys. Lett.* 60B:177 (1976).
- [191] E. Witten, *Nucl. Phys.* B258:75 (1985); E. Cohen, J. Ellis, K. Enqvist, and D. V. Nanopoulos, *Phys. Lett.* 165B:76 (1985); J. L. Rosner, *Comments on Nucl. and Part. Phys.* 15:195 (1986).
- [192] For a review of  $E_6$  phenomenology in the context of superstring theories see J. L. Hewett and T. G. Rizzo, *Phys. Rep.* 183:193 (1989). More recent discussions of extended gauge structures motivated by  $E_6$  include those by P. Langacker and M. Luo, *Phys. Rev. D* 45:278 (1992); P. Langacker, in *Precision Tests of the Standard Model*, edited by P. Langacker (World Scientific, Singapore, 1995), p. 883; M. Cvetič and S. Godfrey, in *Electro-weak Symmetry Breaking and Beyond the Standard Model*, edited by T. Barklow, S. Dawson, H. Haber, and J. Siegrist (World Scientific, Singapore, 1995), and references therein; M. Cvetič and P. Langacker, *Phys. Rev. D* 54:3570 (1996).
- [193] R. Slansky, *Phys. Rep.* 79:1 (1981).
- [194] See, e.g., S. M. Barr, *Phys. Lett.* 112B:219 (1982); J. Ellis, J. L. Lopez, and D. V. Nanopoulos, *Phys. Lett. B* 371:65 (1996); J. L. Lopez, D. V. Nanopoulos, and A. Zichichi, *Phys. Rev. D* 53:5253 (1996); and references therein.
- [195] J. L. Rosner, CERN report CERN-TH/96-209, hep-ph/9607467, submitted to *Phys. Rev. D*.
- [196] P. Langacker and J. Erler, in Ref. [47], p. 103.

- [197] R. W. Robinett and J. L. Rosner, *Phys. Rev. D* 26:2396 (1982); P. G. Langacker, R. W. Robinett, and J. L. Rosner, *Phys. Rev. D* 30:1470 (1984).
- [198] CDF Collaboration, F. Abe *et al.*, *Phys. Rev. D* 51:949 (1995); T. Kamon, Fermilab report FERMILAB-CONF-96-106-E [hep-ex/9605006], presented at XXXI Rencontre de Moriond: QCD and High-energy Hadronic Interactions, 23 – 30 March, 1996; CDF Collaboration, M. K. Pillai, E Hayashi, K. Maeshima, C. Grosso-Pilcher, P. de Barbaro, A. Bodek, B. Kim, and W. Sakumoto, report hep-ex/9608006, August, 1996, presented at *The Minneapolis Meeting: DPF 96* (Division of Particles and Fields Meeting, American Physical Society, Minneapolis, MN, 10–15 August, 1996), to be published.
- [199] CDF Collaboration, F. Abe *et al.*, *Phys. Rev. Lett.* 77:2616 (1996).
- [200] J. L. Rosner, *Phys. Rev. D* 54:1078 (1996).
- [201] CDF Collaboration, F. Abe *et al.*, presented by S. Park, in *Proceedings of the 10th Topical Workshop on Proton-Antiproton Collider Physics*, Fermilab, May 9–13, 1995, AIP Conference Proceedings 357, edited by R. Raja and J. Yoh, (AIP, Woodbury, NY, 1996), p. 62.
- [202] S. Ambrosanio, G. L. Kane, G. D. Kribs, S. P. Martin, and S. Mrenna, *Phys. Rev. Lett.* 76:3498 (1996); Univ. of Michigan reports hep-ph/9605398 and 9607414 (unpublished); S. Dimopoulos, M. Dine, S. Raby, and S. Thomas, *Phys. Rev. Lett.* 76:3494 (1996); S. Dimopoulos, S. Thomas, and J. D. Wells, *Phys. Rev. D* 54:3283 (1996); S. Dimopoulos, M. Dine, S. Raby, S. Thomas, and J. D. Wells, SLAC-PUB-7236 [hep-ph/9607450] (unpublished); J. L. Lopez and D. V. Nanopoulos, Rice University reports DOE/ER/40717-29 [hep-ph/9607220] and DOE/ER/40717-32 [hep-ph/9608275] (unpublished); K. S. Babu, C. Kolda, and F. Wilczek, Institute for Advanced Study report IASSNS-HEP-96/55 [hep-ph/9605408]; J. Hisano, K. Tobe, and T. Yanagida, Univ. of Tokyo report UT-754 [hep-ph/9607234] (unpublished).
- [203] G. Bhattacharyya and R. N. Mohapatra, *Phys. Rev. D* 54:4204 (1996).
- [204] D. London and J. L. Rosner, *Phys. Rev. D* 34:1530 (1986).
- [205] D. Toback, Fermilab report FERMILAB-CONF-96/240-E, August 1996, presented for the CDF Collaboration at *The Minneapolis Meeting: DPF 96* (Division of Particles and Fields Meeting, American Physical Society, Minneapolis, MN, 10–15 August, 1996), to be published.